IEEE EMB

STUDENT CHAPTER, MAGDEBURG

IEEE Engineering in Medicine & Biology

International Student Conference 2019

MAGDEBURG - GERMANY

BOOK OF PROCEEDINGS

Organized by

Partners

BOOK OF PROCEEDING OF THE IEEE EMBS ISC 2019 Magdeburg

30.10.2019, Magdeburg

Edited by

Markus Weinreich, Fadil AL-Jaberi

Published, 2019

ADVISORY COMMITTEE

Prof. Michael Friebe- INKA – Chair of catheter technologies and IGT

Dr.-Ing Axel Boese – INKA – Chair of catheter technologies and IGT

Dr. Alfredo Illanes – INKA – Chair of catheter technologies and IGT

Prof. Debdoot Sheet – IIT Kharagpur, India

Dr. Subhamoy Mandal- The German Cancer Research Center, Heidelberg, Germany

Prof. Steven Wright- Bioengineering and Radiology, Texas A&M

Mr. Alejandro Azocar – EMBS Student Rep and ISC Convener

Ms. Malin Schmidt- VDE, Junges Forum

Ms. Yeshaswini Nagaraj – University of Groningen

Mr. Felix Middelstaedt- Otto von Guericke University, Magdeburg, Germany

Mr. Mathias Makdowski – Otto von Guericke University, Magdeburg, Germany

Mr. Raghu – Student Chair, RIT, Bengaluru

Mr. Rama Reddy R – Student Vice-Chair, RIT, Bengaluru

ORGANIZATION COMMITTEE

Chairman of the Conference

Prof. Michael Friebe, PhD

Members of the Committee

Conference Chair: Elmer Jeto Gomes Ataide

Technical Chair: Dr. Alfredo Illanes

Finance Chairs: Thomas Suehn and Holger Fritzsche

Publicity Chairs: Ali Pashazadeh and Prabal Poudel

Keynotes and workshops Chairs: Marwah Al-Maatoq and Chien-Hsi (David) Chen

Publication Chairs: Prabal Poudel and Marco Kalmar

Local Logistics Chairs: Kimberly Brunstein and Sinja Lagotsky

Hosting and Planning Chairs: Holger Fritzsche and Ivan Maldonado Zambrano

Human Resources Chairs: Jens Ziegle and Elmer Jeto Gomes Ataide

Reception Chairs: Nazila Esmaelli and Naghmeh Mahmoodian

Academic Liaison: Thomas Suehn

Industry Liaisons: Markus Weinreich and Sathish Balakrishnan

Startup Liaisons: Juan Sebastian Sanchez Lopez

Website developement: Maryam Sadeghi

Dear Biomedical Engineering and Medical Students, dear Attendees,

I am very happy and honored to welcome you to Magdeburg, the Otto-von-Guericke-University, and the chair of Intelligent Catheters and Image Guided Therapies (INKA). The organisation of the conference predominantly was carried out by the INKA doctoral students. Thank you very much for that!

*The motto of this years International Student Conference of the IEEE Engineering in Medicine and Biology society is "**Global young professionals addressing todays MedTec challenges for a healthier tomorrow"**.*

*There is one saying that is appropriate ... **you have many wishes and dreams if you are healthy, you have only one when you are sick**. Healthcare is everyone's concern.*

But healthcare is also one of the areas with the biggest change potential and the largest opportunities. We are globally spending more and more on the diagnosis and treatment of diseases, but spend rather little on prevention and moving healthcare responsibility to the patient. All of us want to stay healthy as long as possible, get treated as quickly and empathetically as possible when we are sick, and live as long as possible ... which also will require that we eat well, move more, take care of our environment, and monitor our own health.

Digitization, digital processes and exponential technologies will dramatically change the way we engage in and with the healthcare system. We will have advanced sensors at the fingertip of everyone that process datasets using machine and deep learning. That will give the potential patients an empowerment that was not available before. We will see a shift from evidence based medicine, to a value based personalized approach that will put the patient in the center of attention. We will have massive datasets that we need to make available to the patients. Additionally we are seeing major advances in genetic engineering, 3D tissue and organ printing, robotics in healthcare, and further molecular insights.

All this will lead to major disruptions - not only technologically, but even more pronounced with respect to how healthcare is delivered. Innovation that is valuable in that context is an interdisciplinary development between clinicians, engineers, and other experts with the patient in mind. And, also with a global perspective! Let us not forget that there are still plenty of places in the world with little to no access to medical services. We - biomedical engineers - have a responsibility to work on disruptive innovations that make healthcare accessible to everyone ... and the best way to do that is to work closely with our peers from the clinical disciplines. We also need to understand the need for ethical and empathetic developments and need to assume responsibilities.

Be part of these challenges that also provide huge entrepreneurial opportunities.

I hope that you will learn a lot, expand your horizon, talk to lots of people from all disciplines, and enjoy your time and the great keynote lectures that we offer.

Thank you again organizing team, all the keynote lecturers, and of course the industry sponsors that helped us to finance this student conference.

Stay in touch!

Prof. Michael Friebe, PhD

Chair of Intelligent Catheters Image Guided Therapies

Design of a feedback Loop for improving accuracy of CNN Algorithm for Breast Cancer Lymph Node Metastasis Detection

M. Sadeghi, I. Maldonado, N. Abele, J. Haybaeck, A. Boese, M. Friebe

***Abstract*—This paper, proposes a feedback-based method, aimed to improve the performance of the classification algorithms by utilizing the feedback of the pathologists. The GUI developed for this purpose, is aimed to be simple and adaptive to different classification algorithms. The method showed significant improvement in the classification performance of the applied Convolutional Neural Network (CNN) algorithm.**

I. INTRODUCTION

Digital pathology can be thought of as a model composed of 3 main elements; classification algorithm, Graphical User Interface (GUI) and the pathologists. The diagnosis decision of the classification algorithm is visualized by a GUI and available for the pathologist as an assisting tool. As of until now, there is no way for the pathologist to impact the classification algorithm which can act as an improving tool for the algorithm. Achieving this, necessitates a feedback-based backward path from the pathologist to the classification algorithm through a GUI to achieve a sufficiently high accuracy classification algorithm, which can be a valuable assisting tool for the pathologists in making decisions and save time in time-consuming tasks.

II. METHODS

In order to prepare a dataset to feed to the classification algorithm, certain pre-processing procedures were performed on the Whole Slide Images (WSI) from the Camelyon17 grand challenge [1]. The preprocessing stage included creating tissue mask and tumor mask, patch extraction, and data augmentation. In total, 200k normal and tumor 128x128 pixel patches were prepared to train the Convolutional Neural Network (CNN) as the classification algorithm. In the second stage, the proposed method was tested to evaluate the impact of the feedback of the pathologists on the performance of the algorithm. In order to collect feedback from the pathologists, a graphical user interface (GUI) was created in python using PyQt library. The workflow is as follows. In the GUI, the a probability score heatmap of the selected slide is created and displayed. Then, each patch can be marked by the pathologist as a tumor or normal tissue area respectively by right mouse click and left mouse click, to confirm or contradict the prediction of the CNN algorithm.

In total, 1243 classified patches were evaluated by Pathologist 1, and 1204 classified patches were evaluated by Pathologist 2, and their feedback was recorded. The .CSV files containing the data input by the pathologists are then processed to select the false positive (FP) and false negative (FN) patches. The new set of patches were added to the original training set and the CNN was retrained on the new training set, and the change in the performance of the CNN was evaluated.

*This study was done as a Master thesis in collaboration with the pathology department of Magdeburg University clinic and Intelligente Katheter research group (BMBF Grant Number 03IPT7100X)

III. RESULTS

After retraining the CNN algorithm with the new training set, containing the original training set and the feedback input of the pathologists, both trained algorithms were tested on a set of 10k tumor patches. The accuracy of the CNN algorithm prediction showed significant improvement by this addition. With the mentioned approach, the 25% quantile of the probability score of the predictions increased from 0.48 to 0.89, and the median of the data increased from 0.95 to 0.99 (Fig 1).

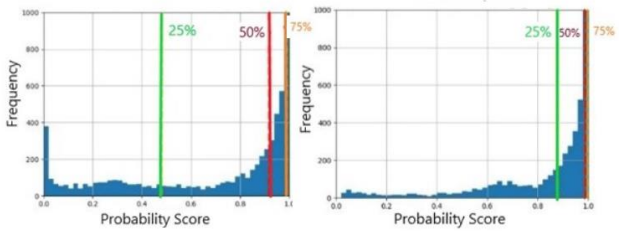

Figure 1. The performance of the CNN algorithm on 10k tumor patches. Top, CNN trained on original dataset. Bottom, CNN trained on a dataset containing the feedback-input.

IV. DISCUSSION & CONCLUSION

The proposed method can be used to improve the accuracy of future diagnostic regarding the real clinical images. The process is based on the feedback path provided by the pathologist for the algorithms of classification through the GUI. Although the pathologist can use different algorithms, feedback path provides more accuracy to automated diagnostics of the tumor area.

ACKNOWLEDGMENT

We thank all the Camelyon Grand Challenge 2016 and 2017 organizers.

REFERENCES

[1] Camelyon 2017, https://camelyon17. grand-challenge.org/, Accessed: 2017-07-24

New Concept for Laparoscopic Magnetic Detection of Sentinel Lymph Nodes

Ana Orive Benito, Melissa M. van de Loosdrecht, Erik Krooshoop, Bennie ten Haken

***Abstract*— A new magnetic detector for minimally invasive detection of sentinel lymph nodes is presented.**

I. INTRODUCTION

A new concept for laparoscopic magnetic detection of sentinel lymph nodes is presented. Superparamagnetic iron oxide nanoparticles (SPIONs) can be used as a tracer for sentinel node biopsy (SNB), a procedure recommended for patients with certain types of cancer that analyses the lymph node status to determine if the tumor has metastasized [1]. Magnetic particles present several advantages over the standard technique, which makes use of a radioisotope and blue dye, and entails safety and logistical issues.

II. METHODS

Several magnetic handheld probes have been developed for SNB, but their main drawback is that they are sensitive to both tissue diamagnetism and surgical instruments. To overcome this disadvantage, the technology we use is Differential Magnetometry (DiffMag) [2], which makes use of the nonlinear magnetization curve of SPIONs to achieve selective detection and avoid the interference from tissue and surgical steel. A first laparoscopic prototype was developed by the separation of excitation and detection coils, to obtain the clinically required depth sensitivity. Both AC and DC excitation coils are big and will be placed underneath the patient and the detection coils are small and placed in a probe [3]. In the new developed system, the DC excitation and detection coils switch positions (Figure 1), avoiding the need to use compensation coils to balance the probe, which is the case in the first prototype. Now, the detection coils can be passively balanced with respect to the AC excitation coil.

III. RESULTS

Both systems are comparable in various static measurements such as detection limit, penetration depth and measurements at different sites of the excitation field. Their performance is also alike in the presence of water, which has diamagnetic behavior as human tissue. The main difference was seen when both setups were compared in a simulated operating room in proximity of different surgical instruments (Figure 2). The big detection coils of the presented prototype seem to be very sensitive to the magnetic properties of stainless steel, making it impossible to differentiate SPIONs from the empty coil.

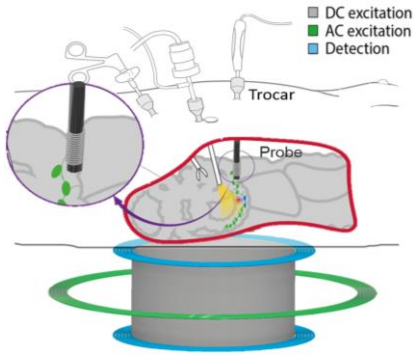

Figure 1. Sketch of the new laparoscopic concept for sentinel node biopsies.

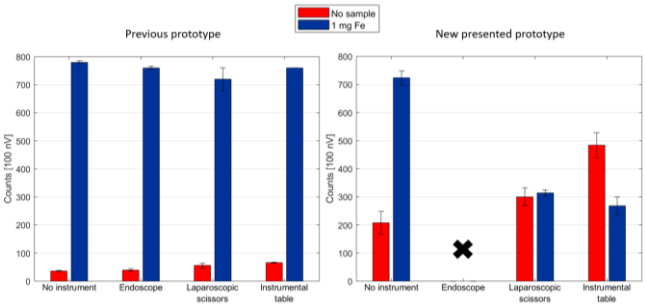

Figure 2. DiffMag counts obtained in static measurements for both laparoscopic prototypes, van de Loosdrecht et al., 2019 [3] (left) and the new concept (right), with and without SPIONs, in proximity of different surgical instruments. The cross represents that it was not possible to measure because the detection signal was saturated due to the presence of an endoscope.

IV. DISCUSSION & CONCLUSION

The presented new prototype is ineligible for sentinel lymph node *in vivo* detection, since it is not possible to measure SPIONs in proximity to laparoscopic instruments. However, the previous prototype looks promising for clinical implementation and is currently being optimized.

*Research supported by the Netherlands Organization for Scientific Research (NWO-TTW), under the research program Magnetic Sensing for Laparoscopy (MagLap) with project number 14322

All authors are with the Magnetic Detection & Imaging group, Technical Medical Centre, University of Twente, the Netherlands; e-mail: m.m.vandeloosdrecht@utwente.nl.

REFERENCES

[1] A. E. Giuliano and A. Gangi, "Sentinel node biopsy and improved patient care," *Breast J.*, vol. 21, no. 1, 2015.

[2] S. Waanders et al., "A handheld SPIO-based sentinel lymph node mapping device using differential magnetometry.," *Phys. Med. Biol.*, vol. 61, no. 22, pp. 8120–8134, Nov. 2016.

[3] M. M. van de Loosdrecht et al., "Separation of excitation and detection coils for in vivo detection of superparamagnetic iron oxide nanoparticles," *J. Magn. Magn. Mater.*, vol. 475, pp. 563–569, Apr. 2019.

Ex-vivo sentinel lymph node mapping in colorectal carcinoma

L. Molenaar, M.M. van de Loosdrecht, J. van Baarlen, B. ten Haken, I.A.M.J. Broeders, D.J. Lips

***Abstract*— This study tests an *ex vivo* sentinel lymph node mapping in order to reduce medical costs without increasing patient invasiveness or decrease the level of medical healthcare.**

I. INTRODUCTION

Worldwide incidence of colorectal cancer (CRC) in 2018 was 1.8 million, causing 861.000 associated deaths [1]. With the ever-increasing healthcare costs, the need to not only improve patientcare but also reduce costs strongly arises. Standard care for CRC patients is a radical resection of tumor including a regional lymph node (LN) dissection. Patients are treated with adjuvant chemotherapy when metastases are found in the LNs. Although this method is effective, it involves a lot of time and money spend on pathological examination of all found LNs.

The sentinel lymph node (SLN) mapping could potentially reduce the amount of researched LNs. SLNs are LNs which directly drain of the tumor, thus having the highest chance of containing metastases. Costs can be reduced by solely investigating the SLNs. However, it is vital that healthcare quality remains and patient burden does not increase. Therefore the manner of finding the SLNs should be as minimally invasive as possible.

To find SLNs, multiple tracers are available [2]. In this study the choice has been made to inject *ex vivo* a magnetic tracer to ensure minimal invasiveness. The goal of this study is to test an *ex vivo* peritumoral injection method, with and without tissue massage.

II. METHODS

Fifteen patients diagnosed with primary CRC and without known metastases were included in this study. The first ten received two to four peritumoral injections with 2ml (diluted to a total of 4ml) Sienna+© (Endomag, UK) and no tissue massage after injection (*group 1*), the second five patients received three to four peritumoral injections with 2ml (diluted to a total of 4ml) Magtrace© (Endomag, UK) and 1-2min of tissue massage after injection (*group 2*). All detected LNs were measured with the SuperParamagnetic Quantifier [3] (SPaQ, developed by the University of Twente based on the DiffMag principle [4]) at pathological examination. An LN was considered to contain magnetic tracer, when a signal at least twice the background noise was measured.

*Financial support from the Netherlands Organization for Scientific Research (NWO-TTW), under the research program Magnetic Sensing for Laparoscopy (MagLap) with project number 14322 is gratefully acknowledged.

L. Molenaar is with the Magnetic Detection & Imaging group, Technical Medical Centre, University of Twente, Enschede, The Netherlands; e-mail: l.molenaar@utwente.nl.

III. RESULTS

Study results are shown in Table 1. Both groups show an 80% SLN detection rate. LN metastases were found in a total of seven patients. In two of those patients metastases were also found in the LNs containing magnetic tracer (29%).

TABLE I. STUDY RESULTS

	Group 1	***Group 2***
Patients (N)	10	5
Mean amount of found LNs	21.3 (5-36)	27.6 (10-44)
Mean amount of found magnetic LNs	1.9 (0-4)	2.4 (0-4)
SLN identification rate	8/10 (80%)	4/5 (80%)
Patients with metastases in LNs	3	4
Patients with metastases in SLNs	1	1

IV. DISCUSSION & CONCLUSION

Distribution of magnetic tracer throughout the lymphatic system is seen (80%) despite the absence of natural lymph flow. Both groups show comparable results with respect to the SLN detection rate. Tissue massage seems to have little effect on lymphatic distribution. In only 29% of the patients with LN metastases, metastases were also found in the SLNs. This means that when only the SLNs in this group of patients were pathological researched, five of the seven patients with metastases would have received inadequate medical treatment. Our next step will be to investigate the feasibility of intratumoral injection. When a successful *ex vivo* injection method has been found, we intend to execute a large study to test whether researching all removed LNs or only all SLNs yield the same clinical result. Ultimately, the goal is to reduce healthcare costs while maintaining the same level of medical care.

ACKNOWLEDGMENT

To Mark Selles and Quinten Eyck thanks for their contribution to this research.

REFERENCES

[1] Arnold et al. (2017), doi: 10.1136/gutjnl-2015-310912
[2] Van der Zaag et al. (2012), doi: 10.1245/s10434-012-2417-0
[3] Van de Loosdrecht et al. (2019), doi: 10.1063/1.5039150
[4] Waanders et al. (2016), doi: 10.1088/0031-9155/61/22/8120

Towards Multi-user Virtual Reality Camera Navigation Training for Laparoscopic Surgery

V. Chheang[1], P. Saalfeld[1], T. Huber[2], F. Huettl[2], W. Kneist[2], B. Preim[1], and C. Hansen[1]

***Abstract*— Training camera navigation in laparoscopic liver surgery is an important part of modern surgical education. We propose a multi-user virtual reality simulation for camera navigation training in laparoscopic surgery. In our scenario, a student trains laparoscopic camera movement and is guided by a surgeon together with an anesthesiologist inside a virtual operating room. Our prototype was shown to surgeons and they underlined the potential of this collaborative training for further clinical evaluation.**

I. Introduction

Laparoscopic surgery allows surgeons to operate inside the abdomen of patients using small incisions with the aid of a camera. Adequate visualization of the surgical field and the navigation of the camera during a laparoscopic surgical procedure is extremely important [1]. However, the laparoscopic camera is often controlled by a surgical trainee who has less experience. An inappropriate handling of the camera can lead to longer operating time, frustration of surgeons, and compromise patient safety [2].

Current simulations for camera navigation training are limited due to the usage of conventional 2D displays, collaborative training in an immersive environment, and lacking realistic scenarios with anesthesia [3], [4]. In this paper, we introduce a collaborative virtual environment for camera navigation training in laparoscopic surgery. Continuous clinical feedback comprised an essential part of scenarios and system development.

II. Design and Implementation

We used patient image data to reconstruct a volumetric model. This model includes the liver and its vascular structures. They are embedded inside a phantom in a virtual operating room. There are three main roles for our training simulation: camera navigation trainee, experienced surgeon, and anesthesiologist (see Fig. 1). For our initial tests, we use three VR-ready computers in a local network and connect the surgical instruments (Simball joysticks) separately for the laparoscopic surgeon and camera holder. Two scenarios are developed for camera navigation training in our collaborative VR. The first scenario is focused on a *steady* camera navigation during the liver resection. The camera holder is required to keep the camera head level in straight horizontal tilt, move the camera smoothly to provide adequate visualization of the surgical area, keep the camera steady, and zoom as close to the resection area as possible.

[1] Faculty of Computer Science, University of Magdeburg, Germany.
[2] Department of General, Visceral and Transplant Surgery, University Medicine of the Johannes Gutenberg-University Mainz, Germany.

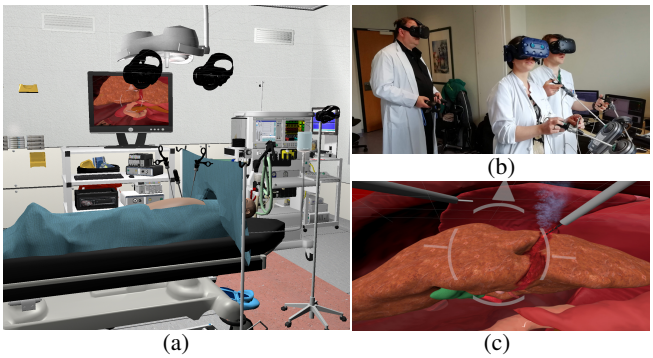

Fig. 1. Overview of multi-user training: (a) surgeons virtually collaborate in VR, (b) surgeons perform in the real world, and (c) camera navigation.

The second scenario is started during the liver resection while the depth of anesthesia is flattened and the patient begins to press. Therefore, the camera holder is required to notice movements of the organ, hold the camera during difficult situation, and communicate with the anesthesiologist to give a muscle relaxant. Once the anesthesiologist gives the muscle relaxant to the patient, the pressing will be paused and the surgeon will continue to perform liver resection.

III. Discussion & Conclusion

Our prototype was evaluated in a pilot study. Two liver surgeons and one anesthesiologist participated and performed the training simulation. They were positive about the usefulness of the simulation. The usage of real patient image data is considered an advantage compared to other simulators. This work builds a basis for clinical evaluation and opens a new direction for laparoscopic surgical training. Future work aims to improve the performance, and add additional scenarios.

Acknowledgement This project has been funded by the Federal Ministry of Education and Research (BMBF) (Number 16SV8054).

References

[1] T. Huber, M. Paschold, F. Schneble, A. Poplawski, F. Huettl, F. Watzka, H. Lang, and W. Kneist, "Structured assessment of laparoscopic camera navigation skills: the salas score," *Surgical endoscopy*, vol. 32, no. 12, pp. 4980–4984, 2018.

[2] A. Bennett, D. W. Birch, C. Menzes, A. Vizhul, and S. Karmali, "Assessment of medical student laparoscopic camera skills and the impact of formal camera training," *The American journal of surgery*, vol. 201, no. 5, pp. 655–659, 2011.

[3] C. Nilsson, J. L. Sorensen, L. Konge, M. Westen, M. Stadeager, B. Ottesen, and F. Bjerrum, "Simulation-based camera navigation training in laparoscopy -a randomized trial," *Surgical endoscopy*, vol. 31, no. 5, pp. 2131–2139, 2017.

[4] T. Huber, T. Wunderling, M. Paschold, H. Lang, W. Kneist, and C. Hansen, "Highly immersive virtual reality laparoscopy simulation: development and future aspects," *International journal of computer assisted radiology and surgery*, vol. 13, no. 2, pp. 281–290, 2018.

Automatic Scar tissue segmentation in CT with Convolutional Neural Networks

Yashbir Singh, Deepa, Tejasri Polana, Gaurav Garttan, Weichih Hu

***Abstract*—This research develops a framework to segment scar tissue in the LV endocardium wall using computer tomography (CT) with a convolution neural network. The dataset was divided into training images (N = 105) and testing images (N = 44) using Pixel value classification concept. We achieved 89.23% accuracy, 91.11% sensitivity and 87.75% specificity in the detection of scar tissue using CNN-based method. This study provides a platform for future algorithms of scar detection techniques.**

I. INTRODUCTION

Myocardial infarction is a well renowned and well warranted fear among all. For when blood flow to the heart is blocked, the muscle cells of the heart undergo hazardous ischemic death that is irreversible. Consequently, replacement myocardial fibrosis or "scar" formation takes place, which is a well- recognized substrate for the development of malignant ventricular arrhythmias and is a principal cause of sudden cardiac death (SCD). Patients having myocardial scar formation are at an elevated risk for subsequent re-entrant-type ventricular arrhythmias. Fortunately, this risk may be managed through device therapy (implantable cardiac defibrillator) or catheter ablation of scar-related re-entrant circuits. Patient selection and delivery of such therapies may be improved through individualized, non-invasive modeling of this arrhythmia substrate. In particular, Computational models must incorporate accurate reconstructions of left ventricular (LV) scar geometry, to accurately represent patient-specific structural remodeling. Here, we developed an automated method based on convolutional neural network (CNN) to detect the LV endocardial scar tissue from delayed enhancement CT cardiac images. To our knowledge, this is the first implementation of CNN for the detection of scar tissue using delayed enhancement CT cardiac images.

II. METHODS

Our study consists of 5 in-patients with chronic ischemic cardiomyopathy. The dataset comprises of 409 images with 512×512 dimension, provided by the National Institute of Hospital of Yang-Ming University. The informed consent procedure and study were approved by the Institutional Review Board (IRB) of National Yang-Ming University Hospital, Taipei. This method mainly involves steps such as Automatic segmentation of left ventricular (LV), Standard deviation (SD) and average calculation of pixel value, Implementation of region growing algorithm, Implementation of morphological operations, Architecture of CNN and Testing Phase.

III. RESULTS

According to previous studies, the presence of scar tissue on the endocardium of the LV plays a significant role in determining function and remodeling. In this study, we developed the method for automatic prediction of scar tissue on the LV endocardial wall. In the evaluation of our proposed method, we found the accuracy of segmentation to be 89.23%, with a sensitivity and specificity of 91.11% and 87.75% respectively using the trained model and then tested using the testing dataset of 44 delayed CT cardiac images. (Table.1).

Accuracy	89.23%
Sensitivity	91.11%
Specificity	87.75%

Table.1 Performance and analysis is summarized

IV. DISCUSSION & CONCLUSION

Computed tomography (CT) with delayed-enhancement images is a highly extensive imaging technique for tissue detection. To our knowledge, deep learning-based methods for endocardial scar detection from cardiac CT images have previously, not been described. This study helps to provide a new platform for future algorithms of scar detection techniques.

ACKNOWLEDGMENT

The author acknowledges support from National Institute of Hospital of Yang-Ming University and this study was also supported by Department of Biomedical Engineering, Chung Yuan Christian University Taiwan.

REFERENCES

[1] Wu KC. Sudden Cardiac Death Substrate Imaged by Magnetic Resonance Imaging: From Investigational Tool to Clinical Applications. Circ Cardiovasc Imaging 2017;

[2] Sun, Yao, and Karl T. Weber. "Infarct scar: a dynamic tissue." Cardiovascular research 46.2 (2000): 250-256.

[3] Ypenburg, Claudia, et al. "Impact of viability and scar tissue on response to cardiac resynchronization therapy in ischaemic heart failure patients." European heart journal 28.1 (2006): 33-41.

[4] Singh, Yashbir, et al. *Effect of left ventricular longitudinal axis variation in pathological hearts using Deep learning*. No. 648. EasyChair, 2018.

[5] Singh, Yashbir, et al. "Cardiac Electrophysiology Studies Based on Image and Machine Learning." 2018.

*Research supported by BME, CYCU, Taiwan.

Machine Learning for comparing the resolution in different Ultrasounds.

Sandra Torres, Prabal Poudel, Alfredo Illanes and Prof. Michael Friebe, INKA, Institute of Medical Technology, Otto-von-Guericke-Universität Magdeburg.

***Abstract*— Ultrasound (US) is a useful method to track the shape and size of thyroid, two things that can give us information about thyroid health. In this context, it is important to compare the accuracies of thyroid segmentation in different US machines to find out if the high price machine achieve better accuracy or not.**

I. INTRODUCTION

Medical images have become a fundamental part of the correct treatment of patients. In this context, Ultrasounds (US) imaging give us an easy way of monitoring some of the organs as in the case of thyroid, where it is fundamental to monitor its shape and the size to diagnose probable diseases. Thyroid segmentation and volume reconstruction are two steps that should be followed to achieve this goal[1]. Taking into consideration the amount of different US systems are on the market nowadays, a compromise between quality and price must be found. Therefore, we want to compare the quality in the different price ranges of the US to see how much the price influences the quality of the thyroid measure.

II. METHODS

Effectively measuring the size and evolution of the thyroid over time imply being able to detect it. Due to the large number of images we have, it will be necessary to use Artificial Intelligence (AI) methods to expedite this procedure, as Machine Learning (ML).

Before training the ML algorithms, we need to extract the images from a DICOM video to have enough information to give to have enough information to feed the CNN. In total, we have sixteen volunteers, and to analyze their thyroid we used for each one four different types of US systems. The second step was extracting the ground truth of those images, differentiating if its thyroid or not depending on if it is black (non-thyroid) or white (thyroid). After that, we divided the image into small patches to analyze each one of them, saving the location, the intensity information from the patch and whether it is a thyroid or non-thyroid patch by comparing with the ground truth. The images had a length of 568 pixels and a width of 455 pixels which implied that to divide it in size of 20x20, some padding was needed.

At this point, the thyroid and non-thyroid regions have different textures, so computing GLCM features gives you the measure of different textures in these regions. These textural features (entropy, homogeneity, shade, energy, contrast, correlation and prominence) were used to train the SVM to classify the different textures in thyroid US images. Also, we used k-means as a ML algorithm to cluster our data into thyroid and non-thyroid.

III. RESULTS

With k-means algorithms we calculated the accuracy for all the patients. In reference to the Support Vector Machine (SVM) algorithm, the accuracy results were not satisfactory, so we decided to omit them.

TABLE I. ACCURACY TABLE FOR K-MEANS

US machines	**Accuracy Patient 1**		
	Correlation	***Shade***	***All***
Chinese US	0.8206	0.8286	0.7243
GE Logiq E	0.5608	0.5588	0.6160
GE Venue 50	0.9194	0.7188	0.7899
GE Logiq E9	0.9303	0.9421	0.7177

Figure 1. Example of accuracy results.

US machines	**Accuracy Patient 1**		
	Homogeneity	***Energy***	***Prominence***
Chinese US	0.3732	0.5514	0.8286
GE Logiq E	0.6895	0.5803	0.7925
GE Venue 50	0.1941	0.2886	0.9112
GE Logiq E9	0.7934	0.4416	0.9421

Figure 2. Example of accuracy results with other features

IV. DISCUSSION & CONCLUSION

In the table, we can see five of the calculated features accuracies and the accuracy of all those features. With these results we can not conclude that a more expensive US will be better than a cheap one for this type of application.

REFERENCES

[1] P.Poudel, "Evaluation of commonly used algorithms for thyroid ultrasound images segmentation and improvement using machine learning approaches"

The effect of viewpoint on fractal dimension of renal vascular tree*

Katarzyna Heryan, *student member IEEE*, Janusz Skrzat, Adrian Goral

***Abstract*— Fractal dimension can be applied to angiography, to evaluate the changes of renal vasculature caused by pathological processes. However, angiograms are 2D representations of 3D structures of varying orientation. In this work, we examined the impact of the spatial orientation of intrarenal vascular tree on the calculated fractal dimension.**

I. INTRODUCTION

Intra-renal blood vessels are commonly diagnosed using angiography. The structure of the kidney's vascular tree can be described by fractal dimension (FD) of the angiogram. FD represents structural complexity which, theoretically, makes it a suitable premise for diagnosis [1]. The main shortcoming of FD is its sensitivity to spatial orientation of 3D structure represented in 2D angiogram. The anatomical studies that propose the use of FD for diagnosis have been conducted *ex vivo*, on corrosive endocasts. The endocasts reproduce the structure of the tree with high fidelity but, unlike a living organ, can be placed in any orientation with respect to the projection plane. Consequently, the structure of the endocast is usually analyzed in a projection that is parallel to the kidney's symmetry plane, and not in the patient's frontal plane, typical for angiography (see Fig. 1). The variation in the FD that results from this misalignment may be greater than any diagnostically relevant difference which brings into question the credibility of such analysis.

The aim of this work is to establish the impact of spatial orientation of a 3D vascular tree on the FD calculated from its corresponding 2D projection. The resulting variability of FD due to spatial orientation is then compared with the estimated change of this parameter that may be a sign of a pathological process.

II. METHODS

A corrosion endocast of the human renal arterial tree was digitized with a micro-CT scanner (Nanotom S, GE) to ensure that the 3D model closely represents the original structure. In order to simulate the projection of an object with varying spatial orientation, the original 3D grayscale images were transformed using 1000 random rotations. This process is equivalent to aligning a fixed structure with 1000 projection axes within a cone (see Fig. 2). Then, the acquisition of the angiogram was simulated by the orthogonal projection of binarized 3D images. The resulting 1000 images were used to calculate the FD, according to the standard algorithm [2].

*This research was supported by the National Science Centre, Poland – NCN PRELUDIUM 2016/21/N/ST7/02351.

K. Heryan and A. Goral are with AGH University of Science and Technology, Dept. of Measurement and Electronics, Kraków, Poland.

J. Skrzat is with the Jagiellonian University Medical College, Department of Anatomy, Kraków, Poland

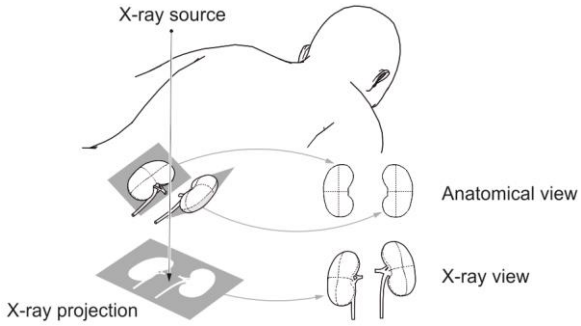

Figure 1. The effect of the projection on the depicted shape of the kidney: anatomical view (endocasts analysis) and X-ray view (angiography).

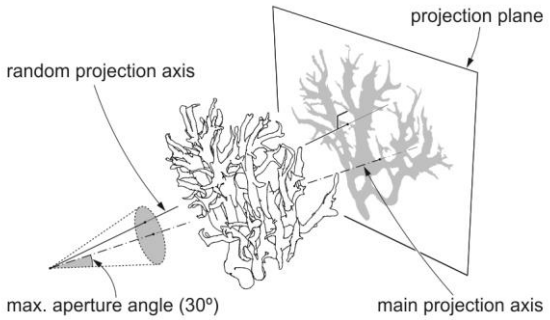

Figure 2. The method used to obtain random orthogonal projections.

III. RESULTS AND CONCLUSION

Depending on the projection axis, FD varied between 1.68 and 1.74. Such variability is significant, considering that a diagnostically relevant difference in FD may be as low as 0.01 [1]. Thus, in some cases, the orientation of the projection axis alone may affect the FD of the angiogram more than a hypothetical pathological condition. This result provokes further questions that will be explored in future studies. First, the experiments need to be extended to a greater number of endocasts to examine the individual variability of FD and to compare it with the variability induced by varying spatial orientation. Larger data volume might also reveal certain patterns, such as the range of spatial orientations that affect the FD the least, a kind of knowledge that can be useful in clinical practice. Lastly, it is necessary to consider the characteristics of imaging devices, such as modality, parameters of the projection, and image resolution affecting FD.

REFERENCES

[1] S. S. Cross, "Fractal geometry of the human renal arterial tree in development, health and disease," in Fractals in Biology and Medicine,. Birkhäuser, Basel, pp. 294-313, 1998.

[2] G. B, So, H. R., So, and G. G. Jin, "Enhancement of the box-counting algorithm for fractal dimension estimation," Pattern Recognit. Lett, vol. 98, pp. 53-58, 2017.

Thyroid Ultrasound Images Synthesis with Generative Adversarial Networks

Onur Gülkokan, Prabal Poudel, *Member, IEEE*

***Abstract*— Thyroid segmentation and volume computation are most important tools used for thyroid diseases diagnosis by tracking the structural changes of thyroid over time. Several deep and machine learning based approaches have been used to segment the thyroid recently. For the machine learning approaches in medical imaging area, diversity and volume of the dataset is a major necessity in this field. It is difficult to obtain large and sufficient images in the medical field due to ethical consideration. However, generating synthetic/fake but realistic images can be a good solution to tackle the data insufficiency in medical imaging field. In this study, we created synthetic thyroid ultrasound (US) images using Generative Adversarial Networks (GANs). Later, several texture patches were extracted manually from the original and synthetic thyroid US images to compare the texture similarities. For this purpose, Mean Squared Error (MSE), Structural Similarity Index (SSIM) and a novel approach based on parametrical modelling was used to compare the texture similarity. The high similarity obtained between the original and computed thyroid images opens the possibilities of using synthetic thyroid US images for training the deep and machine learning classifiers whenever large amount of training images are not available.**

I. INTRODUCTION

Several machine learning based approaches have been used for segmentation of thyroid in US images. However, lack of sufficient data in medical imaging community causes these approaches to produce not highly accurate results. In this study we used deep convolutional generative adversarial networks (DCGANs) to generate synthetic thyroid US images [1]. Later, we extracted texture patches from both original and generated images and compared them using MSE and SSIM. Lastly, a signal based parametrical approach using Autoregressive (AR) modelling [2] was used to compare the similarity between the texture patches from original and generated thyroid US images.

For image synthesis, 2D thyroid US dataset was used. It consisted of 703 thyroid images with image size 752 x 496 pixels. Before training of DCGAN, all images were resized to 256 x 256 pixels. Basic data augmentation methods were applied to prevent overfitting and to improve generalization. For patch extraction and comparison 5 images from original US dataset and 10 images from generated US dataset were chosen. Then from each image, 2 patches were extracted from within the boundaries of the thyroid region to calculate MSE and SSIM values. To compute features based in parametrical approach, 100 images were chosen in total 50 per original and 50 per generated US dataset. From each image, 5 patches were extracted manually within the range of thyroid.

*This work has been funded by Federal Ministry of Education and Research in the context of the INKA Project. [Grant Number 03IPT7100X]. O. G. and P.P are with Otto-von-Guericke University Magdeburg (onur.guelkokan@st.ovgu.de).

II. RESULTS

In this study, MSE and SSIM values were calculated between the texture patches from original and computed thyroid US images. Unlike MSE, SSIM index value was normalized and could vary between -1 and 1, where 1 indicates highest similarity. SSIM was recognized by majority more reliable approach for comparing texture similarity [3]. According to calculations, SSIM comparison values ranged between 0.71 and 0.89 which was very high value for texture similarity. For feature computation, 30 different features were computed from AR parameters per texture patch. It was done using energy ratios for each patch in between different frequencies. In figure 1, distribution of two different features are shown as example.

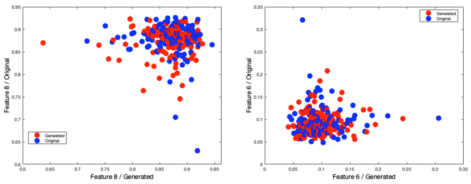

Figure 1. Two AR spectral energy ratios for extracted patches

III. DISCUSSION & CONCLUSION

In this study, thyroid US images were synthesized using DCGAN. Then, three similarity metrics were used to compare the texture between original and generated texture patches. The similarity computation proves that the generated dataset could be used to expand the original dataset.

ACKNOWLEDGMENT

We would like to thank General Electric, USA for providing us with the US machine to conduct our experiments.

REFERENCES

[1] Radford, A., Metz, L., & Chintala, S. (2015). Unsupervised Representation Learning with Deep Convolutional Generative Adversarial Networks. *CoRR, abs/1511.06434*.

[2] Illanes, A., Esmaeili, N., Poudel, P., Balakrishnan, S., & Friebe, M. (2019). Parametrical modelling for texture characterization—A novel approach applied to ultrasound thyroid segmentation. *PLOS*.

[3] Brunet, D. (2012*).* A Study of the Structural Similarity Image Quality Measure with Applications to Image Processing.

Automatic Classification of Contact Endoscopy Images using Artificial Neural Networks Classifier

Nicole Vizhñay Corral[1], Nazila Esmaeili[2], Alfredo Illanes[2], Axel Boese[2], Nikolaos Davaris[3], Christoph Arens[3], Michael Friebe[2].
1. King Juan Carlos University, Community of Madrid, Spain.
2. INKA, Institute of Medical Technology, Otto-von-Guericke University Magdeburg, Magdeburg, Germany.
3. Department of Otorhinolaryngology, Head and Neck Surgery, Magdeburg University Hospital, Magdeburg, Germany.

***Abstract*—As a non-invasive technique, a combination of Contact Endoscopy (CE) and Narrow Band Imaging (NBI) can provide real-time visualization of changes in the structure of blood vessels of laryngeal mucosa. In this study we propose the use of Artificial Neural Networks (ANN) to automatically classify CE+NBI image based on vascular pattern as well as benign and malignant lesions, using a proposed set of features. Four different datasets with 1458 CE+NBI images of 32 patients were used to extract 24 features which describe the level of disorder of vascular patterns. For classification of CE+NBI images based on the vascular pattern, ANN showed an accuracy of 96%. Furthermore, ANN showed an accuracy of 75%, 84% and 86% for classification between benign histopathologies, malignant histopathologies and benign and malignant lesions, respectively. The results prove the ability of the proposed set of features to classify the CE+NBI images using ANN classifier.**

I. INTRODUCTION

Combination of CE and NBI creates a promising optical technique for evaluation of laryngeal lesions by providing real time information of vascular structure and cellular architecture. During recent years, the focus in larynx CE was shifted to the evaluation of vascular patterns, because changes in the structure of these vessels can provide valuable information for surgeons. In a new study [1], a novel approach was proposed to automatically characterize vascular patterns in CE+NBI images and extract a set of features describing the level of disorder of vessel. These features showed robust and acceptable performance to classify CE+ NBI images based on vascular patterns and laryngeal histopathologies, using four different supervised classifiers. The main objective of this work it to go further and use the proposed set of features to train an ANN. ANN as a well-known machine learning based approach is finding many uses in the medical diagnosis application. ANN tries to create artificial models that solve problems difficult to solve using conventional algorithmic techniques. By that, we want to show that the use of features with ANN can obtained acceptable results in comparison to other proposed classifiers.

II. METHODS

Four different datasets were used in this study [1]. Dataset I consist of 1485 images that were labeled into three groups based on vascular patterns. Dataset II include 890 images that were labeled into four groups based on benign histopathologies. 465 image in Dataset III were labeled into three groups based on malignant histopathologies. Dataset IV has 1355 images that were labeled into two groups based on laryngeal lesions. For each image, five indicators were computed after image pre-processing and vessel segmentation. Then 24 features were extracted based on the qualitative properties of these indicators [1]. The classification using ANN was carried out using Python 3.7. First, each dataset was divided into dependent (labels) and independent variables (24 features). Then, each dataset was split into the training and testing sets using 10-fold cross-validation. The Stochastic Gradient Descent Algorithm (SGD) was used as an iterative method to adjust the weights and obtain a minimum cost function and hence an optimal neural network. Some parameters were chosen as the optimum ones: 80 epochs and 2 hidden layers including 12 nodes. Also, a Rectified Linear Unit (ReLU) activation function was used for the activation of the hidden layers. A confusion matrix was computed for the classification scenario and the accuracy, sensitivity and specificity were obtained from it.

III. RESULTS

Following table shows the result of ANN classifier.

TABLE I. CLASSIFICATION RESULTS USING ANN

Datasets	Accuracy	Sensitivity	Specificity
Dataset I	0.9602	0.9571	0.9760
Dataset II	0.7561	0.7479	0.9204
Dataset III	0.8473	0.8477	0.9252
Dataset IV	0.8612	0.8280	0.8787

IV. DISCUSSION & CONCLUSION

In general, there are no notable differences compared to the results of four classifiers proposed in [1], except the results of Dataset II. The created model by ANN is able to classify CE+NBI images based on vascular pattern with an accuracy of 96%. It also can classify CE+NBI images based on benign histopathologies, malignant histopathologies and laryngeal lesions with an accuracy of 75%, 84% and 86%, respectively.

Based on these results, the proposed approach by [1] has the ability to solve the problem of subjective interpretation of vascular pattern in CE+NBI images. It has the potential to operate as an assisting system to help the clinicians make the final decision about the histopathology of the laryngeal tissue in the routine and surgical procedures.

REFERENCES

[1] Esmaeili N, Illanes A, Boese A, Davaris N, Arens C, Friebe M. Novel automated vessel pattern characterization of larynx contact endoscopic video images. International journal of computer assisted radiology and surgery. 2019 Jul 27:1-1.

Nitinol Based Biopsy Needle Design

Asmita S. Doshi, Marwah Al-Maatoq *Member, IEEE*, Marco Kalmar, Axel Boese and Michael Friebe *Senior Member, IEEE*

Abstract— **The proposed work involves the use of Nitinol as a bended tip biopsy needle. Nitinol preforms as the hollow core for tissue sampling. The goal is to show the visibility of the superelastic property of the Nitinol bended needle tip under ultrasound image guidance.**

I. INTRODUCTION

Nitinol (NiTi) is a biocompatible shape memory alloy due to the formation of passive titanium-oxide layer (TiO) which is also present in titanium alloys [1]. The thermoelastic martensitic transformation allows NiTi to inhibit shape memory and superelastic properties [2]. Due to its properties, NiTi has been widely used in medical applications like guide wires, catheters and needles. Especially when it is related with targeting issues [3]. In this paper, NiTi is utilized as a core for biopsy device. The tip of the core has been given the desired shape angle to acquire samples from different locations of the tumor. The performance of the NiTi hollow curve tip was visualized under ultrasound image guiding.

II. METHODS

A 14-gauge NiTi tube (Johnson Matthey Inc., Germany) was used as biopsy needle for tumor size 5 – 10mm. The 15° angle of the NiTi tip was calculated for 5mm tumor size in proposed work. The set-up for bending Nitinol needle tip is shown in Fig. 1.

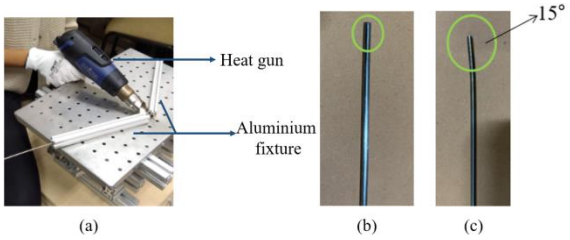

Figure 1: (a) Procedure for bending NiTi, (b) NiTi before bending, (c) NiTi after bending.

The steps for bending NiTi are:

- Insert the NiTi tube into aluminum fixture of desired angle which is 15°.
- Heat the NiTi tube up to 600°C for 90 minutes with Steinel HL 1920 E heat gun.
- Leave the set-up with the NiTi tube inserted for 24 hours to gain the desired angle of 15°.

The NiTi needle with bended tip was fixed in a biopsy device as shown in Fig. 2.

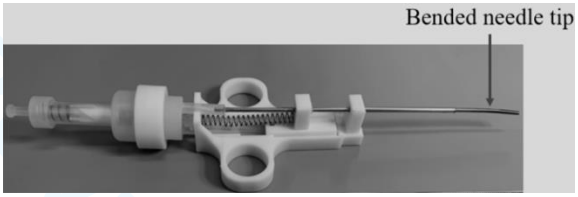

Figure 2: Biopsy device with bended NiTi needle tip.

III. RESULTS

Ultrasound image guidance (GE E6 Ultrasound, Germany) was used for evaluating the performance of bending NiTi core tip at a frequency (f) = 9.0 Hz and Gain (Gn) = 36 of the ultrasound. For this test, the proposed NiTi biopsy needle was inserted inside a gelatin phantom under ultrasound as shown in Fig. 3.

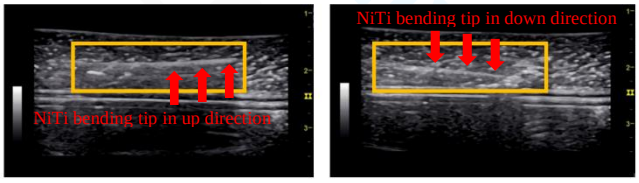

Figure 1: Ultrasound images for NiTi bended tip in gelatin phantom illustrate in two direction.

IV. DISCUSSION & CONCLUSION

In this approach of proposed biopsy device, NiTi material was chosen for inner core biopsy needle as it has the required properties that we are looking for, such as biocompatibility, shape memory effect and superelasticity. Ultrasound findings reported the appearance of NiTi core bending tip with proposed slight angle at two positions in up and down direction. Therefore, NiTi core promised to fulfill the requirement of collecting samples from different areas of the tumor in this proposed work.

REFERENCES

[1] T. Duerig, A. Pelton, and D. Stöckel, "An overview of nitinol medical applications," *Mater. Sci. Eng. A*, vol. 273, pp. 149–160, 1999.

[2] A. Wadood, "Brief overview on Nitinol as biomaterial," *Adv. Mater. Sci. Eng.*, vol. 2016, 2016.

[3] A. Biscarini, G. Mazzolai, and A. Tuissi, "Enhanced nitinol properties for biomedical applications," *Recent Pat. Biomed. Eng.*, vol. 1, no. 3, pp. 180–196, 2008.

* Research is financially supported by the Federal Ministry of Education and Research (BMBF) in context of the 'INKA' project (Grand Number 03IPT7100X and by EFRE funding in context of the ego.- INKUBATOR program (ZS/2016/09/81061/IK)). 01/2015 and Martin Luther University Halle-Wittenberg, phone: 015171982731; e-mail: asmita.doshi@student.uni-halle.de).

Transmission and Visualization of Carotid Auscultation signals in an Android Application

Jahnavi Thimmaiah Cheyyanda, Zeynep Ece Ergin, Thomas Sühn, Michael Friebe

***Abstract*— Carotid Artery diseases occur due to plaque deposition which reduces blood flow to the brain. If untreated, it can increase the risk of stroke, leading to brain damage or death. Currently, carotid auscultation is carried out in the clinical environment. Hence, there is a need for a long-term home-based monitoring system. Health Tracker application is developed in order to control the prototype of the auscultation device in a convenient way. Transmission and communication of the data and control commands between device and smartphone is implemented wireless via Bluetooth. The application allows visualization of audio signals and saving them along with patient data.**

I. INTRODUCTION

Carotid arteries are the large vessels that are located on either side of the neck carrying oxygenated blood to the brain. The narrowing of the carotid arteries can occur due to plaque deposition resulting in reduced blood flow from the heart to the brain. Carotid artery stenosis is considered to be one of the major causes of stroke [1]. Currently, carotid auscultation procedure is being followed for listening to the internal sounds of the body commonly using a stethoscope, an ultrasound or a phonocardiography system. For long-term observation of carotid arteries, there is a need for a remote health monitoring system. The aim of this work is to develop an app-based control interface for a low-cost, computer assisted auscultation device. The audio signal is recorded and transmitted using Bluetooth from an auscultation device to a smartphone. The android application allows the user to visualize and store the audio signal along with patient details [2].

II. METHODS

Raspberry Pi 3 B+ along with the MEMS microphone (SPH0645LM4HB - Knowles Electronics) is used as an acquisition device. The audio signal which is captured via the microphone is saved in the SD card of the Raspberry Pi. On the Raspberry Pi side, a Bluetooth server application is created using the RFCOMM protocol to accept the connections coming from the android phone. A UUID is advertised so that a client knowing the UUID is able to connect to it. When the socket receives a command from the client, the audio file is transferred using Obexftp Service. The user interface on the android application allows managing the Bluetooth features of the phone. The user can connect to the auscultation device and control the transmission of the recorded audio signal. Additionally, by invoking an interrupt, the start and stop of the recording are controlled by the application. The received audio signal is visualized in the time domain. The signal and the corresponding patient details can be stored in a local database of the smart phone organized and analyzed at a late point in time.

III. RESULTS

Mono and stereo audio signals with a bit width of 8 or 16 and a sampling rate of 16 kHz are visualized as shown in Figure 1.

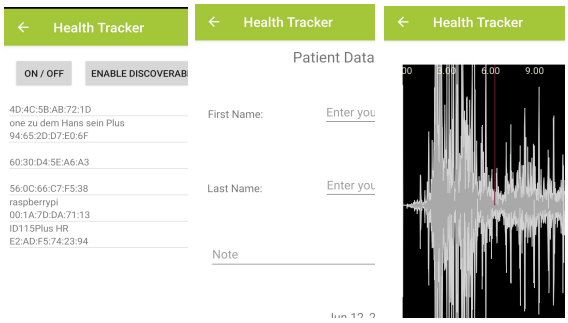

Figure 1. Bluetooth connection, patient data and visualization of signal on the android application.

Real-time transmission and visualization cannot be achieved since Bluetooth API on android supports the devices to only initiate a streaming and does not provide the capability to receive a live stream from a remote device. Other wireless protocols such as Wi-Fi can be chosen in order to have a real-time feature.

IV. DISCUSSION & CONCLUSION

An app-based control interface for a low-cost remote health monitoring system is developed. It enables the patients to track changes in the carotid arteries more frequently in the comfort of their home. When abnormal changes are noticed, the results can be shared with doctors for further analysis.

ACKNOWLEDGMENT

We would like to thank Prof. Dr. Michael Friebe – Chair Catheter Technologies + Image Guided Therapies for the opportunity to conduct this project.

REFERENCES

[1] Flaherty, M. L., Kissela, B., Khoury, J. C., Alwell, K., Moomaw, C. J., Woo, D., … Kleindorfer, D. (2013). Carotid artery stenosis as a cause of stroke. Neuroepidemiology, 40(1), 36–41. doi:10.1159/000341410

[2] Sühn, T.; Mahmoodian, … & Friebe, M. (2019). Computer Assisted Auscultation System for Phonoangiography of the Carotid Artery. Current Directions in Biomedical Engineering 2019 (accepted).

Strategies: Include Cognitive Rehabilitation Training in Daily Life

Mareike Gabele[1,2], Andrea Thoms[3], Steffi Hußlein[2] and Christian Hansen[1]

***Abstract*— The aim of rehabilitation is to use regained skills in daily life. However, in existing software-based training, the improvement of the abilities during training is often set as the focus. Therefore, we propose to combine a medically approved software-based training with strategies that can be learned during training and practiced in the patient's daily life. A feasibility study with 4 patients has shown that the system is perceived as meaningful and the patients are interested in its use.**

I. Introduction and Related Work

Software-based cognitive training is successfully used in the therapy of acquired brain damage. The progress often focuses on the improvement of competences during training. However, the actual goal is to improve and use the skills in daily life [1]. Although some software daily examples are practiced on-screen or in Virtual Reality [2], there is a lack of support in using strategies to solve problems that differ from these examples. This led to the research question 'How to include a system to transfer the software-based rehabilitation training to daily life?' The main contributions of this work are the conceptual and prototypical development of a possible solution and a first feasibility study with patients.

II. Concept and Prototype

We used a medically approved therapy software for cognitive training of verbal memory in clinical use (RehaCom) as a basis. The patient read texts, memorized it and answered multiple-choice questions about the text. We have combined this with the strategy 'Visual Imagination' in a click prototype: The patient imagines a picture of the elements in the text or information received (Figure 1). The strategy is explained in three steps: (1) at the beginning of the training the use of the strategy, (2) after half of training an extension of the strategy and (3) at the end how to train or use it in daily life. Between the steps, the strategy was practiced with examples.

III. Feasibility Study: Methods and Results

We evaluated our prototype in a qualitative feasibility study with 4 patients aged between 17 and 60 years. All had acquired brain damage between and are slightly to moderately affected. They were in phase C to D of the German rehabilitation system and had previous experience in the use of cognitive training. First, we collected disease-related and demographic data. Then, patients used the click prototype during a training session. We asked questions about the subjectively felt effect of the training, understanding and use. These were answered using a Likert scale (1 = strongly agree, 5 = strongly disagree) and open questions. It was shown that the patients understood the strategy (m = 1.5), used it in the training situation (m = 1.5) and want to use it in everyday life (m = 2). All participants stated that they liked to learn strategies and to use them as a working tool in their daily life. It was mentioned that the presented strategy does not help in every situation. However, the enjoyment in this way of training was described as higher than in current training. The division into three steps was perceived as meaningful.

Figure 1: Explanation of how to learn 'Visual Imagination'

IV. Discussion, Conclusion and Future Work

The participants showed both their abilities to use and their interest in using the strategies in daily life. Not only this but also different strategies are needed for different situations. The system can be used as a basis for integrating different strategies and transfer them to daily life. It also may be transferred to different pieces of training and levels of difficulty. The prototype shows the possibility to transfer the learned strategies into daily life. Currently, we build on these results and integrate a sequence of different strategies, like 'PQRST' or 'Learning through processing depth', into existing training exercises. We evaluate this with patients in a comparative study according to the training success parameters and use in daily life.

* This work was funded by the European Regional Development Fund under the operation numbers ZS/2016/04/78123 and ZS/2017/01/83843 as part of the initiative "Sachsen-Anhalt WISSENSCHAFT Schwerpunkte". It was also funded by the European Social Fund (ESF) of Saxony-Anhalt (under the operation number CCI 2014DE05SFOP013) as part of the initiative "Sachsen-Anhalt WISSENSCHAFT Chancengleichheit" with the program title "FEM-Power".

[1] Authors are with the Otto von Guericke University of Magdeburg, Faculty of Computer Science, Germany

[2] Authors are with the Magdeburg-Stendal University of Applied Sciences, Department of Engineering and Industrial Design, Germany

[3] Authors are with the HASOMED GmbH, Paul-Ecke-Straße 1, 39114 Magdeburg, Germany

References

[1] Y. Bogdanova, M. K. Yee, K. D. Cicerone, "Computerized Cognitive Rehabilitation of Attention and Executive Function in Acquired Brain Injury", in *Journal of Head Trauma Rehabilitation*, Vol. 31, Issue 6 , 2016, pp. 419-433

[2] A.L. Faria, A. Andrade, L. Soares, S.B. Badia, "Benefits of virtual reality based cognitive rehabilitation through simulated activities of daily living: a randomized controlled trial with stroke patients", in *Journal of NeuroEngineering and Rehabilitation,* Vol. 13, 2016

Real-time Emotion Detection for Medical and Home Caring

Chao Yan, Bastian Klopfer, Jiahua. Xu

Abstract— Medical diagnosis and caring is an important invention for human diseases treatment and life extension. In recent years, more and more medical equipment has greatly improved the quality of human life. However, there is still much space for improvement, especially in the clinical monitoring of patients with major diseases. It is often impossible for medical workers to acquire in advance the emergency of patients. Based on the integration of medical engineering and artificial intelligence, we propose a patient emotion monitoring and feedback system that can monitor patients' facial expressions in real-time. It predicts those positive or negative emotions and doctors can be given advance reminders so they can provide more effectively care for patients.

I. INTRODUCTION

By a United Nations report from 2017, "it is expected that the number of older persons is expected to double again by 2050, when it is projected to reach nearly 2.1 billion." [1] This development will result in a growing number of people that need to be taken care of and thus in a high demand of caregivers. In recent years, various facial expression recognition (FER) systems have been explored to encode expression information from facial representations. For a real-time detection system, it is usually capturing and processing only a single frame (which can be regarded as an image) from the live-streaming video each time. This paper aims to create an application that can real-timely monitor emotions of patients clinically or homely based on deep learning technology by surveilling the person that needs to be taken care of and recognize dangerous situations. The system consistently predicts the person's emotion based on the facial expression and when the person is feeling unwell for a specified period, it sends out a warning to doctors or family members. The currently available systems do not make use of Computer Vision to make the system smarter or have features to make early warnings. Although the real-time monitoring of parameters such as electrocardiogram, blood oxygen, the respiratory rate which effectively provides clinical decision-making references, it is often impossible for medical workers to acquire in advance the emergency condition. With our system, doctors can get timely reminders and patients can receive corresponding medical treatment as well.

II. METHODS

Several interesting pieces of devices were chosen in order to fulfill "small, easy-portable, high speed" these requirements of the system: Raspberry Pi, Pi Camera and Neural computation stick [2]. In this system, we consider only static image FER, in which the feature representation is encoded with only spatial information from the current single image. And the system consists of two main parts. Face Recognition and Emotion Recognition. The Face Recognition workflow is shown in Figure 1. There are three phases: Data Gathering, Train the Recognizer and Recognition. And The FDR004 model by Intel is implemented to fulfill face recognition task. Only when a known face has been detected successfully in an image will the system continue to do the emotion recognition (ER) task. In conventional FER approaches, the FER is composed of three major steps: (1) face and facial component detection (2) feature extraction (3) expression classification. Deep Learning based FER approaches highly reduce the dependence on face-physics-based models and other pre-processing techniques by enabling "end-to-end" learning to occur in the pipeline directly from the input images [3]. The mode we chose for the system is face-recognition library and Xception CNN Model trained on FER-2013 dataset with more than 35.000 labeled photos [4]. Prototypical facial expressions are labeled angry, disgust, neutral, happy, sad, scared, and surprised among which "Sad", "Angry", "Scared", and "Disgust" are considered negative emotions. This task is solved in our application by processing the emotion label received by the system for each frame. If a negative emotion is detected, the value "1" is stored in an array of specified length. If not, "0" gets stored. For each frame, the next position of the array is addressed. If this sum of values is higher than a certain threshold it means that the monitored person has been in a bad mood for the set time and a warning message should be sent out, see Figure 1.

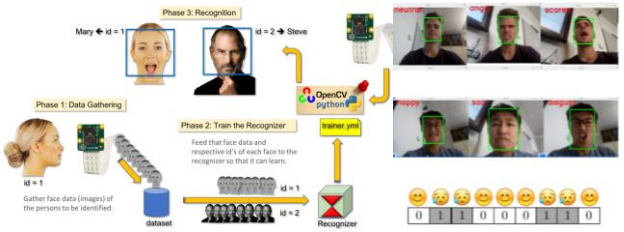

Figure1 [5]. The left part is the workflow of face recognition; the upper right part shows the emotion recognition demonstration of application; the lower right part shows the way of how the trigger of warning works.

III. RESULTS

We proposed this real-time emotion detection and prediction with the deep neural network and implemented it on the Raspberry Pi with NCS, the performance is shown in Table 1. This kind of technology could be implemented later in home or hospital caring. However, due to data limitation, the accuracy of the ER model implemented in the system is not reliable enough. Moreover, it is not guaranteed that patients always look towards the camera. The future work will focus on the trigger for warnings. Whenever an alert is triggered, a photo from the camera should be stored into a specific file in database and sent together with the warning message to the caregivers so they can check the photo to make sure if the situation is urgent or it is a false alarm.

Face Detection Model	FDR004 + NCS
Capture and Prepare Time	0.01s
Face Detection Time	0.06s
Emotion Recognition Model	Tensor Flow only
Emotion Recognition Time	0.03s
Whole Loop Time	0.10s

Table1: the time cost of the each section with or without the help of NCS.

*Research supported by CSC Foundation.

Jiahua. Xu is with the Faculty of Computer Science in University of Magdeburg, Germany, e-mail: Jiahua.xu@med.ovgu.de).

REFERENCE :

[1] World Population Ageing, United Nations, Department of Economic and Social Affairs, 2017.
[2] https://software.intel.com/en-us/movidius-ncs
[3] Walecki R., Rudovic O., Deep structured learning for facial expression intensity estimation, Image Vis. Comput. 2017;259:143–154
[4] Chollet, Xception: Deep Learning with Depthwise Separable Convolutions. arXiv:1610.02357.
[5]https://www.hackster.io/mjrobot/real-time-face-recognition-an-end-to-end-project-a10826

Smart Balance Board for Stability Training and Gaming

Maik Ehses[1], Laureen Polenz[1], Max Joris Hubmann[1]
[1]Otto-von-Guericke-University Magdeburg, Faculty of Electrical Engineering and Information Technology, Germany

***Abstract*— Deep muscles are essential for general health especially when recovering from an injury. One method of enhancing the rehabilitation process is stabilization training, which can be increased by using a Balance Board. This paper introduces a Balance Board, which provides visual feedback on the board and on a mobile phone application.**

I. INTRODUCTION

After an occurrence of a torn ligament or similar injuries it is advised to take physiotherapy to strengthen the affected region and ensure a faster recovery process [1]. This may be achieved by stabilization exercises performed by the patient. The efficiency and intensity of these kind of exercises can further be enhanced by using a Balance Board (BB). Additionally, the usage of a BB activates the musculature in the trunk of a patient and can therefore also improve the posture [2]. Furthermore, it has been shown that especially the Nintendo Wii BB can enhance the condition of children with cerebral palsy [3]. The goal of this paper is to introduce a BB with an accurate positioning system, which can be used by the physician and the patient to check the execution of an exercise.

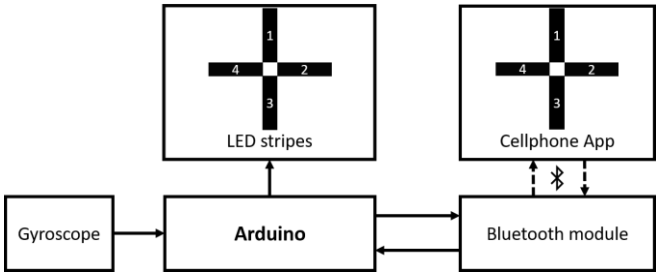

Figure 1: Setup schematic with Arduino Uno R3, MPU6050 gyroscope, HC-05 Bluetooth module and RGB LED stripes.

II. METHODS

The components mentioned in Figure 1 are placed inside of a customary BB casing. The LED stripes are arranged in a cross formation and are responsible for the direct feedback of the slant of the BB. The real time feedback on the app follows the same formation and color codes from the BB's LEDs. This has the purpose that the patient and the physician may observe the slant separately and independently. A further requirement is to implement a game system, so that the patient may have a sense of progress by reaching higher scores while undergoing the physical therapy treatment. The application can be paired with the Bluetooth module to track the training. The Arduino is powered by a Lithium ion battery pack, which can be recharged via an USB cable. It is connected to the gyroscope, from which it receives data about the slant of the BB and processes it. Thereafter, the LED stripes indicate the slant by displaying different color codes. The data is simultaneously sent to the app via the Bluetooth module ensuring the real time display on the app. The game structure provides a variety of exercises, which rewards the user with points depending on the exercise's difficulty and the achieved performance.

* Funding received from Institute of Medical Technology, Faculty of Electrical Engineering and Information Technology, Otto-von-Guericke-University Magdeburg, Germany.

III. RESULTS

To validate the BB a user survey has been carried out. The participants were between 21 and 61 years old with an average age of 29.5 years. Most of the participants gave a positive feedback regarding the general liking, handling and the visibility of the direct feedback. The displayed color codes were found to be intuitively recognizable and differentiable. The main problem was to keep the BB in balance. Another side problem was, that most participants were not overly motivated by a simple high score game but would rather enjoy more complex games like running through a maze.

IV. DISCUSSION & CONCLUSION

The first prototype offers all functionalities that were expected. An adaption to a self-constructed casing with a softer tip will solve the issue of the tough balancing challenge. The current high score game should be complemented by more complex games to ensure the patients permanent motivation. The physiotherapeutic benefits of the presented BB still need to be validated and confirmed by a further case study. Based on those results and in combination with the mentioned improvements a broad usage in the physiotherapeutic field should be targeted, but also an implementation in the gaming industry is conceivable.

REFERENCES

[1] Brooks et al. - Treatment for partial tears of the lateral ligament of the ankle: a prospective trial. BMJ, 1981, 282, 606-607
[2] Szczygieł et al. - The Impact of Deep Muscle Training on the Quality of Posture and Breathing. Journal of Motor Behavior, 2018, 50, 219-227
[3] Gatica-Rojas et al. - Does Nintendo Wii Balance Board improve standing balance? A randomized controlled trial in children with cerebral palsy. Eur J Phys Rehabil Med 2017;53: 535-44.

Vascular Pattern Enhancement and Extraction in Contact Endoscopy Images of Larynx

Nazila Esmaeili (Member, IEEE), Alfredo Illanes, Axel Boese, Nikolaos Davaris, Christoph Arens, Michael Friebe (Senior Member, IEEE)

***Abstract*— Vascular patterns in Contact Endoscopy (CE) + Narrow Band Imaging (NBI) images provide valuable information about the stage of cancer. The use of automatic characterization of vascular patterns in CE+NBI images can solve the problem of subjective interpretation. Vessel enhancement and extraction is the first step toward the automatic characterization. In this study the Jerman filter is applied to CE+NBI images to enhance the vessels and is followed by skeletonization to extract the vessels. The visual and qualitative results showed an acceptable response across all vascular structures.**

I. INTRODUCTION

Laryngeal cancer is one of the most common cancers. As larynx becomes involved in cancer, the organization of blood vessels in tissue goes through changes. Therefore, a high magnification imaging technique is needed to evaluate the changes. Contact Endoscopy (CE) in combination with Narrow Band Imaging (NBI) can visualize vascular structures in the most superficial layer of mucosa. Characterization and evaluation of these structure in CE+NBI images can provide valuable information for the surgeons to find the stage of cancer and to manage the treatment plan. But the interpretation of vascular patterns is a subjective procedure and depends on the experience of surgeons. To solve this issue, an approach was proposed in [1] to automatically characterize vascular patterns in CE+NBI images. A pre-processing step including Frangi filter was first applied on CE+NBI images. Frangi is a multiscale Hessian based filter. The established enhancement function applied in Frangi generally produces a rather poor and non-uniform response for natural variations of vascular morphology. Jerman et al [2] came up with a novel enhancement filter that can solve this problem. As a new pre-processing step, we aim to use Jerman filter on CE+NBI images followed by the skeletonization process to enhance and extract vascular patterns and prepare the images for the automatic characterization process.

II. METHODS

Three test images that represent different vascular patterns in CE+NBI images were selected from Datasets I, used in [1].

Jerman filter is a multiscale Hessian filter using a novel enhancement function which overcomes the deficiencies of Frangi filter and has properties close to an ideal enhancement function. Sigma (σ) and Tau (τ) are two main parameters of the enhancement function in Jerman filter. σ is a vector of scales on which the vesselness is computed. This parameter was set between *0.5* mm to *2.5* mm with the step size of *0.5* mm to cover all the possible vascular structures. τ is a parameter that controls response uniformity. The empirical tests in [2] showed that a value between *0.5* to *1* is the proper value for τ. For that, in this study τ was set as *1*. The resulting image was converted to a binary image followed by the skeletonization procedure using iterative thinning to reduce vessels to one-pixel-wide lines. The algorithm was implemented in MATLAB 2019a.

III. RESULTS

Fig. 1 shows the results of vessel enhancement and extraction for three different patterns in CE+NBI images, using Jerman filter.

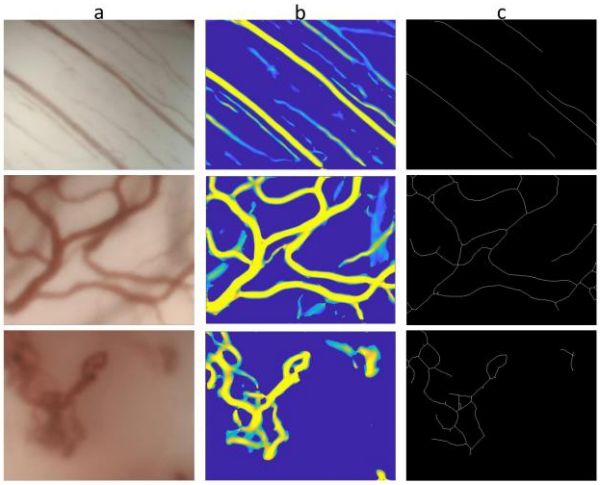

Figure 1. a) Original image, b) Jerman filter, c) Skeletonization.

IV. DISCUSSION & CONCLUSION

In this study, Jerman filter was used for vessel enhancement in CE+NBI images, followed by the skeletonization for vessel extraction. The visual evaluation of Fig. 1.b showed that Jerman filter yielded good segmentation performance in CE+NBI images and has high and uniform response across all vascular structures. In the end, this process resulted in a detailed vessel extraction (Fig. 1.c).

REFERENCES

[1] Esmaeili N, Illanes A, Boese A, Davaris N, Arens C, Friebe M. Novel automated vessel pattern characterization of larynx contact endoscopic video images. International journal of computer assisted radiology and surgery. 2019 Jul 27:1-11.

[2] Jerman T, Pernuš F, Likar B, Špiclin Ž. Enhancement of vascular structures in 3D and 2D angiographic images. IEEE transactions on medical imaging. 2016 Apr 4;35(9):2107-18.

* This work was financially supported by the Federal Ministry of Education and Research (BMBF) in context of the 'INKA' project (Grand Number 03IPT7100X)

Nazila Esmaeili is with INKA, Institute of Medical Technology, Otto-von-Guericke University, Magdeburg, Germany; (e-mail: nazila.esmaeili@ovgu.de).

Proximal Audio Emissions Measurement for Veress Needle Guidance during Laparoscopic Entry

A. Schaufler, A. Illanes, A. Boese, M. Friebe, *Senior Member, IEEE*

***Abstract*— Improved insertion guidance can help avoid injuries during laparoscopic abdominal access. The presented investigation examines whether distal measurement of audio emissions on a Veress needle is appropriate for providing meaningful information for insertion guidance.**

I. INTRODUCTION

In order to perform laparoscopic keyhole surgery, initial access to the abdomen is often done by blind puncture with a Veress needle. This step is the cause of most, and partially life-threatening, iatrogenic injuries throughout the procedure [1]. Numerous sensor-based approaches aim to provide additional guidance information at this stage to minimize the risk. However, the integration of sensors in laparoscopic equipment is always associated with high complexity and cost as well as miniaturization and safety issues. In a recently published approach, audio emissions (AE) are used as a source of information about intracorporeal instrument tip/tissue interactions [2]. AE propagate as slight vibration along the instrument and can be recorded extracorporeally with a sensitive microphone at the proximal instrument end. This study addresses the applicability of this AE approach to laparoscopic Veress needles entry guidance.

II. METHODS

A series of insertions were carried out into a multi-layered phantom consisting of porcine fat enclosed in gelatin with a 120 mm long Veress needle (KLS Martin GmbH, Freiburg, Germany). The insertions were done automatically by means of a material testing system (Zwicki, Zwick GmbH & Co. KG, Ulm, Germany) at a constant speed and a perpendicular angle. The system simultaneously measured the axial forces as reference. A 3D printed adapter attached to the distal needle valve houses the MEMS microphone for AE recording. The setup can be seen on the left of Fig. 1. To allow a clear assignment of events during an insertion, videos of all measurements were recorded.

III. RESULTS

On the right side of Fig. 1, an example of the recorded audio and force curve of one insertion is shown. The layer transitions are indicated by the boundaries B1-B4 in the phantom depicted as well as in the signals. The transitions are between B1) air-gelatin, B2) gelatin-fat, B3) fat-fat separated by a fascia, and B4) fat-gelatin separated by a fascia. The fasciae formed a considerable resistance and simulated significant punctures in the experiment. In the force curve, the punctures of fasciae were identifiable by a pronounced peak. There was a clear increase in transient changes in the audio signal as soon as the needle penetrated into fat. The puncture of the fascia was even more evident by increasing dynamics in the signal. In addition, a strong artifact seen immediately after each fascia puncture was caused by the clicking sound of the inner needle obturator.

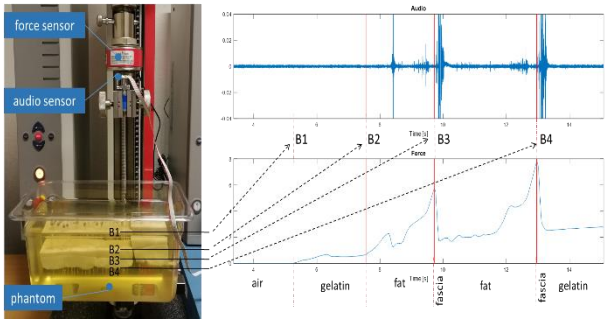

Figure 1. Experimental setup and relation between the needle path trough the specimen and corresponding audio and force signals

IV. DISCUSSION & CONCLUSION

The present study confirms the suggestion that tip/tissue interactions of insertion needles are detectable by proximal recording of the audio emissions. Punctures of major layers are clearly visible in the signal course. The next step will be to use a comprehensive database to define characteristic features of different events in the signal to enable automated position recognition. This is a promising new method of assisting orientation in abdominal access, free from the disadvantages of existing solutions.

ACKNOWLEDGMENT

This research was financially supported by the Federal Ministry of Education and Research (BMBF) in the context of the INKA Project (Grant Number 03IPT7100X).

REFERENCES

[1] G. Ahmad, *Laparoscopic entry techniques*. Cochrane database of systematic reviews, 2015

[2] A. Illanes, "Novel clinical device tracking and tissue event characterization using proximally placd audio signal acquisition and processing" in *Scientific reports*, 1st ed. vol. 8, pp. 1-11.

All authors are with the INKA, Institute of Medical Technology, Otto-von-Guericke University, Magdeburg, Germany; e-mail: anna.schaufler@ovgu.de.

Development of an embedded device for the acquisition of audio signals produced inside human body

Ghazanfar Ali, Ivan Maldonado, Michael Friebe

***Abstract*— The human body produces numerous audio signals, which contain important information about a medical condition. It is fairly challenging to acquire these signals from the human body especially within the noisy operating room environment. Here in this work, a robust, accurate and safe way of acquiring audio signals from the human body is presented. This setup works with the existing INKA audio sensor setups for auscultation, robotic surgery, veress needle penetration and guidewire penetration.**

I. INTRODUCTION

The human body produces numerous audio signals, which contain important information about a medical condition. This information can be used to diagnose or predict potential diseases. For example, listening to the pulse or heart beat via a stethoscope can provide sufficient information to doctors about some specific diseases. Acquiring and processing these signals digitally, may help doctors in prevention and diagnosis of several diseases.

It is fairly challenging to acquire audio signal from the human body especially within the noisy operating room environment. The noise level of devices and other ambient noises degrade the audio signal acquired from the body.

Here in this work, a robust, accurate and safe way of acquiring audio signals from the human body is presented. The proposed device is based on an embedded system and have many capabilities i.e. it can acquire an audio signal from an audio sensor or from any other audio device attached to the body.

II. METHODS

The device communicates with other devices via different protocols i.e. Bluetooth Low Energy, WIFI, I2S and I2C. Selection of these protocols depends on the application, which makes this device highly configurable.

The device has several features like low energy consumption, filtered noise acquisition, wireless data transfer, real-time acquisition and is adaptable to any kind of operating room environment. The device is able to be programmed to perform pre-processing tasks like cyclic redundancy check (CRC) for safety, storage and decimation. The features like decimation, filtration, sampling frequency, resolution and signal size should be easily configurable.

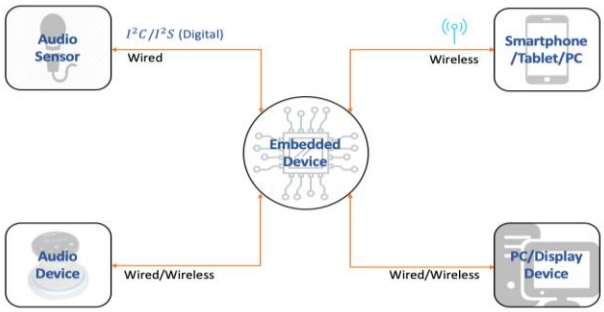

Figure 1. Setup

III. RESULTS AND CONCLUSION

This setup works with the existing INKA audio sensor setups for auscultation, robotic surgery, veress needle penetration and guidewire penetration.

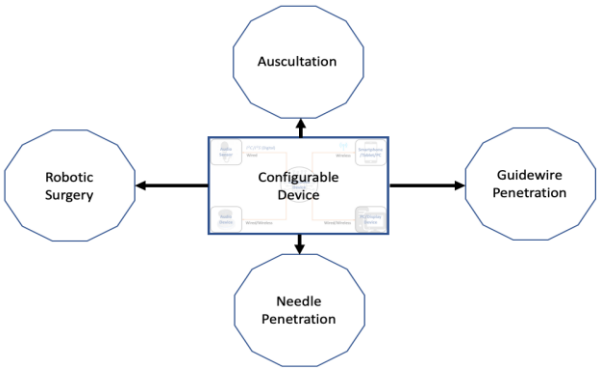

Figure 2. Applications

Retinal Screening Using an Open Source Ophthalmoscope and Deep Learning for Retinal Vessel and Optic Disc Segmentation

Tobias Holmes, Klaus Drechsler

***Abstract*— This paper explores the development of automated retinal screening using an open source medical device for image capture, and convolutional neural networks for semantic retinal image segmentation.**

I. INTRODUCTION

Automated screening devices play a significant role in the development of accessible global healthcare. Especially in regions with few medical professionals.

In this context, an image processing pipeline was developed for use with a handheld open source ophthalmoscope. The aim of this pipeline is to provide an extensible and modifiable base for automated retinal screening. The primary focus was vessel segmentation, as many biomarkers can be derived from retinal vessel shape, diameter or tortuosity [2]. Vessel tortuosity has been associated with diabetic retinopathy (DR) [4] as well as obstructive sleep apnea (OSA) [3]. A machine learning approach was deemed contemporary and appropriate.

II. METHODS

The open indirect ophthalmoscope (OIO) is a handheld retina camera developed at the LVPEI* in Hyderabad, India. It uses a Raspberry Pi, camera module and optic mirror setup.

Images are transferred from the ophthalmoscope via a python socket to a more powerful backend server. Two Unet [1] based convolutional neural networks (CNN) were used to segment the optic disc and retinal vessel tree from the retinal images. Using the equivalent diameter of the optic disc, a ROI is defined between 0.5 and 1 disc diameters from the equivalent disc margin.

After vessel segmentation, an algorithmic calculation of tortuosity is performed on separated vessel braches within the ROI using Equation 1.

$$\tau = L / L_0 = \text{length of vessel / shortest path} \qquad (1)$$

Each vessel branch is then redrawn onto the original image in a colour matching the degree of tortuosity. After augmentation of the original image, it is returned to the OIO and displayed to the operator.

III. RESULTS

Due to the current operational state of the OIO, demo images were used to simulate the use of the image processing pipeline. The complete process requires approximately 25 to 40 s with vessel segmentation requiring approximately 20 to 25 s.

Fig. 1 shows the original retinal image, whereas Fig 2 shows the augmented image with tortuosity colouring. The tortuosity of each branch is displayed appropriately in green, yellow or red, according to local tortuosity in relation to the image average. L_0 is exemplarily given for two vessels.

Figure 1: Original retinal image

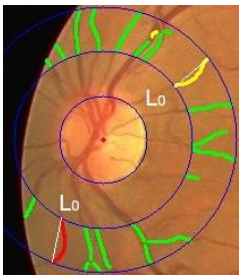

Figure 2: Augmented image

IV. DISCUSSION & CONCLUSION

The diagnostic power of classifying vessel tortuosity by referencing the images mean tortuosity is questionable, as tortuosity usually affects all vessels in a similar manner. However, it would be trivial to replace the classification thresholds to reflect current research on tortuosity values and their relation to various diseases, such as OSA. Threshold values could be obtained from retrospective case-control studies similar to Mohsenin et al. [3].

The use of portable medical screening devices, such as the OIO, in combination with automated image processing enables dedicated medical diagnostics in remote regions and without the need for a medical professional to perform the test. In future, functionality could be expanded by adding further diagnostic modules, such as CNN's for the calculation of the cup-disc ratio or arterio-venous ratio. Moreover, a non-mydriatic OIO is being developed at the FH Aachen.

V. REFERENCES

[1] O. Ronneberger, P. Fischer, and T. Brox. U-net: Convolutional networks for biomedical image segmentation. In Intl. Conference on Medical image computing and computer-assisted intervention, pages 234-241. Springer, 2015.

[2] J. Almotiri, K. Elleithy, and A. Elleithy. Retinal vessels segmentation techniques and algorithms: a survey. Applied Sciences, 8(2):155, 2018

[3] A. Mohsenin, V. Mohsenin, and R. A. Adelman. Retinal vascular tortuosity in obstructive sleep apnea. Clinical ophthalmology (Auckland, NZ), 7:787, 2013.

[4] M. Sasongko, T.Wong, T. Nguyen, C. Cheung, J. Shaw, and J.Wang. Retinal vascular tortuosity in persons with diabetes and diabetic retinopathy. Diabetologia, 54(9):2409-2416, 2011.

* L V Parasad Eye Institute https://lvpmitra.com/oio

Combining Formlabs Resins to cover multiple mechanical properties

Oleksandr Savysko, M.Sc. Marco Kalmar, Dr.-Ing. Axel Boese, Prof. Dr. Michael Friebe

***Abstract* - Most of the 3D printers are not able to print parts out of different materials in one print job. For the Formlabs printers, there are various materials covering different properties available. In this work, a method is explained on how to connect components with different materials (Resin) through their own resin as connector and to test their resilience.**

I. INTRODUCTION

The *Form 2* (*Formlabs, Massachusetts, USA)* is a stereolithographic (SLA) based 3D printer using engineering resins to manufacture prototypes or tools. Layer by layer the UV-laser is polymerizing a liquid resin. After a print job is done the remaining not polymerized resin needs to be removed with an isopropanol bath (Form Wash). The Form Cure is an ultraviolet post-curing system and should be applied after cleaning.

Sometimes it is necessary to create two-component-prints using different resins for special mechanical tasks. The Form 2 is not adapted to print both resins simultaneously. Typical processes to join different parts like drilling or welding are using more space, limiting the design and needs unnecessary time. We tested an approach for combining parts out of different resins by design of connection surfaces and using the resin itself as a glue. To realize that, two material combinations and their properties were evaluated by tensile strength tests.

II. METHODS

This work is based on DIN EN ISO 527-2. Half parts of the tensile specimen are printed in different materials (resin) and treated like recommended by Formlabs [1]. Later on, the parts are connected with either a resin of one of the used materials or instant glue (Loctite 406, Henkel, Düsseldorf).

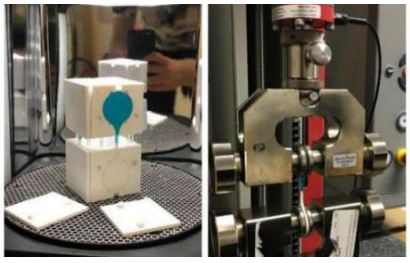

Figure 1. Connection, curing and loading.

To hold the specimen in the correct position while connecting them a holder was designed (Figure 1 left). This holder can keep up to 4 specimens in position at the same time while the connection is curing.

All tensile specimens are tested for their strength with a tensile test machine (Fig.1 right) (500 N Zwicki, Zwick/Roell, Ulm).As test resins four types of *Formlabs* resins (*tough, durable, clear* and *white*) were chosen. These resins cover a spectrum of mechanical properties, from hyperelastic to hard. In total two material combinations were tested. *White* paired with *tough* (pair 1) and *durable* paired with *clear* (pair 2). Each of the combination was fixed either with their own resin or with instant glue.

III. RESULTS

Results revealed that instant glue demonstrates a very unsustainable and weak connection. For example, pair 1 could not even be tested with instant glue, because the connection was destroyed during the installation process. Pair 2 showed significant dissimilarity of results, which could be provoked by the difficult process of joining and the creation of additive areas of connection beside the main connecting surfaces.

All other connections showed that resin itself could be a very effective and useful connector. For example, pair 1 with *white* liquid resin as the connector has tensile stress 26 MPa and with *tough* liquid resin - 20,5 MPa compared to the pure material with a tensile stress of 27 MPa (“Fig. 2”).

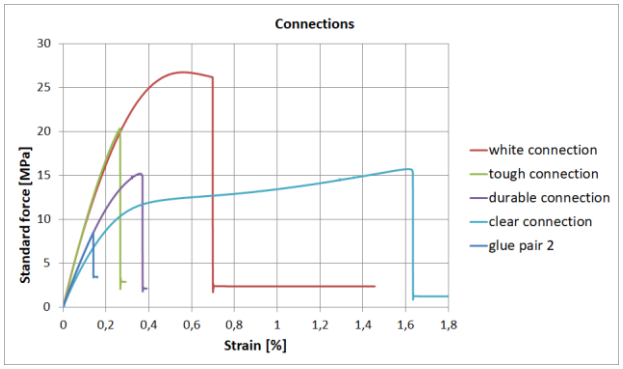

Figure 2. Stress-strain curve of connections.

IV. DISCUSSION & CONCLUSION

Resin itself as a connector of two different materials can be a useful tool to create two component materials. Other than expected the compound is stronger than the compound with instant glue. It provides strong enough connections in comparison with adhesives. However, the advantages lie in the fact that no further materials are required than those already used for 3D printing with the Form2.

V. REFERENCES

[1] Formlabs. Erreicbar: https://formlabs.com/materials/engineering/.

Electrophysiological measurement of the perturbed calcium-phosphate homeostasis in Charophycae *chara braunii*

Pöbel Andreas

***Abstract*—Rare metabolic diseases, like hypophosphatasis, have shown enormous loss in life quality, especially in young children. The experimental setup within this project was designed to examine the electrophysiological behaviour of the calcium-phosphate (Ca-P) homeostasis of armchandelier algae in the target and perturbed state. The transmembrane current in dependence of concnetration perturbation is observed using the voltage-clamp measuring technique. Insight into the transmembrane transport of Ca-P in different milieu is hoped to provide deeper understanding on the deposition of aggregates caused by metabolic disorder of the Ca-P levels.**

I. INTRODUCTION

As the equilibrium state of the human metabolism is perturbed numerous processes in the body are affected. Diseases occur that severely impair the life of the person pertained and reduce the quality of life enormously. This is particularly dramatic in young children, who still have their entire lives ahead. Due to the rarity of hypophospahtasia only limited research is carried out to discover the basic interrelationships [1]. Futhermore the underlying mechanisms are complex and difficult to observe in-vivo. As a result, there is little hope to prevent or cure the diseases in an early stage.
However, the disease is characterized by a perturbed Ca-P equilibrium caused by a the reduced enzyme activity of tissue-unspecific alkaline phosphatases, which is influenced by a gen-defect that occurs already in the early childhood [1]. The consequences include a malformation of the skeletal system or anomalies in the tooth cement but also premature tooth loss [2]. Instead of storing calcium into the bones, calcium pyrophosphate crystals are stored in the muscle tissue, causing rheumatic pain [3]. Similar effects are observed in storage disorders such as gout, essential familiar hypercholesterolemia and amyloidosis [4]. Since the research on the human organism turns out to be extremely complex many influencing factors have to be considered, so that we investigate parts of the Ca-P metabolism in *chara braunii*, a well-studied candelabra alga, which often occurs in European waters. The aim of this project is to establish a measuring-setup designed to observe transmembrane current in different milieu of Ca-P concentration to get insight into the basic metabolic mechnaisms.

II. METHODS

The measurement of the transmembrane electrical potentials and currents of the algae is carried out using the voltage/current clamp technique, which is connected to a computer-controlled high-precision measuring device [5]. On the one hand the transmembrane currents are measured on the algae in its natural, and on the other hand in its perturbed state, where the environment is artificially modified, i.e. with an in-/decreased Ca-P concentration. The recording of the applied transmembrane ion distribution and corresponding currents lead us to a concentration dependent set of membrane current time series that characterise each state.

III. RESULTS

The variety of influencing factors within the calcium-phosphate metabolism makes it difficult to find a set of optimal parameters to start the experiments. This instance lead us to analyse a primary set of pertubed physiological parameters. The natural state, maximum and minimum values for the analysis are shown in table 1. The measured values are successively perturbed from the ground state in the direction of their extreme values.

Tab.1: Parameter perturbtion of the natural homeostasis condition.

state	pH	$Ca^{2+}[mg/l]$	P^{-} $[mg/l]$	Cl^{-} $[mg/l]$
min.	3.8	0.0	0.000	0
natural state [6]	8	50	0.001	50
max.	11.2	536	1.000	3020

IV. DISCUSION AND CONCLUSION

The experimental setup was designed to map the correlations of the target and perturbed state of the homeostatic system. This knowledge will enable us to influence and test disease-related perturbations observed in the human organism and ultimately to bring forward new methods for recovery.

ACKNOWLEDGMENT

I wish to record my deep sense of gratitude to my resesarch supervisor Prof. Dr. Stefan Bernhard, Faculty of Life Science Engineering, THM University of Applied Sciences for his very huge interests, constant encouragement with this work during the research and writing process, to create this paper.

REFERENCES

[1] C. Beck, M. Stenzel, P. Schneider and H. J. Girschick, Hypophosphatasie – Aktuelle Diagnostik und Therapie, vol. 221, 2009.
[2] Ö. Ljunggren and J. Gustafsson, Hypophosphatase 2016, Akademiska Pediatric Hospital.
[3] K.-I. Iida, J.-I. Fukushi, T. Fujiwara, Y. Oda, and Y. Iwamoto, "Adult hypophosphatasia with painful periarticular calcification treated with surgical resection," vol. 30, pp. 722–725, 2012, Journal of bone and mineral metabolism.
[4] C.-P. Adler, Knochenkrankheiten, 3rd ed. Springer-Verlag Berlin Heidelberg, 2005.
[5] B. Gunsé, C. Poschenrieder, S. Rankl, P. Schröeder, A. Rodrigo-Moreno, and J. Barceló, "A highly versatile and easily configurable system for plant electrophysiology," vol. 3, pp. 436–451, 2016, Journal of MethodsX
[6] I. Blindow und K. van de Weyer, "Armleuchteralgen," Springer Spektrum Berlin Heidelberg, 2016.

SPONSORS


SIEMENS
Healthineers


INTERVENTIONAL
systems


VISUS


MR:comp


IEEE Xplore®
Digital Library


sanaone®

Lightweight Residual Network for The Classification of Thyroid Nodules

Nikhila Ponugoti, Sabari Nathan, Elmer Jeto Gomes Ataide , Alfredo Illanes, Dr. Michael Friebe, Srichandana Abbineni

***Abstract*—Ultrasound is a useful technique for diagnosing thyroid nodules. Benign and malignant nodules that automatically discriminate in the ultrasound pictures can provide diagnostic recommendations or, improve diagnostic accuracy in the absence of specialists. The main issue here is how to collect suitable features for this particular task. We suggest here a technique for extracting features from ultrasound pictures based on the Residual U-net. We attempt to introduce significant semantic characteristics to the classification. Our model gained 95% classification accuracy.**

I. INTRODUCTION

The thyroid is one of the endocrine glands, which generates hormones that assist the body to regulate the metabolism and is situated in the throat just below the epiglottis. Ultrasound scans are most often used for the initial diagnoses of thyroid gland abnormalities. Computer-aided diagnosis (CAD) helps radiologists and physicians improve this diagnostic accuracy, decrease biopsy percentage. Fewer researchers are more focused on Image processing and ROI detections in CAD systems, classify the thyroid nodule is still very difficult because of the feature extraction process. Deep network models are good at image classification and object detection tasks. Here we use a Residual U-Net Encoder part for the classification of ultrasound thyroid nodules. We trained the Residual U-net with randomly initialized weights and learned the encoder features based on a segmentation mask.

II. METHODS

In this paper, we used 99 images in those 17 benign and 82 malignant images.We augmented the images using different techniques like flip, blur so totally training (1010 images) and testing (590 images). The proposed network has the properties of the encoder and decoder structure of vanilla U-Net [1]. The input image is passed to coordinate the convolution layer [2], the output of this image passed to the encoders. During down-sampling four blocks are used in the encoder phase. In each block, the first layer is a 3×3 convolutional layers, followed by two residual blocks are added and at the end, 2 × 2 max-pooling layers are attached. In the decoder phase, the same blocks have been used except the max-pooling layer which is replaced with an up-sampling layer. Convolutional Block Attention Module (CBAM) attention layer is connected between Encoder and decoder, the output of the decoder is connected with the softmax layer. Connected the attention layer with Global average pooling for the classification. We trained the models into two parts. Part one is trained U-net with Segmentation and Part two trained the encoder as a classifier with previous weight.

III. RESULTS & DISCUSSION

TABLE I. TABLE RESULT OF TRAINING AND TESTING DATA

	Dataset	Accuracy	Sensitivity	Specificity	Dice
Training	1010	0.945	0.875	1	0.556
Testing	590	0.9507	0.883	0.997	0.5811

Light weight model gained the accuracy of 95% on unseen data with 96% F1 score for the classification of benign and malignant nodules. In this model binary cross entropy loss used to update the encoder weights. Segmentation model weights help to obtain the features from the thyroid region and trained model has 1.3million parameters.

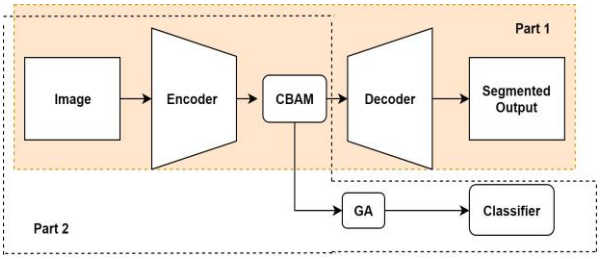

Figure 1. Flow chart of proposed network

IV. CONCLUSION

Compared to other studies we used the lightweight model to improve the feature extraction process for the thyroid nodule classification and Qing Guan et.al [1] proposed inception-v3 method it exhibits the 90% accuracy on validation data. Compared with Inception-v2 [1] model our model is giving higher accuracy.

References

[1]. Guan Q, Wang Y, Du J, Qin Y, Lu H, Xiang J, Wang F. Deep learning based classification of ultrasound images for thyroid nodules: a large scale of pilot study. Ann Transl Med 2019;7(7):137. doi: 10.21037/ atm.2019.04.34

[2].Liu R, Lehman J et.al. An intriguing failing of convolutional neural networks and the coordconv solution. In ANIPS, pp. 9605-9616, 2018.

Single-Image Super-Resolution for Fast 4D OCT Acquisition

Philipp Caspers, Max-Heinrich Laves, Tobias Ortmaier

***Abstract*—We present fast acquisition of 4D optical coherence tomography by upsampling sparse acquisitions with single-image super-resolution. The use of convolutional neural networks (CNN) provides a $4\times$ speed-up in imaging rate while maintaining delicate details in the upsampled images.**

I. Introduction

Optical coherence tomography (OCT) is a 4D (volumes over time) high-resolution trans-sectional imaging modality for biological tissue. Acquisition of a volume requires raster scanning with single depth scans (A-scans). Modern commercially available OCT devices provide an A-scan rate of up to 250 kHz, which translates to a volume rate of ≈ 0.95 vol/s at 512×512 A-scans per volume. This prevents imaging of dynamic processes and limits the potential of 4D OCT.

Prior work has addressed this problem with scan patterns beneficial for acquisition rate (e.g. spiral or Lissajous paths) [1]. While this can reduce dead times in raster scans, the main limitation of the volume rate remains the A-scan rate. In this paper, 4D OCT volume rate is increased by using fewer A-scans per volume and subsequently upscale the volume to full resolution using CNN-based super-resolution (SR) methods, as CNNs have been reported to achieve state-of-the-art performance with highest reconstruction quality.

II. Methods

Two recent deep learning architectures for single image super-resolution were implemented. The first one is based on an autoencoder for real-time semantic segmentation [2], which we modified for the task of super-resolution (SR-AE). The second architecture is the enhanced super-resolution generative adversarial network (ESR-GAN) [3]. The data set was created by keeping every fourth A-scan of pathological retinal OCT scans. We used 20.000 images for the training set and 3.000 for the test set. Both networks were trained to reconstruct the full-resolution image from a single low-resolution image. This corresponds to quadrupling the volume rate of the OCT device. SR-AE was trained with the following loss functions: ℓ_1, ℓ_2, SSIM and a perceptual loss which was achieved by extracting low-level image features from a pretrained VGG-16 network. The perceptual loss delivers the sharpest and most detailed image, but also has the worst contrast. Therefore, we combined the perceptual loss with SSIM and ℓ_2 to achieve the best possible result. ESR-GAN uses a similar combined loss function consisting of an ℓ_1 loss, a perceptual loss and an adversarial loss created by the discriminator, which has led to sharp and detailed reconstructions. The training took about 10 hours on a single NVIDIA GeForce RTX 2070S.

This work has received funding from EU EFRE project *OPhonLas*. All authors are with the Institute of Mechatronic Systems, Leibniz University Hannover, Germany. (e-mail: laves@imes.uni-hannover.de).

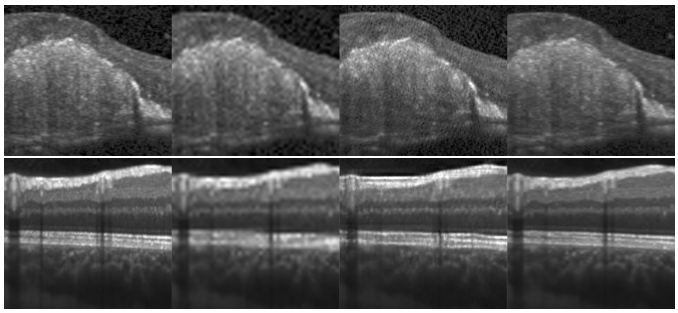

Ground Truth Bicubic ESR-GAN SR-AE

Fig. 1. Qualitative results of two arbitrarily picked test set images.

III. Results

Fig. 1 shows two OCT scans from the test set. Results from bicubic upscaling are given as comparison. ESR-GAN is able to create textures with high sharpness but has problems with replicating the speckle noise and tends to create artifacts. Apart from that, most reconstructions look valid and outperform the bicubic interpolation consistently. SR-AE provides comparable results and does not suffer from artifacts. Although the reconstructions show a slight blur and lack of intensity, they are considerably better than those from bicubic interpolation.

IV. Discussion & Conclusion

In this paper, sparse raster scans and subsequent SR upsampling is discussed to provide $4\times$ speed-up in OCT volume rate. Due to adversarial training, GAN based image reconstruction is prone to *hallucination* of patterns, that are not present in the input image. These artifacts look natural and are not easy to identify. This prohibits the use of GANs for any image reconstruction in medical imaging. SR-AE provides smooth upsamling while preserving details, which was achieved by using a combined loss function.

References

[1] O. M. Carrasco-Zevallos, C. Viehland, B. Keller, R. P. McNabb, A. N. Kuo, J. A. Izatt, "Constant linear velocity spiral scanning for near video rate 4D OCT ophthalmic and surgical imaging with isotropic transverse sampling," Biomed Opt Express, vol. 9(10), pp. 5052–5070, 2018.

[2] E. Romera, J.M. Álvarez, L.M. Bergasa, R. Arroyo, "ERFNet: Efficient Residual Factorized ConvNet for Real-Time Semantic Segmentation," IEEE Trans Intell Transp Syst, vol. 19(1), pp. 263–272, 2018.

[3] X. Wang, K. Yu, S. Wu, J. Gu, Y. Liu, C. C. Dong, Y. Qiao, C. Change Loy, "ESRGAN: Enhanced Super-Resolution Generative Adversarial Networks," IEEE ECCV Workshops, 2018.

Markerless 6 DoF Needle Pose Estimation in 3D OCT

Marc Alexander Kühn, Max-Heinrich Laves, Tobias Ortmaier

***Abstract*—In this paper, markerless 6 DoF needle pose regression from volumetric optical coherence tomography using deep convolutional networks is presented. We achieve sub-voxel accuracy for both translational and rotational degrees of freedom.**

I. Introduction

Optical coherence tomography (OCT) is a cross-sectional imaging modality for biological tissue with micrometer resolution. We envision the use of volumetric (3D) OCT for intraoperative navigation. An important step towards this is pose estimation of surgical instruments within the surgical scene. This enables robot-assisted control of instruments with an accuracy required for e. g. ophthalmic interventions.

Pose estimation in OCT has already been addressed in prior work. Weiss et al. proposed 5 DoF pose estimation using single OCT cross-sections [1]. The manually engineered image features limit their approach to needles and the missing DoF can be problematic for non-cylindric instruments. Gessert et al. have presented 6 DoF pose estimation from volumetric OCT using convolutional neural networks (CNN) [3]. Their results indicate superior performance of machine learning approaches to pose estimation. However, this method relies on the use of an artificial marker within the scene. To overcome this drawback, this work presents markerless 6 DoF pose estimation of a surgical needle in volumetric OCT using 3D CNNs.

II. Methods

We implement two different 3D CNN models based on ResNeXt architecture by Xie et al. [2]. Model A is an adaption of ResNeXt for regression of pose coordinates from 3D OCT data with a resolution of $32 \times 32 \times 32$ voxels. Three stacks of residual blocks are used in this model. In model B the following modifications were implemented [3]. The complexity was reduced by using two stacks of residual blocks and halving the spatial dimension of the input data at the beginning. The early spatial downsampling of the input data allows processing of OCT data with doubled resolution of $64 \times 64 \times 64$ voxels (GPU: NVIDIA Tesla K80 12 GB).

The automated generation of training data with ground truth poses was conducted as follows. An injection needle was placed on a hexapod robot that moves randomly in all six degrees of freedom. Each time the needle reaches a new position, a 3D OCT scan is saved along with the corresponding pose relative to the pivot point of the hexapod. This process is used to generate 5,000 individual scans. The implemented models are trained with an SGD optimizer and an initial learning rate of 0.01. During training the mean squared error (MSE loss) between the estimated pose coordinates and the data labels is minimized. Due to different units between translational and rotational coordinates, two identical neural networks were trained to predict these coordinates separately.

This work has received funding from EU EFRE project *OPhonLas*. All authors are with the Institute of Mechatronic Systems, Leibniz University Hannover, Germany. (e-mail: laves@imes.uni-hannover.de).

III. Results

A test data set was used to evaluate the trained networks. The resulting mean absolute errors (MAE) between the estimated pose coordinates and the data labels for the different model are shown in Tab. I. One voxel processed in model A corresponds to a volume of $156.25\,\mu m \times 156.25\,\mu m \times 93.75\,\mu m$ and one voxel in model B corresponds to a volume of $78.13\,\mu m \times 78.13\,\mu m \times 46.88\,\mu m$. Therefore, model A can estimate the pose with almost the precision of voxel resolution and model B can estimate the pose even more accurately with a precision that is 2–4 times higher than voxel resolution.

TABLE I: MAE results for different models.

Architecture	Mean Absolute Error	
	Translation	Rotation
Model A	$(165.9 \pm 0.06)\,\mu m$	$(0.76 \pm 0.34)°$
Model B	$(23.25 \pm 0.01)\,\mu m$	$(0.15 \pm 0.07)°$

IV. Discussion & Conclusion

This work shows that it is possible to estimate the 6 DoF needle pose with sub-voxel accuracy. Reduced memory demands are demonstrated by early downsampling of the input data, allowing the processing of full-resolution OCT data and further increasing the precision. The inference time of the model is 89 ms, enabling real-time processing of OCT data with an acquisition rate of current high-speed OCTs. In future work, the algorithm can be made more robust by using tissue samples in the background during data acquisition. Different surgical instruments should be evaluated, as our model has been used for the detection of one specific surgical needle.

References

[1] J. Weiss, N. Rieke, M. A. Nasseri, M. Maier, A. Eslami, N. Navab, "Fast 5DOF needle tracking in iOCT," Int J Comput Assist Radiol Surg, vol. 13, no. 5, pp. 787–796, 2018.

[2] S. Xie, R. Girshick, P. Dollár, Z. Tu, K. He, "Aggregated Residual Transformations for Deep Neural Networks," 2017 IEEE Conf Comput Vis Pattern Recognit, pp. 5987–5995, 2017.

[3] N. Gessert, M. Schlüter, A. Schlaefer, "A deep learning approach for pose estimation from volumetric OCT data," Med Image Anal, vol. 46, pp. 162–179, 2018.

Artefact-reduced MRI imaging by using fibre-bundle core based needles

Marwah AL-Maatoq *student Member, IEEE,* A. Boese, H. Henke and M. Friebe *Senior Member, IEEE*

***Abstract*— This study describes a concept for MRI compatible core needles based on a plastic sheet filled with a fibre-bundle core. Standard MRI needles still show huge artefacts in imaging because due to materials interactions with the magnetic field. Different prototypes were built up and compared to a standard MRI core needle.**

I. INTRODUCTION

Positioning core needles into soft tissue is common in minimally invasive procedures. These procedures require accurate placement into a target. Imaging modalities such as magnetic resonance imaging (MRI) and computed tomography can assist placement [1]. Particularly, for core needles that are used in MRI, ferromagnetic materials must be avoided because of the risk of magnetic attraction. Likewise, the visibility in the MRI image is highly important. In this context, standard MRI core needles based on non-magnetic metals are not attracted. However, they still suffer from huge artefacts presenting in the MRI images [2-3]. As a result, they do not allow the precise placement of the core needle. Therefore, a new design for an MRI compatible core needle based on plastic sheet enforced with fibre-bundle (FB) was designed and build up. In order to achieve a sharp tip, one prototype was equipped with a glass tip and a second one with a NITINOL tip.

II. MATERIALS & METHODS

A non-metallic concept based on the combination of different materials was used to formulate the core. The needle core is composed of fibre-bundle (FB) (FibreCableConnect, (FCC), Germany). The fibres are embedded into a matrix from shrink (SH) material. The first core tip was made from sharpened Glass rod (GR) (Hilgenberg, Innovative Glass Products, Germany. The second tip was made from Nickel-Titanium alloy (NiTi) (ITP Innovative Tomography Products, Germany). Both tips are bundled with an outer plastic tube Polyimide (PI) (Vention Medical Andorson, USA). In the sequel, the core needles corresponding to the first and second tip are denoted as the core needle no. 1 and no. 2, respectively, as shown in Fig. 1.

III. RESULTS

To evaluate the proposed core needles, we employ a 3T MRI machine (Skyra, Siemens, Germany). For this operation, we compare their image quality with a standard MRI needle (ITP) based on the produced amount of artefact. Based on the parameters involved in a real MR intervention [3], we use a FLASH sequence t1_fl2d_tra_7m, flip angle = 20, repetition time = 8.6, and echo time = 4. During the MRI-based test, the

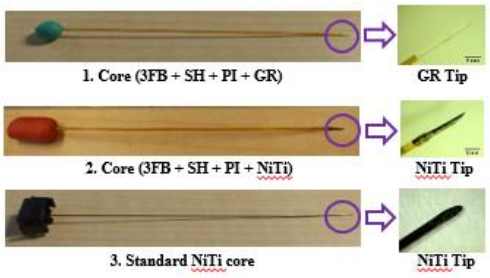

Figure 1: Core needle structures used in the work.

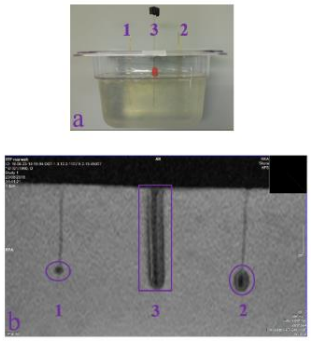

Figure 2: (a) Three core needles, FB based needles no.1 & 2 placed on the sides while the standard core needle is located in middle, (b) MRI image of cores.

three core needles were embedded into a gelatine phantom as presented in Fig 2. The core needle no. 1 appears with an air bubble artefact at the tip. Here, the glass rod tip shows only a linear artefact, whereas the core needle no. 2 shows bigger artefact than the previous one. Nevertheless, it is significantly smaller compared with the standard needle, which produces a huge amount of artefact along with the complete core.

IV. DISCUSSION & CONCLUSION

The proposed core needle concept showed seven times smaller artefacts under MRI test than the standard needle. However, for their use in clinical practice, the proposed approach still needs to be optimized and examine from a mechanical perspective.

REFERENCES

[1] H. H. Quick, "Mr-compatible instruments for interventional mri," in Interventional Magnetic Resonance Imaging. Springer, pp. 35- 51, 2011.

[2] M. Al-Maatoq, J. W. Krug, and M. H. Friebe, "The tip is the key-rfa needle modification using peek for reduced susceptibility artifact in mri," Conference of the international Society for Medical Innovation and Technology, (SMIT), Delft, 2016.

[3] M. Al-Maatoq, A. Boese, H. Henke and M. H. Friebe, Primary Design Concept for Non-metallic Needle for MRI Guided Spinal Applications. 41st International Engineering in Medicine and Biology Conference (EMBC 2019), Berlin. Germany, July 2019.

*Federal Ministry of Education and Research (BMBF) in context of the 'INKA' project (Grand Number 03IPT7100X and by EFRE funding in context of the ego.-INKUBATOR program (ZS/2016/09/81061/IK)).

01/2015. Marwah AL-Maatoq, INKA, Institute of Medical Technology, Otto-von-Guericke University Magdeburg, Universittspl. ; E-mail: marwah.al@ ovgu.de.

A Study on the Classification Performance of Cardiotocographic Data vs. Class Formation Criteria

Patricio Fuentealba, *Student Member, IEEE*, Alfredo Illanes, and Frank Ortmeier

***Abstract*— This work focuses on studying the classification performance of cardiotocographic data in relation to the class formation criterion. For this purpose, we first extract a set of signal features based on CEEMDAN and conventional features. Then, their classification performance is evaluated according to different class formation criteria based on the pH value. Results reveal that the classification performance significantly depends on the class formation criteria, whose best performance is achieved by considering a class formation based on a pH=7.05.**

I. INTRODUCTION

Fetal monitoring during labor commonly relies on the analysis of the fetal heart rate (FHR) and uterine contraction data obtained by a Cardiotocograph (CTG). Currently, the interpretation of such data is difficult because it involves a visual analysis of highly complex signals. For this reason, several approaches based on signal processing and classification have been proposed [1]. Most of the CTG classification approaches use class formation criteria based on the pH value, which is considered as a gold standard measure for postpartum evaluation. However, at birth, the association of a precise value of pH with the neonatal outcome is still inconclusive [2], which makes the classification training a difficult task. In this work, we examine how the CTG classification performs in relation to different values of pH as criteria for the class formation.

II. METHODS

For the analysis, we employ the feature extraction and classification strategy presented in a previous approach [3], where the complete ensemble empirical mode decomposition with adaptive noise (CEEMDAN) method was used. Here, we computed a set of 69 features based on both CEEMDAN and conventional time-domain features proposed in the literature, whose performance was evaluated by using a support vector machine classifier. For more details of the employed feature extraction and classification methodology, please refer to [3].

In this work, the CTG signal classification involves two classes (normal and acidotic cases), which are labeled by using different thresholds of pH values such as 7.05, 7.10, 7.15, and 7.20. Them, we have four different class formation criteria, one for each pH value. Besides, taking into account that there is no precise definition about an optimal *epoch* for CTG analysis [1], we decided to consider different signal lengths just before delivery in the range of 20 and 60 min in steps of 5 min. The analysis was performed using real CTG data extracted from the CTU-UHB Database [4]

* This work was supported in part by the National Commission for Scientific and Technological Research CONICYT, Chilean National Scholarship Program for Graduate Studies.

Patricio Fuentealba is affiliated with the Faculty of Computer Science, Otto-von-Guericke University, Magdeburg, Germany, and Universidad Austral de Chile, Valdivia, Chile; e-mail: patricio.fuentealba@ovgu.de.

III. RESULTS AND DISCUSSION

Table I presents the classification performance achieved for each epoch vs. the used class formation criterion.

Results reveal that the classification performance significantly depends on both the selected pH value for the class formation and the epoch used for feature extraction. In particular, an epoch of 20 min length and a class formation based on a pH=7.05 achieves the higher classification performance (75,63%). Although a pH=7.10 shows a slightly better performance for epochs of 35 and 40 min, according to the obtained average, a pH=7.05 is the optimal criteria for the class formation for the used CTG dataset. However, to validate our results, more investigation is needed, which would include a larger set of formation criteria, different classifiers, and different CTG databases.

TABLE I. CLASSIFICATION PERFORMANCE (%) FOR EACH EPOCH

Epoch (min)	Class formation criteria			
	pH=7.05	**pH=7.10**	**pH=7.15**	**pH=7.20**
20	**75,63**	73,11	67,14	64,01
25	74,25	70	67,68	65,49
30	73,24	72,95	70,43	67,80
35	72,12	72,14	68,89	67,13
40	71,97	72,16	67,33	66,81
45	75,48	72,06	65,97	66,83
50	74,31	70,06	66,39	65,73
55	74,14	69,60	65,55	65,57
60	70,20	68,28	65,16	65,59
Average	**73,48**	**71,16**	**67,17**	**66,10**

REFERENCES

[1] M. Haritopoulos, A. Illanes, and A. K. Nandi, "Survey on cardiotocography feature extraction algorithms for foetal welfare assessment," in *XIV Mediterranean Conference on Medical and Biological Engineering and Computing 2016*, 2016, pp. 1187–1192.

[2] F. Perveen, A. Khan, T. Ali, and S. Rabia, "Umbilical Cord Blood pH in Intrapartum Hypoxia," *J Coll Physicians Surg Pak*, vol. 25, no. 9, pp. 667–670, 2015.

[3] P. Fuentealba, A. Illanes, and F. Ortmeier, "Cardiotocograph Data Classification Improvement by Using Empirical Mode Decomposition," in *41st Annual International Conference of the IEEE Engineering in Medicine and Biology Society*, 2019, pp. 5646–5649.

[4] V. Chudáček *et al.*, "Open access intrapartum CTG database," *BMC Pregnancy Childbirth*, vol. 14, no. 1, p. 16, 2014.

Emphysema classification in low dose computed tomography data based on semi-supervised anomaly detection

Yeshaswini Nagaraj[1,2], Jiapan Guo[1,2], Ludo Cornelissen[1,2], Mieneke Rook[3,4], Hendrik Joost Wisselink[3], Jiali Cai[8], Rozemarijn Vliegenthart[3], Raymond Veldhuis[5], Matthijs Oudkerk[6,7], Peter M.A. van Ooijen[1,2]

Abstract— Emphysema is a type of chronic obstructive pulmonary disease characterized by lung parenchyma destruction. Low-dose computed tomography can be used as an imaging modality for early detection of emphysema. Minimum intensity projection (minIP) on LDCT improves the eminence of subtle changes in the density of the lung parenchyma and hence better characterization of emphysema can be achieved. Here, we propose a minIP with a deep neural network (dnn) model for classification of emhysematous and non-emphysematous scans in LDCT. The proposed model provides an area under the curve (AUC) of 90 % for classification.

I. INTRODUCTION

Chronic obstructive pulmonary disease (COPD) has a high disease burden and is a leading cause of death worldwide. COPD includes emphysema and chronic bronchitis. An important risk factor for COPD is smoking, which also increases the risk for lung cancer. Lung cancer screening with low dose computed tomography (LDCT) can reduce lung cancer mortality [1]. Furthermore, emphysema can be detected in an early stage using LDCT. Lung cancer screening leads to large amounts of LDCT scans, which makes visual to detect emphysema a time-consuming process. We introduce a minIP based dnn model for automatic classification of emphysematous and non-emphysematous participants in LDCT scans.

II. MATERIALS & METHODS

We included 103 LDCT scans from participant of the population-based study "ImaLife"*. Each scan was annotated as emphysematous or non-emphysematous by two experienced radiologists and a medical trainee for this study. Slice numbers were specified to indicate the presence or absence of emphysema. The scans were pre-processed with and without minIP (Fig. 1). A generative adversarial network-based anomaly detection (GANomaly [2]) model was trained to classify tissue in being emphysematous or not. The model performs classification on participant-level, such that to classify a participant as negative, all slices considered from the scan had to be classified as non-emphysematous. The network was trained with 53 non-emphysematous scans from the 103 included scans, 30 scans were used for validation (15 emphysematous and 15 non-emphysematous) and 20 (10 emphysematous and 10 non-emphysematous) for testing.

III.RESULTS

The cross-validation with and without minIP yielded an area under the curve of 0.90 [95% CI = 0.87-0.91] and 0.80 [95% CI = 0.77-0.83], respectively. The independent test set with minIP resulted in a participant-level classification sensitivity of 100% [95% CI = 63.06% - 100.00%] and specificity of 83% [95% CI = 51.59% - 97.91%], for classification of emphysematous cases.

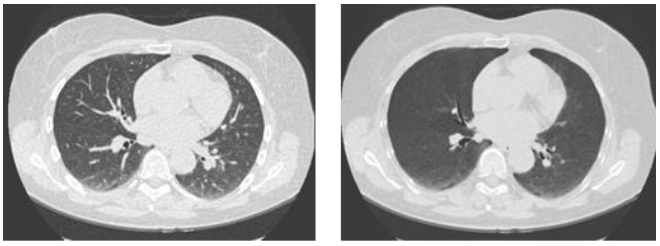

(a) (b)

Figure 1 Fig.1 Example of axial slices of LDCT scans before (a) and after (b) minIP.

IV. DISCUSSION & CONCLUSION

Our proposed model accurately classifies non-emphysematous LDCT scans, thereby potentially reducing visual inspection time required for non-emphysema detection. Our minIP based model can also be a potential computer aided tool for screening of emphysema.

REFERENCES

[1] D. R. Aberle *et al.*, "Reduced lung-cancer mortality with low-dose computed tomographic screening.," *N. Engl. J. Med.*, vol. 365, no. 5, pp. 395–409, 2011.

[2] S. Akcay, A. Atapour-Abarghouei, and T. P. Breckon, "GANomaly: Semi-supervised Anomaly Detection via Adversarial Training," in *Lecture Notes in Computer Science (including subseries Lecture Notes in Artificial Intelligence and Lecture Notes in Bioinformatics)*, 2019.

AFFILIATIONS

[1] University of Groningen, University Medical Center Groningen, Department of Radiation oncology, Groningen, The Netherlands
[2] University of Groningen, University Medical Center Groningen, Machine learning lab, DASH, Groningen, The Netherlands
[3] University of Groningen, University Medical Center Groningen, Department of Radiology, Groningen, The Netherlands
[4] Martini Hospital Groningen, Department of Radiology, Groningen, The Netherlands
[5] University of Twente, Faculty of Electrical Engineering, Mathematics & Computer Science (EWI), Data management & Biometrics (DMB). Groningen, The Netherlands.
[6] University of Groningen, Faculty of Medical Sciences, Groningen, The Netherlands.
[7] Institute for DiagNostic Accuracy Research B.V., Groningen, The Netherlands.
[8] University of Groningen, University Medical Center Groningen, Department of Epidemiology, Groningen, The Netherlands

Robotically customizable thermal ablation volumes

Iwan Paolucci, Jan Hermann, Raluca-Maria Sandu, Daniel Candinas,
Pascale Tinguely and Stefan Weber, *Member, IEEE*

***Abstract*— Stereotactic percutaneous ablation is a fast advancing modality for treatment of tumors in soft solid organs such as the liver, kidney and lung. Ablation needles typically deliver ellipsoidal shaped ablation volumes varying in size as a function of ablation time and power. As a result, irregularly shaped tumors can only be ablated by delivering volumes significantly larger than the target itself or by the use of several needles. In this study, we have investigated the possibility of creating ablation volumes with configurable shapes through synchronous modulation of ablation power and applicator position, in an ex-vivo porcine liver model.**

I. INTRODUCTION

Thermal ablation of liver tumors of less than 30 mm becomes more and more standard for these cases. In most recent studies, tumor size of > 30 mm has been reported to be a risk factor for recurrence [1], [2]. Furthermore, irregularly shaped tumors have to be ablated with a large margin, which involves ablating large portions of healthy tissue. Due to the drastically increased quality of life for patients who undergo an ablation vs a resection, we aim to develop the procedure and the technology further to accommodate tumors irregularly shaped or larger than 30 mm. The shape of an ablation can be increased laterally by using parallel needles. However, there currently exists no reproducible way of increasing the size longitudinally, which is a prerequisite for fully customizable ablation shapes. One possibility to achieve this would be to dynamically modulate the energy level in space, time.

In this exploratory study, we investigated the possibility of achieving a superposition of ablation zones by modulating the energy level depending on the position along a trajectory using robotic technology in an ex-vivo study.

II. METHODS

In an ex-vivo experiment, we evaluated whether a superposition of ablation zones can be achieved by synchronously moving the ablation needle and modulating the energy level. Therefore, we created ablation profiles where the applied energy depends on time and location. These dynamic ablation profiles were then applied to ex-vivo bovine livers using an interventional robotic platform (Figure 1), which moves the ablation needle according to the planned profile. The energy was set manually on the ablation device according to the profile using the provided timer on the screen. After the ablation profiles were applied, we dissected the specimens along the needle trajectory to visualize the resulting ablation zones.

Figure 1: Interventional robotic platform consisting of an ablation and a surgical robotic device, moving the needle through the specimen.

III. RESULTS

In this study, we have performed 8 ablations in ex-vivo bovine liver with different ablation profiles (Figure 2). The profile with two stationary ablations produced two spherical ablation shapes (left). The profiles with a constant energy over a path (center) produced an almost rectangular ablation shape, and the increasing/decreasing energy (right) yielded a large elongated ellipsoid.

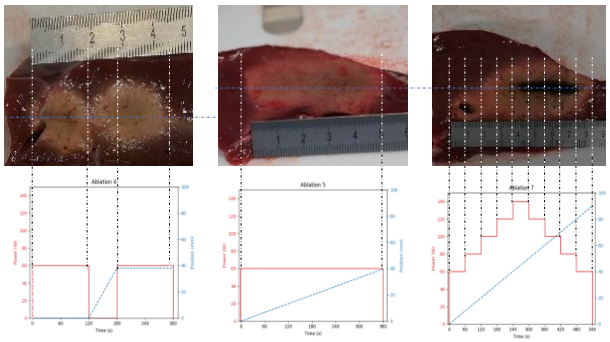

Figure 2: Results of three different ablation profiles

IV. DISCUSSION & CONCLUSION

Dynamic energy delivery during ablation procedures using robotic technology could achieve reproducible large or irregular ablations customized to the tumor shape. However, more investigation is needed to confirm these findings, as this was a rather exploratory analysis.

REFERENCES

[1] M. Beermann *et al.*, "1000 consecutive ablation sessions in the era of computer assisted image guidance – Lessons learned," *Eur. J. Radiol. Open*, vol. 6, pp. 1–8, Jan. 2019.

[2] K. S. Ahn and K. J. Kang, "Appropriate treatment modality for solitary small hepatocellular carcinoma: Radiofrequency ablation vs. Resection vs. Transplantation?," *Clin. Mol. Hepatol.*, Apr. 2019.

I. P., J. H., R. S., and S. W. are with the ARTORG Center for Biomedical Engineering Research, University of Bern, Bern, Switzerland;. D. C. and P. T. are with the Department of Visceral Surgery and Medicine, Inselspital, Bern University Hospital University of Bern, Bern, Switzerland

Adjustable Bone Plate Design

G. Huri[1], M.N. Doral[2], O.S. Bicer[3], O. Demirak[4], P.Y. Huri[4]

***Abstract*— One of the most important factors affecting success of treatment in bone fracture and bone defect is closeness of the fracture ends. None of the bone plates currently used allow shortening and lengthening, requiring refixation and repeated drilling and screwing operations. We have presented the potential of the new generation dynamic bone plate for use in future clinical applications.**

INTRODUCTION

Surgical treatment of bone fractures may be made by various devices such as intramedullary nails and external fixators[1]. However, traditional external fixators and intramedullary devices causes pain and provides large residual scars and can cause severe complications such as failure of lengthening mechanism and migration of locking screws[2]. Additionally, existing plates allows only 2 mm compression in the fracture line and not any further distraction. It may cause the surgery period becomes 2 or 3 times longer[3]. This situation results in a similar increase in the duration of anesthesia in a patient, and risks of complication as well[4].

Based on these requirements and knowledge, we have produced a new adjustable bone plate that replaces the attractive qualities of expandable intramedullary nail as well as external fixator device by minimalizing the risk of deep infection and no damage to growth plates.

METHODS

Plate prototypes were produced matching the dimension requirements of the sheep tibias. 3D design of the plates was made on *Solidworks* and the static, dynamic and fatigue analysis were conducted in *silico*.

Adjustable bone plate (ABP) is composed of static and dynamic parts. Static part is fixed to the bone with its proximal screws (Figure 1). Dynamic part is fixed with its special screws to the bone. Osteotomy is performed between the closest screws in the static and dynamic part or fracture site is adjusted.

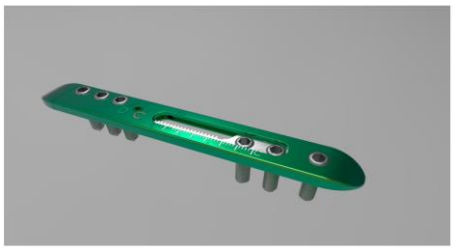

Figure 1. ABP showing static and dynamic parts. Distraction obtained with sliding in D direction, while compression is achieved in C direction.

Biomechanical properties of the plates were assessed with ASTM F382 static compression and dynamic test.

Adjustable bone plates were evaluated on the segmental tibia defect of the sheep. Radiological evaluation was performed in order to evaluate the regeneration efficiency of the fracture site and the bone union. Histopathological evaluation was performed to observe tissue response and bone regeneration at the bone-plate interface.

RESULTS

Mean displacement, mean compressive bending yield load, mean bending strength, mean bending stiffness, mean bending structural stiffness, mean peak load and mean displacement at peak load according to ASTM static compression test are shown in Table 1. No fractures occurred during four point bending test. Radiological evaluation revealed that the free bone segment was completely transferred at the proximal direction throughout the defect. Histopathologic evaluation validated formation of the healed bone at 12th week.

TABLE I. RESULTS OF BENDING PROPERTIES OF ABP

.

Specimen	Displacement at yield (mm)	Compressive bending yield load (N)	Bending strength (Nm)	Bending stiffness (N/mm)	Bending structural stiffness (Nm²)	Peak load (N)	Displacement at peak load (mm)
1	4.231	1417.809	25.52056	335.126	26.928	1617.66	5.00
2	4.221	1365.419	24.57754	323.467	25.991	1570.78	4.99
3	3.985	1356.665	24.41997	340.443	27.355	1585.38	5.00
4	4.295	1425.981	25.66765	332.028	26.679	1615.15	5.00
5	4.381	1552.277	27.94099	354.330	28.471	1729.70	5.00
6	4.229	1484.468	26.72043	350.988	28.202	1614.31	4.68
Average	**4.224**	**1433.770**	**25.80786**	**339.397**	**27.271**	**1622.16**	**4.94**
S.D.	0.132	74.225	1.33605	11.702	0.0940	56.014	0.130

DISCUSSION & CONCLUSION

ABP successfully transferred 14.6±1.2 mm bone segment on sheep tibia model without any complications. This result validated our hypothesis. Unique designs of ABP not only allows distraction in the osteotomy site but also has the ability of compression. It is thought to be used in fracture treatment by using its adjustable compression utility.

References

[1] Hernigou, P. and J. Pariat, History of internal fixation (part 1): early developments with wires and plates before World War II. Int Orthop, 2017. 41(6): p. 1273-1283.

[2] Novikov, K.I., et al., Cosmetic lower limb lengthening by Ilizarov apparatus: what are the risks? Clinical orthopaedics and related research, 2014. 472(11): p. 3549-3556.

[3] Rouhi, G. and M. Amani Hamedani, A BRIEF INTRODUCTION INTO ORTHOPAEDIC IMPLANTS: SCREWS, PLATES, AND NAILS. 2012.

[4] Bilen, F.E., et al., Fixator-assisted nailing and consecutive lengthening over an intramedullary nail for the correction of tibial deformity. Vol. 92. 2010. 146-52.

* This project is funded by The Scientific And Technological Research Council of Turkey (TEYDEB-1511) (Project No: 1150410).

Beyond Tool Motion Analysis: Exploring Potential Innovations for Augmenting Laparoscopic Surgery Skill Analysis and Training

Harold Jay M. Bolingot, Tomohiro Shibata

Abstract— **Laparoscopic surgery requires extremely precise and careful hand-eye coordination due to the nature of the procedure. The laparoscopic interface demands an intensive learning curve to ensure that surgeons are capable of conducting the correct actions during an operation. Currently, tool motion analysis is the prevalent system component in automatic skill assessment systems for laparoscopy training. However, overall surgical competency is not just dependent on the quality of tool motion, but also takes account of certain criteria such as tissue handling and resilience through long hours of operation. This work presents a brief exploration of potential innovations for future laparoscopy skills training and analysis beyond the framework of tool motion analysis.**

I. Introduction

The increasing demand for laparoscopy operations brought by the benefit of less trauma to patients demanded more sophisticated and scalable ways of cultivating the right laparoscopy skills to future surgeons. Modern systems for laparoscopy training have since emerged, with the example CGI simulators for training of different kinds of laparoscopy operations, and physical simulators that consists of plastic-based representations of tissues and hardware tools for practice. In most of these modern systems, tool motion analysis has become integral. It refers to the visual and/or kinematic tracking of tool use during laparoscopy training and operations, through which the performances of novices are evaluated by comparing them to the performances achieved by experts, thus quantitatively defining a rubric for high quality tool motion.

But in accordance with the officially accepted standards for laparoscopy skills, achieving high quality tool motion on its own is inadequate to achieving overall excellent surgical competency [1]. The Objective Structured Assessment of Technical Skills (OSATS) and Global Operative Assessment of Technical Skills (GOALS) are two standards that are used in certifying surgical competency. Based on an analysis of the criteria covered by tool motion analysis in these two standards, emphasizing the quality of tool motion alone does not capture meaningfully well the overall capacity of a surgeon in performing laparoscopy [1].

II. Methods and Implementation

Two potential methods are proposed to improve the overall automatic skills training and assessment framework for laparoscopy: surfaced-based EMG (sEMG) analysis [2], and automatic visual inspection [1].

sEMG analysis refers to the recording and analysis of the state of muscles of the surgeon for identifying how much the muscles have fared throughout the laparoscopy training regime, and detecting instances of muscular fatigue which can severely affect the performance of surgeons throughout their career [3]. An implementation is demonstrated in [2] that used the Myo Armband to track the forearm muscle fatigue during repetitive trials of a modified peg transfer exercise. The Myo Armband consists of eight surface-based EMG electrodes and an IMU module packaged in a wearable band.

Automatic visual inspection refers to the visual analysis of the surgical objects and actions performed on the surgical field view. This entails the simultaneous recognition and tracking of surgical tools and tissues, and programmatically ascertaining whether the correct action is performed as well as whether the desired outcome is attained. An implementation is demonstrated in [1] that used deep learning-based instance segmentation to detect the pegs and tools during peg transfer exercise that was set up on a 3D-printed box trainer. The instance segmentation method was based on YOLACT, which achieved 61.09 mAP on bounding box accuracy and 39.71 mAP on masks accuracy.

III. Discussion and Conclusion

By artificially inducing fatigue to the forearms, it has been demonstrated that the EMG data from the Myo Armband is reliable enough to recognize the effect of forearm fatigue on the subject's performance on the peg transfer exercise. For automatic visual inspection, the work demonstrated the use of deep learning to accurately classify the objects in the surgical training scene, for the purpose of visually inspecting the states of those objects. These two frameworks for surgical skill understanding are potential augmentations to the current state of laparoscopy training.

H. Bolingot and T. Shibata are with the Graduate School of Life Science and Systems Engineering, Kyushu Institute of Technology, Kitakyushu City, Fukuoka Prefecture, Japan 808-0196, phone: +818087082109; e-mail: bolingot.harold681@mail.kyutech.jp).

References

[1] H. J. Bolingot, "Automatic Visual Inspection in a Laparoscopy Box Trainer using a Deep Learning-based Object and Motion Tracking System," *Thesis*. Kyushu Institute of Technology, Kitakyushu City, Fukuoka Prefecture, Japan, 2019.

[2] H. Bolingot et al., "Simulated Laparoscopic Training and Measurement Systems Based on a Low-Cost sEMG and IMU Armband," presented at the 39th Annual International Conference of the IEEE Engineering in Medicine and Biology Society, Jeju, South Korea, 2017.

[3] D. A. G. Reyes, B. Tang, and A. Cuschieri, "Minimal access surgery (MAS)-related surgeon morbidity syndromes," Surg Endosc, vol. 20, no. 1, pp. 1–13, Jan. 2006.

Polymer bonding approach in microfluidics for organ-on-a-chip applications

L. Bakhchova, N. Sajwani and U. Steinmann

***Abstract*— Organs-on-a-chip are microfluidic devices made for the cell culture and emulating *in vivo* conditions. Structures designed for the organ-on-a-chip applications require single or a number of closed microfluidic channels. This paper presents an experimental study of obtaining microfluidic structure from Polydimethylsiloxane and Polycarbonate and shows bonding approach for these materials.**

I. INTRODUCTION

Polydimethylsiloxane (PDMS) is a flexible, transparent and highly hydrophobic polymer. There are microfluidic structures made of PDMS for cell-growing into vessels, tissues and spheroids [1, 2]. It is possible to separate two types of the cell tissues by a thin membrane or layer of polymer. Such membrane can be obtained from the chip-body material itself or any other, which is bondable to it. One typical material is polycarbonate which is biocompatible, flexible and durable. One of the possible microfluidic configurations for the organ-on-a-chip is a "sandwich" structure of two PDMS channels divided by 12 µm thick porous polycarbonate membrane [2].

II. METHODS

The master structures were done by standard soft lithography with photoresist SU-8 on 4' silicon wafer. The PDMS structured layers were made by molding technology. The mixing ratio of PDMS (Dow Sylgard 184 Elastomer) and curing agent was 10:1 respectively. After 48 hours, cured PDMS layers were released from master wafers, cut and the holes for inlets and outlets were done by biopsy punch 1.5 mm. On the flat area around the channel the liquid PDMS was applied with brush and stencil. The polycarbonate membrane (Sterlitech Inc.) with pore size 1 µm was applied on top and left for 10 min to allow liquid fill the pores. The next curing was done on ceramic hot plate at 80 ˚C during 15 min. Once the PDMS on membrane was cured and surface was activated with O_2 plasma (1 min., 0.5 mbar, 100 W), two structured parts were brought in contact. To achieve a robust bonding the device was backed on ceramic hot plate 10 minutes at 80 ˚C. The chips were characterized by optical microscopy, scanning electron microscopy and leakage test.

III. RESULTS

The microfluidic "sandwich" structures contain 2 channels with 100 µm width and 50 µm height each. They are divided by the polycarbonate membrane. The photo and 3D CAD model of the prepared device are shown on the Fig. 1. Due to the fact that PDMS has high viscosity (5500 mPas, and after mixing with curing agent 4000 mPas), using it as an adhesive layer, which has to fill pores of the polycarbonate membrane with pore size less than 0.4 µm is not efficient. The reason is that as long polydimethylsiloxane cannot fill the pores, the robust connection to the membrane cannot be made without extra adhesion coating or chemical surface modification. Filling 0.1 µm pores was possible by mixing PDMS with Isopropanol (1:2). Once the PDMS was cured there, both surfaces are bondable to the structured top and bottom parts of the chip. The results of the leakage test show stability of the device during constant pumping water based solutions through the channel. Flow rate was increasing from 1 µl/min to 50 µl/min.

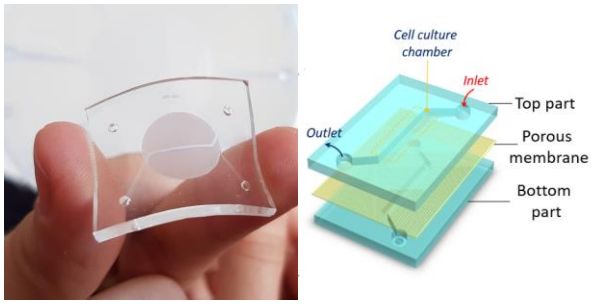

Figure 1. Photo and schematic view of the obtained microfluidc structure.

IV. DISCUSSION & CONCLUSION

Biocompatible polymers show big potential for obtaining stretchable, flexible and reliable microfluidic structures, which, in turn, help to emulate in vivo conditions.For this, a tight bonding of all parts under typical process conditions and for a sufficient time frame is necessary. Once a chip is verified accordingly, the cell culture can be proceeded from few hours to several days in line with e. g. drug testing experiments and fluorescence measurements.

REFERENCES

[1] K.-J. Jang, A. P. Mehr, G. A. Hamilton, L. A. McPartlin, S. Chung, K.-Y. Suh, D. E. Ingber, "Human kidney proximal tubule-on-a-chip for drug transport and nephrotoxicity assessment" in *Integr. Biol.*, vol. 5, 2013, pp. 1089-1198.

[2] A. U. R. Aziz, C. Geng, M. Fu, X. Yu, K. Qin, B. Liu, "The role of microfluidics for Organ on Chip simulations" in *Bioengineering*, vol. 4, issue 2, 2017.

L. Bakhchova is with Otto-von-Guericke University, Magdeburg, 39104 Germany, phone: 003916757238; e-mail: Liubov.bakhchova@ovgu.de).

Intraoperative Distance Estimation using AR-Visualization and Auditory Display

Gerd Schmidt[1], David Black[1,2], Florian Heinrich[1], Christian Hansen[1]
[1] *University of Magdeburg, Faculty of Computer Science & Research Campus STIMULATE, Germany*
[2] *Fraunhofer Institute for Digital Medicine MEVIS, Germany*

***Abstract*— Instrument placement in intraoperative environments demands accurate estimation of distance between surgical tools and obstacles. In this work, AR visualization concepts were combined with real-time auditory display. A pilot study showed that enhancing AR visualization with auditory display provided qualitative and quantitative advantages but showed differences in the acceptance of simple and complex auditory display.**

I. INTRODUCTION

An accurate estimation of distance from surrounding structures in intraoperative environments is essential. Information should optimally be displayed within the user's field of view; otherwise, complications with hand-eye coordination may arise [1]. Our previous work evaluated various AR visualization concepts using a Microsoft HoloLens [2]. Distance information was virtually displayed at the tip of a tool. Our separate previous work [3] also focuses on the use of auditory display (real-time sound guidance) to aid placement of medical instruments. In the current work, we combine these promising concepts and evaluate AR visualization with two novel auditory methods.

II. METHODS

The distance sensor visualization consists of 2 elements. The first visualizes distance between obstacles and the tip of a tool with a pointer. This pointer starts at the tip and continues along the main tool axis and its color is interpolated according to 3 proximity ranges (green > 10 mm; yellow > 5 mm; red < 5 mm). For larger distances, the ray is shaded by stripes every 5 mm. The second element visualizes the lateral distance with red circle sectors that appear when a tool tip moves laterally below a safety distance of 10 mm to obstacles (see Figure 1).

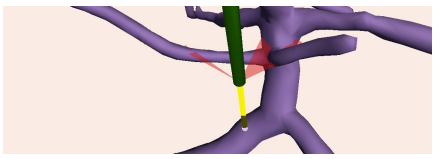

Figure 1. Distance sensor visualization in a virtual liver model. Tool is green, pointer is yellow, and circle sectors are red, indicating nearby vessels.

Two auditory display methods were provided. For the 'simplified' method, the front obstacle distance is mapped to the intra-onset interval of sequential sine tones, becoming faster when approaching the target. If the lateral safety distance is too small and circle sectors occur, a 3-tone chord is played in alternation. In the second 'extended' auditory method, the number of surrounding obstacles (visualized by circle sectors) is mapped to the number of individual pulsed sine tones. The duration of the tones increases as more area is covered by sectors (objects are closer). Moreover, the steady pulsing of the simplified method that encodes front obstacle distance is replaced by a complex rhythmic sequence.

This project was funded by the DFG (HA 7819/1-2).

III. RESULTS

A pilot study with 6 participants was performed. In a navigation task, an instrument was used to navigate to marked points through virtual liver models. The distance to blood vessels should be maximized. Volunteers were asked to rank the concepts. Simplified auditory display was ranked as the most helpful (extended auditory display 2nd place, pure visualization 3rd place). Using the BUZZ audioUX scale [4] with a maximum score of 77, average scores of 54.3 for the reduced sound concept and 47.5 for the extended sound concept were measured. The results of the Van der Laan et al. system acceptance questionnaire [5] show that concepts with sound achieved better usefulness, although pure visualization provided higher satisfaction. The concept with the simplified sound achieved the highest percentage of time in a safe working area and the shortest percentage in critical areas.

IV. DISCUSSION & CONCLUSION

Our concept is the first to provide such a multidimensional warning system using auditory display for needle placement. Using simplified auditory display helped reduce time in critical areas and was found to be particularly useful and preferred over extended auditory display or pure visualization. Due to the limited number of participants, a one-way ANOVA did not show any significant differences.

REFERENCES

[1] B. Wentink. "Eye-hand coordination in laparoscopy -an overview of experiments and supporting aids" in Minimally Invasive Therapy & Allied Technologies 10, 3 2001, 155–162.
[2] F. Heinrich, G. Schmidt, F. Jungmann, C. Hansen. "Augmented reality visualisation concepts to support intraoperative distance estimation" in Proceedings of the 25th ACM Symposium on Virtual Reality Software and Technology, 2019.
[3] D. Black, S. Lilge, C. Fellmann, A. V. Fellmann, L. Kreuer, A. Nabavi, H. K. Hahn, R. Kikinis, J. Burgner-Kahrs, "Auditory Display for Telerobotic Transnasal Surgery Using a Continuum Robot." in Journal of Medical Robotics Research, 4(02), 2019 1950004.
[4] B.J. Tomlinson, E. N. Brittany, B. N. Walker. "BUZZ: An auditory interface user experience scale." Extended Abstracts of the 2018 CHI Conference on Human Factors in Computing Systems, 2018.
[5] J.D. Van der Laan, A. Heino, D. De Waard. „A simple procedure for the assessment of acceptance of advanced transport telematics" in Transportation Research - Part C: Emerging Technologies, 5, 1997.

To go: Gameful Extension for Cognitive Rehabilitation Software

Annika Endler[1], Mareike Gabele[1,2], Tom Heidel[1], Steffi Hußlein[1] and Christian Hansen[2]

***Abstract*— Regular use of software-based cognitive training in the patient's environment can promote rehabilitation success after acquired brain damage. However, existing pieces of training are often conducted without motivation support or lack of therapeutic guidance. We present a prototypical connection of a gamefully motivating training to a medically approved training software. In an expert interview, this was evaluated as well suited for patients and a high potential for use.**

I. Introduction and Related Work

Software-based cognitive training is successfully used in the therapy of acquired brain damage [1]. It is mainly used in in-patient and out-patient therapy under the supervision of therapists during specified training times. Rehabilitation success is based on regular and long-term use, but workplaces must be available for this purpose. Frequent independent use of the learned skills in the own environment can promote rehabilitation. However, this requires an appropriate level of motivation of the patient: In addition to enjoyment and personal responsibility, autonomy as part of the self-determination theory contributes to support motivation [2]. Our research question, therefore, dealt with how these required elements can be used according to the needs and abilities of patients to supporting training. In this work, we propose to extend the existing cognitive training in a casual mobile game with short training sequences on a smartphone or -watch. Our contributions are its conceptual and prototypical development of this approach and the first evaluation of the system.

II. Design Considerations and Prototype

As a basis, we used an existing cognitive training for logical reasoning (RehaCom). Logical reasoning allows us to recognize patterns and establish coherence. The developed mobile casual training game is designed to complement the cognitive training given by the therapist. By a server-based connection of the app to the training profile of the patient, an adjustment of the difficulty to the abilities of the patient is possible. We created a video prototype of the function, screens and interactions. Within the game, shapes are displayed in a row must be logically completed. If the answer is correct, the row disappears. If the answer is wrong, it remains. The goal is, similar to the game 'Tetris', to get as few as many remaining rows as possible, or to achieve a number of correct rows. Figure 1 shows a gameplay situation in current and mobile training.

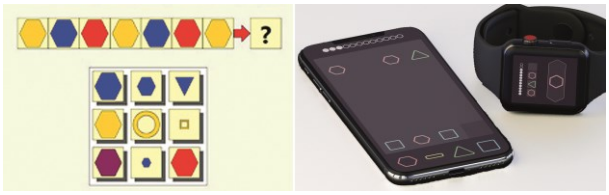

Figure 1: Left: Current Training (Computer), Right: Mobile Training

III. Qualitative Evaluation and Results

We presented the concept and our video prototype to a psychologist and a product manager of the rehabilitation software used as a basis. Then, we conducted a semi-structured qualitative interview of 30 minutes. We asked questions about the use for patients as support for motivation, patient skills and possible use. It was found that the time-reduced task at their own ability level is suitable to promote the practice that is necessary for rehabilitation. A changing environment makes training more challenging, but promotes the learning effect. The gameful approach expands the current training in a motivating way and thus shows a high potential for use in clinics and home training. The combination with an existing training system separates it from existing brain-jogging apps and provides a reliable therapeutic background.

IV. Discussion, Conclusion and Future Work

The selection of the mobile device should be flexibly adapted to the patient's abilities, as additional visual and motor limitations may exist. Rental devices can be a possibility here. The presented concept extends the potential of cognitive therapy flexibly in the personal situation of the patient. This can have a positive influence on the extent and period of rehabilitation success. The next step is to analyze the effect of the system on patients in terms of effect, use and training success parameters.

* This work was funded by the European Social Fund (ESF) of Saxony-Anhalt (under the operation number CCI 2014DE05SFOP013) as part of the initiative "Sachsen-Anhalt WISSENSCHAFT Chancengleichheit" with the program title "FEM-Power". It was also funded by the European Regional Development Fund under the operation numbers ZS/2016/04/78123 and ZS/2017/01/83843 as part of the initiative "Sachsen-Anhalt WISSENSCHAFT Schwerpunkte".

1 Authors are with the Magdeburg-Stendal University of Applied Sciences, Department of Engineering and Industrial Design, Germany

2 Authors are with the Otto von Guericke University Magdeburg, Faculty of Computer Science, Germany

References

[1] C. Yoo, M. Yong, J. Chung, J. Yang, "Effect of computerized cognitive rehabilitation pro-gram on cognitive function and activities of living in stroke patients", *in Journal of Physical Therapy Science*, Vol. 27, 2015, pp. 2487–2489.

[2] R.M. Ryan, C.S. Rigby, A. Przybylski, "The motivational pull of video games: A self-determination theory approach", in *Motivation and Emotion* Vol. 30, 2006, pp. 347-363.

ADHD Neurofeedback: Gameful gestures as a transfer into daily life

Mareike Gabele[1,2], Christoph Schubert[2], Abdullatif Alomar[2], Steffi Hußlein[2] and Christian Hansen[1]

***Abstract*— The goal of neurofeedback training for ADHD is to learn to focus on daily life. However, many software-based pieces of trainings support success on the computer but neglect the use of the ability in daily life. By the use of gestures in a mobile application, we show a possibility to support the transfer of the learned focus in daily life. In an expert interview, this was assessed as very promising for training success.**

I. Introduction and Related Work

ADHD (Attention deficit hyperactivity disorder) is the most common psychiatric disorder among children between 8 and 14 years and leads to problems in behavior and mental development. It is expressed by high distractibility, impulsiveness and restlessness. This often causes problems in social life or at school. At the same time, ADHD also brings positive characteristics such as deep immersion in a task (hyperfocus), a need for harmony and creativity. Instead of focusing on the negative traits, as is often the case today, the positive traits should be brought to the fore [1]. The relevance of positive reinforcement has been shown in an endless runner game [2]. Currently, ADHD is often treated with medication. An alternative is neurofeedback training, which is frequently described by children as uninteresting. The 30-60 minute training is carried out in up to 60 sessions in clinics or practices. However, the actual goal is to use the skills in daily life or to get support and to be reminded inconspicuously on the learned focus skill. Therefore, in this paper, we propose a training game on a tablet, which is controlled by neurofeedback as well as a hand gesture, which can be used as a reminder. The contributions are a concept and a prototype to transfer the training into everyday life, to address the positive, and also a first qualitative evaluation on a psychological basis.

II. Design Considerations and Prototype

We have designed a casual game for training at home and on the go that can complement the current training. After previous interviews with therapists and children with ADHD, who quickly find their hyperfocus in the game 'Minecraft' (Mojang AB), the concept is based on building with blocks. The goal is to build a tower or other constructs (Figure 1). The background varies depending on the height. A MindWave

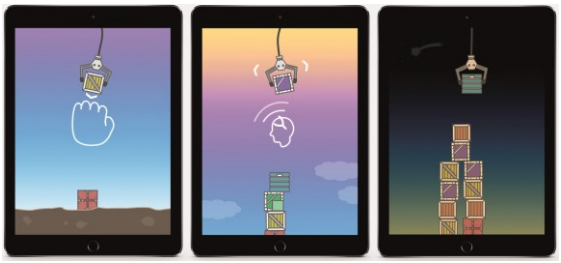

Figure 1: Left: Gesture to control the crate, Middle: Focus to influence the gripper, Right: Tower under construction

Headset (NeuroSky) measures the height of the focus by a sensor. This is represented in the game: The higher the focus, the calmer is the gripper arm. The gesture is tracked by a Myo armband (Myo). A fist holds the crate on the gripper arm while stretching the fingers lets the crate fall. For better memory, the gesture is carried out with the non-dominant hand. This inconspicuous gesture can be used, for example, in school to remind of the way to focus.

III. Qualitative Evaluation – Method and Results

We presented the project to a psychologist. In a semi-structured qualitative interview (duration: approx. 30 minutes) we asked questions about the possible effect of the game on children and the use of the gesture in play and everyday life. It has been found that automating the gesture in the game creates a connection with the focus. The gesture can, when used in everyday life, be a reminder of the way how to focus. The combination with the game supports the learning of the gesture positively and is well tailored to the target group.

IV. Discussion, Conclusion and Future Work

The gesture used may support the success of neurofeedback focus training for children with ADHD in daily life. Whether it is used, probably depends on whether it is inconspicuous enough to avoid stigmatization. The next step is to evaluate the effect of the game on children. This may create an opportunity to use gestures as a supportive expansion in ADHD therapy.

* This work was funded by the European Social Fund (ESF) of Saxony-Anhalt (under the operation number CCI 2014DE05SFOP013) as part of the initiative "Sachsen-Anhalt WISSENSCHAFT Chancengleichheit" with the program title "FEM-Power". It was also funded by the European Regional Development Fund under the operation numbers ZS/2016/04/78123 and ZS/2017/01/83843 as part of the initiative "Sachsen-Anhalt WISSENSCHAFT Schwerpunkte".

[1] Authors are with the Otto von Guericke University of Magdeburg, Faculty of Computer Science, Germany

[2] Authors are with the Magdeburg-Stendal University of Applied Sciences, Department of Engineering and Industrial Design, Germany

References

[1] K.P. Lesch, "'Shine bright like a diamond!'. Is research on highfunctioning ADHD at last entering the mainstream?", in *The journal of child Psychology and Psychiatry*. Wiley, New York, 2018, pp. 191-192.

[2] A. V. Reinschluessel, R. L. Mandryk. "'Using Positive or Negative Reinforcement in Neurofeedback Games for Training Self-Regulation." *Proceedings of the 2016 CHI' play Annual Symposium on Computer-Human Interaction in Play*, ACM Press, New York, 2016, pp. 186-198.

Quantitative Volumetric Assessment of CT-guided Ablation Treatments for Colorectal Liver Metastases

Raluca-Maria Sandu, Iwan Paolucci, Pascale Tinguely, Jacob Freedman, Stefan Weber

***Abstract*— In image-guided percutaneous ablations of liver tumors, the technical intra-procedural success of the treatment is defined by achieving complete tumor destruction plus a circumferential ablation margin of at least 5 mm. In the current setting, the ablation success is visually evaluated by an interventional radiologist who compares the differences between the pre- and post-ablation images. To address this limitation, we have developed an image-based analysis pipeline to compute radiomics for evaluating the volumetric coverage of the ablation. In this work, we present preliminary results after applying the radiomics extraction pipeline to a retrospective cohort of 102 patients that were treated with image-guided percutaneous microwave ablations for colorectal liver metastases.**

I. INTRODUCTION

Percutaneous thermal ablation is a minimally invasive technique generally performed under image-guidance based on CT, MRI or ultrasound. The patients undergoing this treatment benefit from a drastically improved quality of life, since they go home the next day and repeat the treatment when necessary. The ablation treatment has not yet taken over surgical resection due to the high local tumor progression (LTP) rates, which in these cases reach up to 48% [1]. It has been shown that the risk of LTP can be reduced by achieving complete coverage of the tumor including at least a 5 mm ablation margin. In the clinical routine, the ablation is visually assessed by the expert eye of the radiologist which is a subjective technique limited by repeatability and exact numerical quantification.

To address the current limitations in CT-guided ablations, we developed an image-based quantitative analysis pipeline to assess the volumetric ablation coverage using radiomics. We are currently evaluating this analysis pipeline on the MAVERRIC patient cohort [2].

II. METHODS

A software tool for semi-automatic segmentation of tumors and ablations has been developed and integrated into a commercially available navigation system for percutaneous ablations. The seeding point for the semi-automatic Fast-Marching algorithm is taken from the target point of the ablation probe. Based on the DICOM segmentation images, several radiomics which include volumes, diameters, intensity levels and surface distances are computed. The surface distance was calculated as the Euclidean distances between each surface voxel of the tumor and ablation w.r.t the percentage of tumor surface covered and used to evaluate the ablation coverage and ablation margin.

The study included 102 patients with 1-5 tumors < 31 mm in diameter, treated with thermal microwave ablation under CT-image guidance. The post-operative scan for evaluating the ablation success was taken immediately after ablation was performed. In total, 177 tumors were treated.

III. RESULTS

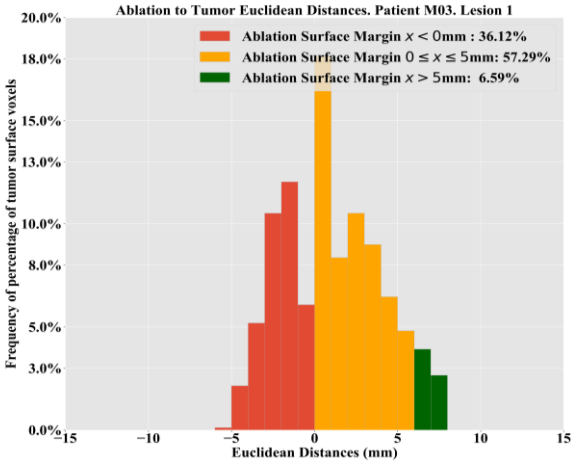

Figure 1 Percentage of tumor surface covered by ablation margins.

Fig. 1 depicts one result from the radiomics analysis pipeline showing an insufficiently treated tumor. The histogram employs a traffic-light color scheme relating to the ablation margin convention. This tumor had an LTP at the patient's 6-months follow-up.

IV. DISCUSSION & CONCLUSION

This work proposes a volumetric image-based quantitative analysis for measuring the technical success of the ablation treatment. This metric, together with other radiomics, could enable a precise measurement of ablation shape, size and margins that could be utilized to identify patients with increased risk of LTP. Eventually, this method might provide an important intra-operative feedback that would allow re-ablations in the same treatment session.

REFERENCES

[1] X. Wang *et al.*, "Margin Size is an Independent Predictor of Local Tumor Progression After Ablation of Colon Cancer Liver Metastases," *Cardiovasc. Intervent. Radiol.*, vol. 36, no. 1, pp. 166–175, Feb. 2013.

[2] "Microwave Ablation Versus Resection for Resectable Colorectal Liver Metastases - Full Text View - ClinicalTrials.gov." [Online].

R.M.S, I.P. and S. W. are with the ARTORG Center for Biomedical Engineering Research, University of Bern, Switzerland; P. T. is with the Department of Visceral Surgery and Medicine, Inselspital, Bern Switzerland; J.F. is with Danderyd Hospital, Karolinska Institute, Department of Clinical Sciences, Stockholm, Sweden;
e-mail: ralucam.sandu@gmail.com

Assessment of the performance of a new gamma-ultrasound scanner: preliminary results of ultrasound imaging

L. Fomanka, A. Pashazadeh, M. Kalmar, and T. Sühn,

Chair for Image Guided Procedures, Otto von Guericke University, Magdeburg

***Abstract*—Hand-held gamma cameras are valuable tools that provide functional information of the body inside operating rooms. However, they cannot acquire anatomical information. Recently we have developed a new hand-held hybrid scanner for surgical procedures which can get both anatomical and functional information of the body. In this study, we report the initial result of testing the scanner in anatomical imaging.**

I. INTRODUCTION

Dual-modality scanners have been developed to integrate structural and functional information obtained from the body of the patient. The resultant hybrid images have more clinical information than those acquired by a single modality scanner. The current hybrid scanners (e.g., SPECT/CT, PET/MRI) are commonly-used tools for preoperative diagnosis or post-operative follow-ups. In surgical settings, however, they cannot be used because of their bulkiness.

To have portable scanners to be used in operating rooms, hand-held gamma cameras have been developed. These lightweight scanners can be held by one hand; therefore, be easily used in operating rooms. These scanners provide only functional information of the body and suffer from the lack of anatomical data. In order to acquire both functional and anatomical information of the body inside the operating room, we have recently proposed a new concept for developing a hand-held gamma/ultrasound (US) scanner [1]. The core of this concept is a reflecting plate used to reflect US wave in the desired direction. This configuration allows using a gamma camera next to a US transducer, performing simultaneous gamma/ultrasound imaging. In the current study, we assessed the performance of this hybrid scanner in US imaging.

II. METHODS

We used a transducer of a US probe (9L, LOGIQ E9, GE Healthcare, U.S.A.) in our scanner. A standard resolution phantom (model 044, CIRS, U.S.A.) was used to do distance accuracy test. To this end, the distance of targets in the phantom in the vertical and horizontal directions was measured. In order to have a reference data, the experiment was replicated with a normal US probe of the same type. Then the results of the two scanners were compared. To reduce statistical error, each measurement was repeated at least three times, and the mean values were reported.

*Research supported by Federal Ministry of Education and Research (BMBF) in the context of the 'INKA' project (Grand Number 03IPT7100X).

L. F. Author is with Chair for Image Guided Procedures, Otto von Guericke University, Magdeburg; e-mail: lfomanka@yahoo.com).

III. RESULTS

Images obtained by the hybrid scanner and a normal US scanner are presented in Fig. 1. Also, the measured vertical and horizontal distances are shown in Table 1.

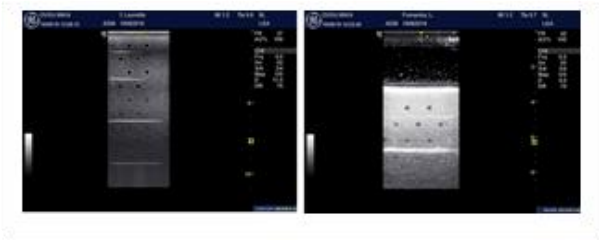

Figure 1. Scanning of the targets of a US phantom by a normal US scanner (left) and the hybrid scanner (right) for distance accuracy measurement

TABLE I. RESULTS OF DISTANCE ACCURACY MEASUREMENT WITH THE HYBRID SCANNER AND A NORMAL US SCANNER

Parameter	***Distance (mm) with Normal US Scanner***	***Distance (mm) with hybrid Scanner***	***Error (%)***
Vertical distance	18.8	18.6	1.1%
Horizontal distance	12.8	12.3	3.9%

IV. DISCUSSION & CONCLUSION

Reflection of the US wave by the aluminum plate and extra traveling of the wave inside the scanner was expected to lead to loss of part of the US signal. However, according to Table 1, the hand-held hybrid scanner can present vertical and horizontal distances with accuracies of, respectively, 98.9% and 96.1%, compared to a normal US probe.

REFERENCES

[1] A. Pashazadeh, T. Karkhanis, M. Kalmar, A. Boese, and M. Friebe, "*Combination adapter with switchable collimator for gamma-ultrasound guided surgery of sentinel lymph nodes*", 18th Annual Meeting of the German Society for Computer- and Robot-Assisted Surgery, Reutlingen, September 2019

Prototype for a surgical tool attachment to reduce tool maintenance costs

Matti Kaupenjohann, Jörg Thiem, University of Applied Sciences and Arts Dortmund

***Abstract*— Construction of a prototype to reduce costs by using manual tools in robotic surgery. This paper describes necessary steps from acquiring tool dimensions to the manufacturing process. This research provides two major results of the manufacturing process of the prototype.**

I. INTRODUCTION

Nowadays *Da Vinci* surgical robots are the de facto standard ones used in robotic surgery. One of its highlights is a wide range of tools, provided by its manufacturer *Intuitive Inc*. Anyway, the tools come with a disadvantage in terms of reusability. Most of the tools use a technology called "EndoWrist", which makes it possible for the tooltip to imitate hand movements [1]. This technology uses a sophisticated mechanism, that must be cleaned like any other MIS (Minimal invasive surgery) tool. The cleaning procedure is one of the potential reasons for the small number of times a MIS tool can be reused. In comparison, manual tools can be cleaned according to the Instrument Reprocessing instructions [2] on-site. The usage of these tools for robotic surgery could reduce the costs by increasing the tool uses. The paper aims to create the first prototype for these type of tools.

II. METHODS

This paper describes the construction of a prototype, which uses a robotic gripper to handle a manual surgical tool. We used a surgical needle holder "PL414R" from *Aesculap* and a robotic gripper "WSG50" from *Weiss Robotics.* There are three viable options in order to obtain the dimensions of a surgical tool. The first one is CAD (Computer aided design) -files provided by the manufacturer. The second is to obtain the data from a 3D scanner and optimize the results by post processing. The third option is the measurement of some selected segments of the tool, connected to the robotic gripper. As the first two options were not available, we could not but take the third one.

As the surgical gripper cannot be directly connected to the robotic gripper, it is necessary to construct a connecting tool. This tool is referred as Medical Gripper Automatic (MGA) hereinafter.

The prototype under research is a 3D printed model manufactured by FDM (Fused Deposition Modeling) Technology. It is extended by bearings and guides that help to translate the robotic gripper movement to the surgical gripper. Finally, the maximum tip movement of the complete construction was tested. To obtain the test data and to scale the movement, an approach based on the second theorem of the intercept theorem, was used [3].

III. RESULTS

In order to fit the limitations for this contribution, we will present just two results of this research.

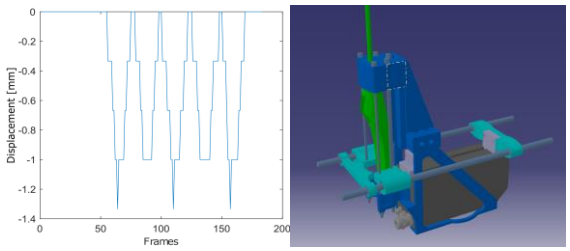

Figure 1. Measurement and final construction

The figure on the left shows the translation in one euclidian direction, which was measured by counting quantized steps on an underlying board. The figure on the right shows a CAD file of the final construction by highlighting different cohesive parts.

As Figure 1 (left) shows, the peaks, which lie between absolute values of 1.2 - 1.4 mm, relative to the neutral position. The measurement was experimental. The parts in Figure 1 (right) were colored to highlight different sections of the MGA. The moving parts (turquoise) are connected to the "WSG50" gripper. The lever of the "PL414R" gripper, not visible in the picture, is pressed by the moving parts. The gripper (green) is statically connected (blue) to the "WSG50" gripper.

IV. CONCLUSION

Our research confirms the possibility to create a prototype with tolerances less than those, achieved by manual guidance of the medical gripper. The comparison with the *Da Vinci* robot tools is still pending. As the FDM parts are often very flexible, the tolerance could be reduced by other manufacturing processes, which are also more viable for medical use.

ACKNOWLEDGMENT

The work has been supported by the Laboratories for Information Technology (LIT) at the University of Applied Science and Arts Dortmund.

REFERENCES

[1] Schilling, D.; *10 Jahre Roboterassistierte Chirurgie* (Presentation), Klinik für Urologie – Universitätsklinikum Tübingen, pp. 7.

[2] Working Group Instrument Reprocessing: *Instrument Reprocessing* (Brochure). Gütersloh, 2017, pp. 57–58.

[3] Müller-Philipp, S.; Gorski, H.-J.: *Leitfaden Geometrie: Für Studierende der Lehrämter*. Braunschweig [u.a.]: Vieweg, 2001, pp. 182.

RGB and IR-sensor fusion for low-cost detection of injured Human beings

Archana Gupta , Matti Kaupenjohann, Andreas Sutorma and Jörg Thiem - *University of Applied Sciences and Arts Dortmund*

***Abstract*— Thermal imaging is emerging as a viable solution to overcome the limitations of RGB cameras in providing effective object detection in low or no light environmental conditions, mostly due to technological advances and availability of low-cost IR sensors. These low-cost IR sensors, when used together with RGB camera sensors, offer capabilities to overcome the existing shortcomings of the RGB cameras and improve system performance.**

I. INTRODUCTION

Object recognition and detection is still one of the most challenging fields in Computer Vision domain, in particular in biomedical applications. Commercially available RGB cameras, due to their ease of use and low price have found use in a plethora of these applications including affordable systems for detecting injured or wounded human beings, e.g., in search and rescue missions or mobile first aid robots. Although being effective in well-illuminated environments, these systems suffer from drawbacks of not being able to capture sufficient information in low contrast, dark, or foggy conditions. Thermal imaging, also known as *thermography*, does not suffer from any such constraints owing to limited or no illumination. They effectively detect the thermal radiation from a human body in long wavelength infrared light range *(LWIR)*, even in low light, fog, or complete darkness. In addition, by the combination of color and thermal image sensors it will be possible to implement diagnostic functions for handheld or light-weight devices. Here, most of the commonly used algorithms for color image processing can be easily adopted for thermographic images as well thus eliminating the need of any additional efforts while integrating them into the system. Besides these future applications, our application initially aims to detect an injured or wounded person by a compact embedded RGB-thermal camera setup mounted on a drone or a mobile robot for indoor environments. Consequently, to make our system more robust, we propose to combine the conventional RGB camera with low cost commercially available IR Camera sensor thereby improving efficiency without blowing up the system cost.

II. METHODS

The proposed system consists of a PiCamera (640x480) and a FLIR Lepton3.5(160x20) connected to a RaspberryPi 3 B+ board. Latter has a LWIR sensor working in wavelength 8 to 14 µm and a thermal sensitivity of <50mK. Calibrating the heterogeneous stereo camera system with a considerable difference in image resolutions posed twofold challenges. Firstly, the system required the use of a calibration pattern which is visible in both visible and IR spectrums. Secondly, neither OpenCV nor MATLAB provided calibration methods which could be employed directly for calibrating images with different resolutions. These challenges were addressed in following ways -1).by creating a custom checkerboard pattern Fig.1(ii), inspired from the work done in [1]. A milled checkerboard pattern on a PCB allowed capturing of images by both the camera sensors with a distinctively visible checkerboard. 2). Stereo Calibration was performed by first individually finding the detection points in both set of images using MATLAB functions and then combining these points to achieve stereo calibration [2]. The resulting images were then fused together using a suitable fusion algorithm to combine information from both the camera sensors.

* Laboratories for Information Technology at the University of Applied Sciences and Arts Dortmund

III. RESULTS

Fig.1 shows the original and stereo-rectified image pairs from both the sensors which are obtained after calibration.

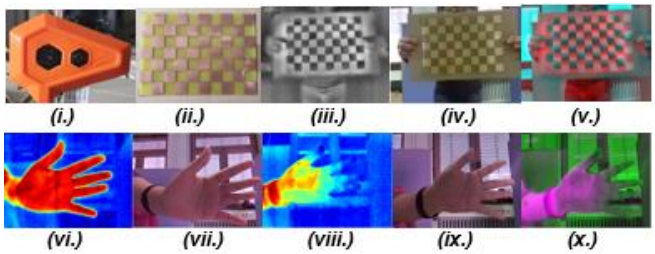

Figure 1.i) Multicamera setup, ii) Checkerboard pattern on PCB, iii) & iv) IR and RGB images of checkerboard respectively, v) Stereo-rectified image pair, vi) & vii) IR (with 'jet' colormap) and RGB images of the hand before applying disinfectant, viii) & ix) IR and RGB images of the hand after applying disinfectant, x) Stereo-rectified image pair with clearly visible hand boundaries.

IV. DISCUSSION & CONCLUSION

In addition to the task of rescue and search, such a system can be used for other medical cases like the hygienic hand disinfection. Many nosocomial infections are the result of a lack of hand hygiene. A thermal image can rate and improve the quality of the hand disinfection. When using alcoholic disinfectants, the hand surface cools down, this change in temperature can be measured by the IR camera sensor. The RGB camera supports the detection of the hand, especially in situations where the hand temperature only slightly deviates from the background and it cannot be separated from background solely based on thermographic images[3].

ACKNOWLEDGMENT

The work is supported by the LIT*.

REFERENCES

[1] Kechiche, Abir Zanzouri et al. "Shape from polarization in the far IR applied to 3D digitization of transparent objects." (2016).

[2] Stereo Camera Calibration Under Different Resolution https://github.com/muhammetbalcilar/Calibration-Under_Different-Resolution

[3] M. Smieschek1 et al. „Unterstützte Handerkennung in Thermographie -bildern zur Validierung der hygienischen Handedesinfektion", p.147, Bildverarbeitung für die Medizin 2017, Informatik aktuell, DOI 10.1007/978-3-662-54345-0_35.

Surface Quality Assessment of Screen-Printed Low-Cost MR Compatible Electrically Conductive Polymer

Sanchit Rathi[1,2)*], Martin Deckert[1)], Sven Brinkhues[1)], Michael Brosch[2)], Bertram Schmidt[1)]

***Abstract*— The aim of this study is to assess the print quality of screen-printed PEDOT:PSS structures. Tests performed in accordance to the ISO 4287 standard give a maximum and average height of the roughness profile of 2.34 µm ± 200 nm and 1.61 µm ± 200 nm for 6-layered PEDOT:PSS structures, respectively. MR imaging compatible test structures with a line resolution of 0.3 mm ± 0.08 mm are printed successfully on top of commercially available Polyimide sheet. In future, the brain stimulation/recording electrodes produced using PEDOT:PSS as a transparent conductive material will facilitate to gain from both the spatial supremacy of optical imaging as well as temporal preeminence of electrophysiology.**

I. INTRODUCTION

The traditional metal-based electrodes suffer from the downside of optical opaqueness. Therefore, such electrodes are unsuitable for tasks that require any optical imaging to be performed during the electrophysiological investigations of the brain. Hence, a MRI compatible, transparent electrically conducting polymer such as PEDOT:PSS opens new avenues of consolidating the benefits of MR imaging and optical imaging during the electrophysiological tasks.

II. METHODS

Unprocessed, out-of-box 5.0 wt.% PEDOT:PSS screen printable polymer paste from Sigma-Aldrich is used to print test structures on spin coated and cured polyimide (PI-2611 HD-MicroSystems), commercially available PI sheets as well as on ceramic plates. Scanning optical profilometer µScan by NanoFocus is employed for measuring the surface profile of the printed layer. MR compatibility test was performed using a Philips clinical 3T-MRI setup at LIN, Magdeburg

III. RESULTS

For the 6-layered PEDOT:PSS structures the measured maximum and average height of the roughness profile were 2.34 µm ± 200 nm and 1.61 µm ± 200 nm, respectively. The unprocessed polymer paste is found unsuitable for printing structures with line resolution of 0.1 mm. However, structures with line resolution of 0.3 mm ± 0.08 mm are printed successfully on top of commercially available PI sheet.

IV. DISCUSSION & CONCLUSION

PEDOT:PSS exhibits the potential to be a promising transparent, bio- & MR- compatible electrically conducting polymer. Nevertheless, further analysis in terms of improved ink formulation & processing methods are required to improve the print resolution and surface qualities of the printed structures.

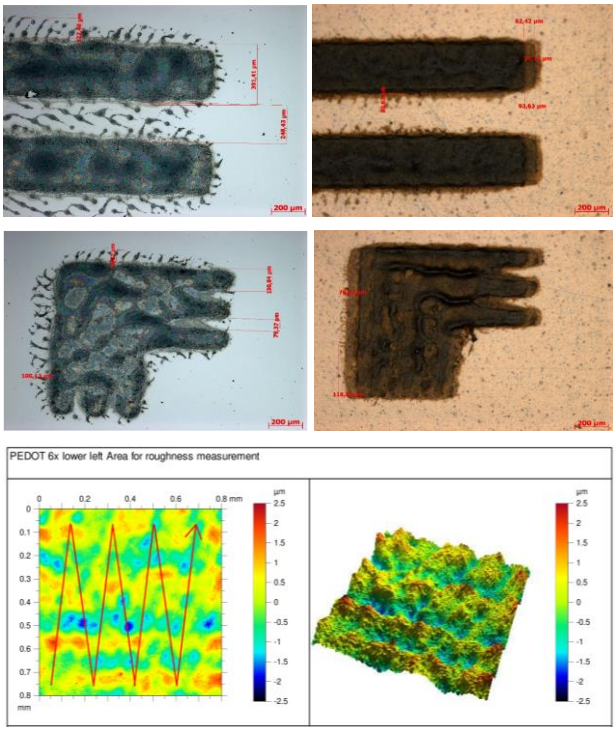

Figure 1. Screen printed single layered PEDOT:PSS structures on PI coated wafer. Line resolution 0.3mm (top row left) and 0.1mm (middle row left). Screen printed six layered PEDOT:PSS structures on commercially available PI sheets. Line resolution 0.3mm (top row right) and 0.1mm (middle row right). Roughness profile of a test structure fabricated using unprocessed out of the box printing paste (bottom row).

ACKNOWLEDGMENT

The authors would like to thank Dr. Markus Detert from OvGU Magdeburg and Dr. Marco Luniak from TU Dresden for their support with optical profilometer scans and advise during this work.

REFERENCES

[1] Khodagholy, D., Doublet, T., Gurfinkel, M., Quilichini, P., Ismailova, E., Leleux, P., Herve, T., Sanaur, S., Bernard, C., Malliaras, G.G.: Highly conformable conducting polymer electrodes for in vivo recordings. Advanced materials (Deerfield Beach, Fla.) (2011).

[2] Sanchit Rathi; Martin Deckert; Sven Brinkhues; Markus; Michael Brosch; Bertram Schmidt: Development of Low Cost Transparent Electrode Arrays for Brain Stimulation in Large Animals. Poster presentation: BMT 2019 - the Biomedical Engineering Congress

[3] Venkatraman, S., Hendricks, J., King, Z.A., Sereno, A.J., Richardson-Burns, S., Martin, D., Carmena, J.M.: In vitro and in vivo evaluation of PEDOT microelectrodes for neural stimulation and recording. IEEE transactions on neural systems and rehabilitation engineering (2011).

Funding: Graduate research scholarship, Sachsen-Anhalt, Germany.

Sanchit Rathi Email: srathi@lin-magdeburg.de.

1. Otto-von-Guericke University (OvGU), Magdeburg
2. Leibniz Institute for Neurobiology (LIN), Magdeburg

Brain-Computer Interaction in Virtual Reality with Low-Cost BCI Devices

Tung-Lung Liu, Zhenglei Wu, Jiahua Xu

***Abstract*—Brain-computer interface (BCI) has gained great attention from the public, which directly measures the brain activities from the users and translates the signals into corresponding defined commands. This usage can be beneficial for movement disorder patients to compensate for their dysfunctional physical capacities. Meanwhile, virtual reality (VR) has been implemented as a new interaction environment with an immersive experience in various fields. Based on BCI and VR, this paper proposes and evaluates a real-time system using low-cost BCI to rotate the robotic arm in VR by motor imaging the movement of left and right hand. It is hoped to help people who have paralyzed or neurodegenerative diseases.**

I. INTRODUCTION

Electroencephalography (EEG) brain signals can be acquired with brain-computer interface (BCI) directly from the scalp. BCI measures the neural oscillations to detect event-related potential (ERP) brain activity that responses to a particular sensory, cognitive, or motor event [1]. Meanwhile, motor imagery is the brain activity changing from the previous idle state oscillatory to another when performing mental imagery of a movement. This feature can be employed for BCI to distinguish the intention of movement of left or right hand by comparing the differences of potentials between two sides of the motor cortex [2]. Furthermore, to explore the possibilities for intuitive human-robot interaction of using BCI, this paper includes Virtual Radiality (VR) for feedback displaying.

II. METHODS

To achieve the abilities mentioned above, a designed framework shown in Fig. 1 consists of four parts; data acquisition, offline training, online classification, and robotic arm in VR. For data acquisition, mu and beta wave over the motor cortex at the positions of C3 and C4 of two different subjects were recorded for electroencephalogram (EEG) for motor imagery (100 trails per subject) for movement of left and right hand (label) as our datasets which were then fed into different combinations of feature extractions as well as machine learning algorithms for the evaluation of classification accuracy based on five-fold cross-validation. For offline training, Filter Bank Common Spatial Pattern (FBCSP) and classical Common Spatial Pattern (CSP) were used to maximize the differences between two classes, right and left hand, while Linear Discriminant Analysis (LDA), Support Vector Machine (SVM), and Decision Tree were used for classification. For online classification and VR, real-time EEG streams were transformed into commands predicted by the classifier and sent to Unity via Open Sound Control protocol to control the robotic arm.

*Research supported by CSC Foundation.

Jiahua. Xu is with the Faculty of Computer Science in University of Magdeburg, Germany, e-mail: Jiahua.xu@med.ovgu.de).

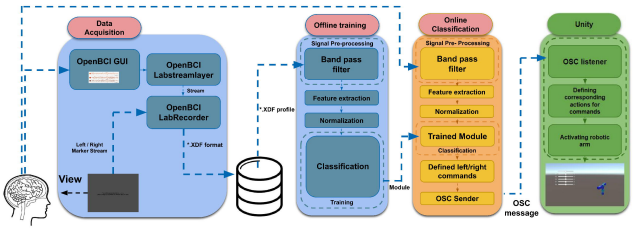

Figure 1. Framework

III. RESULTS

Our best result of accuracy for off-line classification shown in Fig. 2 was LDA with FBCSP (five filter bands) at 55%. And Fig. 3 illustrates the robotic arm in Unity.

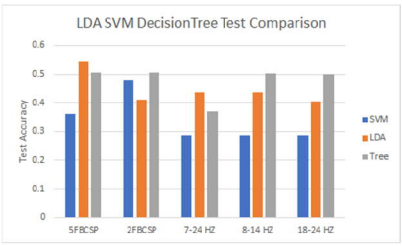

Figure 2. Test accuracy comparison

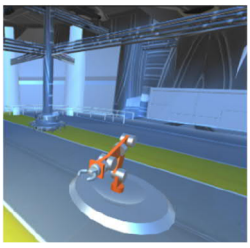

Figure 3. Robotic arm in VR

IV. DISCUSSION & CONCLUSION

This system performed an average of 51% of classification accuracy on our EEG datasets for the left and right hand (class). This result is comparable comparing to another research having an average of 54% also with low-cost BCI [1]. Yet, it also shows that low-cost BCIs are not yet optimized for clinical researches because the acquired data are not as good as medical-grade BCIs. Factors, such as subject performance, hardware capability, and algorithms can affect the performance of a BCI. The designed framework has shown that it can still be reused in other researches with further improvement. For future work, we will consider recording more data for training the algorithms to improve accuracy.

REFERENCES

[1] S. J. Luck, *An Introduction to the Event-Related Potential Technique*, The MIT Press, 2005.

[2] B. Blankertz, R. Tomioka, S. Lemm, M. Kawanabe, and K. Muller, "Optimizing Spatial filters for Robust EEG Single-Trial Analysis", IEEE Signal Process. Mag., vol. 25, no. 1, 2008, pp. 41–56.

[3] B. Estermann, "Evaluation of Low-Cost EEG Hardware in a Motor Imagery Based Brain Computer Interface," B.S. thesis, Department of Computer Science, ETH Zurich, Sep. 2017.

SPONSORS


SIEMENS
Healthineers


INTERVENTIONAL
systems


VISUS


MR:comp


IEEE Xplore®
Digital Library


sanaone®

Time Series Classification of Physiological Data

Moritz Spiller

***Abstract*— An increasing amount of time series data in the healthcare sector requires efficient and accurate machine learning algorithms to analyze them. In this study, state-of-the-art deep learning classifiers for time series classification (TSC) are evaluated on eye tracking data acquired during a user study and their performance is compared to a baseline classifier. While every deep learning classifier significantly outperforms the baseline classifier, the results suggest that MLSTM-FCN is the superior performing model in terms of F1-Score. As it also requires the highest inference time, ResNet and FCN still have to be considered for time-critical applications.**

I. INTRODUCTION

Modern medical devices like electrocardiography (ECG), electroencephalography (EEG) acquire an increasing amount of observational time series data in various clinical applications. Researchers have applied machine learning classifiers such as Multi-Layer Perceptron (MLP) and Support Vector Machine (SVM) [3] to the classification of such data. However, these static classifiers might miss relevant information present along the time scale of the data and require additional feature extraction as well as feature selection. Deep learning models overcome these limitations and have shown to achieve state-of-the-art performance on TSC problems [2,6]. This study aims to provide insight into the classifiers' performance to assist researchers during the selection of a promising classifier by evaluating three deep learning classifiers on eye tracking data and compare their performance to a baseline classifier.

II. METHODS

The used dataset was gathered during an eye tracking user experiment using information visualizations [1] and contains 480 time series (40 participants x 12 questions) with a length of 2700 time steps (45 s time limit x 60 Hz sampling rate), which are labeled by the correctness of the answer to the respective question. A multivariate Long Short-Term Memory – Fully Convolutional Network (MLSTM-FCN) with attention mechanism [2], a simple FCN [6] and a Residual Network (ResNet) [6] are trained on the data for 1000 epochs with a batch size of 128. Logistic Regression (LR) [4] is chosen as the baseline classifier since it has been found to work well on eye gaze data [5]. As the dataset is slightly unbalanced, the F1-Score is chosen as the evaluation metric. To measure the models' efficiency, their inference time in milliseconds (ms) is also reported.

III. RESULTS

Tab. I shows the average performance and standard deviation of the classifiers after 10-fold cross-validation. All deep learning models significantly outperform the baseline classifier in terms of F1-Score. FCN and ResNet yield similar F1-Score, but FCN has a clear advantage in inference time. MLSTM-FCN is the superior performing classifier but requires up to 150 ms to infer the class of one sample.

TABLE I. PERFORMANCE OF THE CLASSIFIERS

Classifier	F1-Score	Inference Time per Sample [ms]
MLSTM-FCN	0.825 (0.08)	104.58 (49)
ResNet	0.675 (0.07)	15.83 (0)
FCN	0.68 (0.15)	4.17 (0)
LR	0.605 (0.12)	0.83 (0)

IV. DISCUSSION & CONCLUSION

MLSTM-FCN is the classifier to be chosen in applications where accuracy is the primary concern. ResNet and FCN are better choices when near real-time classification is required. That these models yield similar performance is unexpected since ResNet is due to its residual connections by design more suitable for TSC. Even though this study used eye tracking data for classification, the results can be transferred to a broad variety of medical and biological applications and help to identify a promising classifier there.

REFERENCES

[1] Md Zakir Hossain, Tom Gedeon, and Atiqul Islam. 2018. Understanding Two Graphical Visualizations from Observer's Pupillary Responses and Neural Network. In *Proceedings of the 30th Australian Conference on Computer-Human Interaction* (OzCHI '18), 215–218.

[2] Fazle Karim, Somshubra Majumdar, Houshang Darabi, and Samuel Harford. 2019. Multivariate LSTM-FCNs for time series classification. *Neural Networks* 116, (August 2019), 237–245.

[3] Hamid Khorrami and Majid Moavenian. 2010. A comparative study of DWT, CWT and DCT transformations in ECG arrhythmias classification. *Expert Syst. Appl.* 37, 8 (August 2010), 5751–5757.

[4] Susan Li. Machine Learning with Python. Retrieved from https://bit.ly/2W5SYfK

[5] Ben Steichen, Cristina Conati, and Giuseppe Carenini. 2014. Inferring Visualization Task Properties, User Performance, and User Cognitive Abilities from Eye Gaze Data. *ACM Trans. Interact. Intell. Syst.* 4, 2 (July 2014), 1–29.

[6] Zhiguang Wang, Weizhong Yan, and Tim Oates. 2016. Time Series Classification from Scratch with Deep Neural Networks: A Strong Baseline. (November 2016). Retrieved from https://github.com/cauchyturing/

*Research supported by Australian Research Council Linkage Project 140100995. Author is with the Australian National University, Canberra, Australia and the Otto von Guericke University, Magdeburg, Germany; e-mail: moritzspiller@gmail.com

Registration techniques for computer-aided endopancreatic surgery

Benjamin Peter Eigl, Caroline Haslebacher, and Philip C. Müller

***Abstract*— Endopancreatic surgery stands for an experimental minimally invasive technique, where a pancreatic resection is performed with a rigid endoscope from inside the pancreas. This phantom study aims to evaluate suitable registration techniques to combine the novel surgical procedure with computer assistance for endopancreatic tumour resection. We evaluated ultrasound-based registration as the suitable technique for a safe resection of two invisible pancreatic tumours.**

I. INTRODUCTION

Open and minimally invasive pancreatic surgeries are still associated with a high morbidity, thus current research is looking for further reduction of the surgical trauma to improve the perioperative outcome.[1] We have previously developed endopancreatic surgery (EPS) as an experimental technique.[2] In the experimental setting, the resections were made according to the visual feedback from the endoscope; however, the study demonstrated the risk of organ perforation with this technique. Furthermore, the orientation inside the pancreas was challenging and structures not visible by the endoscope are impossible to target. In a phantom study we evaluated suitable registration techniques to deliver image guidance for endopancreatic resections. The most promising technique was used to mark and partially resect two pancreatic "tumors" invisible in the endoscopic image.

II. METHODS

The purpose of the study was to evaluate three techniques to achieve best possible local registration. In the first study group only surface landmarks were chosen (Papilla, superior pancreatic border, V. mesenterica superior). In the second group two landmarks were registered by ultrasound (two tumors) and one surface landmark was chosen (Papilla). While in the third group, landmarks were all acquired by ultrasound (three tumors). The measures taken were the Fiducial Registration Error (FRE) as well as the time for the registration attempt. Therefore, a pancreas phantom comprised of intrapancreatic "tumors" and structures at risk with CT, US and electrosurgical characteristics was developed. A rigid endoscope is inserted via a duodenotomy into the pancreatic duct to perform resection using a monopolar loop under visual and virtual guidance.

The study was conducted by a trained medical professional and each registration attempt was conducted 5 times.

III. RESULTS

Pure intraparenchymal landmark registration showed the best accuracy. Computer assistance based on intraparenchymal landmarks enabled the surgeon to resect and mark the correct path from the duct to the invisible tumours (see Fig. 1).

TABLE I. COMPARISON OF REGISTRATION APPROACHES

Study group	Landmarks	Fiducial Registration Error (mm)	Registration Time (min)
1	Surface	3.46 (2.25-4.85)	01:51 (01:33-02:05)
2	Surface and intraparenchymal	2.46 (1.60-3.35)	02:12 (01:54-02:33)
3	Intraparenchymal	2.24 (1.40-2.85)	02:58 (01:42-04:04)

Median (interquartile range)

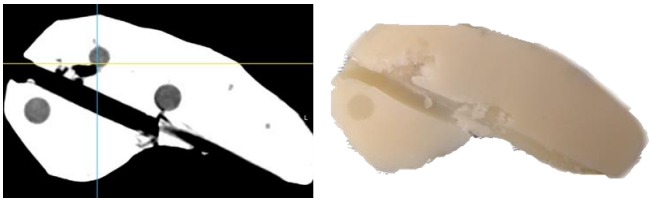

Figure 1. Pancreatic resection marks (CT, left; midline cut, right)

IV. DISCUSSION & CONCLUSION

The combination of computer assistance and the endopancreatic surgery allowed a safe pancreatic tumour resection from inside the organ. Computer assistance is of paramount importance for the orientation and the safety of endoscopic pancreatic surgery. We will evaluate the feasibility of the workflow in a phantom study consisting of 7 phantoms with a total of 14 resections. If endopancreatic surgery can be performed safe and precise, this novel technique has the potential to replace open pancreatic surgical treatments that are known for major morbidity and mortality.

ACKNOWLEDGMENT

This project was funded by the Swiss Pancreas Foundation.

REFERENCES

[1] D. C. Steinemann *et al.*, "Meta-analysis of hybrid natural-orifice transluminal endoscopic surgery *versus* laparoscopic surgery," *Br. J. Surg.*, vol. 104, no. 8, pp. 977–989, Jul. 2017.

[2] P. C. Müller *et al.*, "Transduodenal-transpapillary endopancreatic surgery with a rigid resectoscope: experiments on ex vivo, in vivo animal models and human cadavers," *Surg. Endosc.*, Mar. 2017.

Spinal Ultrasound Bone Segmentation

Alba Rivera, Sathish Balakrishnan, Alfredo Illanes and Michael Friebe, *Senior M*ember, *IEEE*

***Abstract*—Ultrasound (US) imaging is a more useful alternative to guide spine interventions due to it is non-ionizing, real time and economical nature. Thus, it is advisable to enhance, segment and classify US images in order to ease medical procedures.**

I. INTRODUCTION

Ultrasound (US) imaging is a real-time, low-cost, non-invasive and portable medical imaging modality. In interventional surgeries, these advantages of US, makes it a potential replacement for traditional imaging modalities like X-Ray and CT. But still in the case of orthopedic interventions, US has still not made considerable progress because automatic detection of bones in an US image is fundamentally a complicated problem. In this work, we propose a method for US bone segmentation using unique properties exhibited by a bone in an US image.

II. METHODS

In this work, ultrasound images of spinal bone were acquired from 3 different subjects. In total, 600 images were acquired using Logiq E9 US machine (9L-linear probe). Each of these images has an axial resolution of 457*284 pixels and a depth of 7cm.

In order to find the correct method to segment bones, it is necessary to understand the properties of a bone in an US image. Bone has a very high attenuation coefficient and high absorption to US waves compared other tissues. This property creates a very high intensity value followed by a shadowing effect along the depth axis. The figure below shows this property.

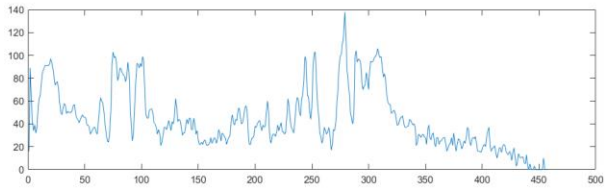

Figure 1. Example of a figure caption.

For the generation of ground truth, we manually annotate the bone regions in order to extract the ground truth information of bone surface. We used the 'imfreehand' function of Matlab to achieve this (Figure 2).

In order to extract the features from the signals from bone and non-bone categories, we started with applying simple polynomial fitting methods. These methods did not provide enough information. Then we applied Auto-Regressive (AR) modeling and extracted 30 best features for each of the signals in bone and non-bone category.

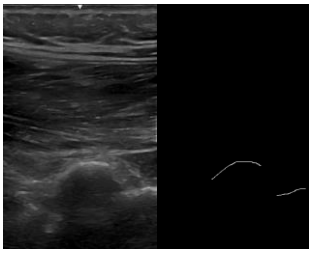

Figure 2. Example of a figure caption.

A linear SVM based classification model and k-nearest neighbor classification, were trained and tested for 2 classes. In total, we had features from 6000 bone signals and 29020 non-bone signals. From this data, 66% was used for training and 34% for testing. So finally, features from 23113 signals were used for training and 11907 signals for testing.

III. RESULTS

Using the features extracted from AR model with a linear SVM based training process, we achieved a testing accuracy of 94.063%. But when testing the same features with K-nearest neighbor model, we achieved a slightly better accuracy of 96.170%.

TABLE I.

Learning Method	Accuracy
SVM	94.063%
K-nearest neighbor	96.170%

IV. DISCUSSION & CONCLUSION

This work impacts in medical field because of the increase of the accuracy obtained, that in spinal bone clinical procedures it is very important to ensure the best results in order to avoid possible failures beyond repair.

ACKNOWLEDGMENT

I want to thank Sathish Balakrishnan, Dr. Alfredo Illanes and Prof. Dr. Michael Friebe, all from INKA, for giving me this opportunity.

REFERENCES

[1] Wang, P., Patel, V.M., Hacihaliloglu, I.: Simultaneous Segmentation and Classification of Bone Surfaces from Ultrasound Using a Multi-feature Guided CNN.

Parametrization of an audio signal

N. Pawaskar, S. Pal, and I. Maldonado

***Abstract*— The audio signal, acquired with an attached audio transducer located in the proximal part of a biopsy needle, had demonstrated to contain information from the distal part or tip. The information is such enrichment that it is possible to identify a puncture or the transition between two materials with different textures and densities. The implementation of a basic experimental setup allowed a controlled environment for the calculation of different mechanical stress forces and displacements. In the end, three main parameters were defined.**

I. INTRODUCTION

The implementation and constant innovation in medical interventional devices (IMD) provide different benefits to patients, medics, industry, and academia. To mention some benefits: induce minimal damage, reduce time recovery, compatible with different noninvasive imaging devices, in most of cases disposable and, it is an excellent platform for new ideas and research. The use of sensors in medical applications demands a complete study and full understanding of the information acquired. The miniaturization and compatibility with different image devices can position a sensor in an entirely new environment, inside or outside the human body. This complete new environment can induce information that can be misinterpreted and generate false expectations and diagnostics. The medical needs, quality standards, and technological advances demand robust applications with a solid theoretical background. The objective of this work is to identify and estimate parameters contained in an audio signal acquired after attach an audio transducer to a biopsy needle excited by an impulse [1][2].

II. METHODS

The experimental setup (ES) consisted of a pair of steel wires with different diameters excited by an actuator located to a specific distance from the audio transducer. All the information was registered and stored in an audio format. The diameters implemented were 1.2 and 1.5 millimeters with a total longitude of 210 millimeters. An audio transducer (MEMS microphone SPH0645LM4H-B, Knowles, Illinois, USA) was attached to the proximal end. A 3D printed holder from our design made the assembly between the audio transducer and the needle. A Raspberry Pi 3 (Raspberry Pi Foundation, Cambridge, UK) computer stored and received all data acquired by the audio transducer via I2S. The programming language that was implemented to collect and store the data was Python 2.7. An electric actuator induced the excitation in the wire with a force of 0.6 N and in two different points (15 and 20 mm) distance from the 3D holder. The actuator consisted of a solenoid (Pressing solenoid ITS-LZ-1949-D-6VDC, Intertec, Hallbergmoos, Germany). The programming environment to analyze and visualize all results was on Matlab 2018b.

A total of 160 audio WAV files were acquired and analyzed. The estimated parameters were the point of maximum amplitude and the constant of decay of the form

$$y' \approx a \cdot e^{b \cdot x} \qquad (1)$$

III. RESULTS

The point of maximum amplitude and constant decay describe the behavior of the audio signal when excited. Both parameters provide information about the system surrounding the needle.

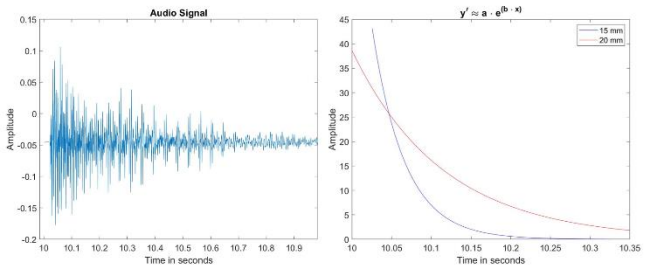

Figure 1. Left, example of audio signal. Right, differences between points of impact, where ***a*** is the maximum amplitude and ***b*** constant of decay.

IV. DISCUSSION & CONCLUSION

The parametrization of the maximum amplitude and constant of decay had contributed to a better understanding of the audio-needle system.

ACKNOWLEDGMENT

Thanks to INKA and its members for the opportunity to collaborate on the audio-needle project.

REFERENCES

[1] A. Illanes, A. Boese, I. Maldonado, A. Pashazadeh, A. Schaufler, N. Navab, and M. Friebe, "Novel clinical device tracking and tissue event characterization using proximally placed audio signal acquisition and processing," Scientific reports, vol. 8, no. 1, p. 12070, 2018.

[2] I. Maldonado, A. Illanes, A. Boese, and M. Friebe, "Characterization of a carotid distension waveform from audio signal acquired with a stethoscope," Computing, vol. 44, p. 1, 2017.

*Research supported by the German BMBF (grant 03IPT7100X) and CONACYT Mexico.

N. Pawaskar and S. Pal are with the Chair of Catheter Technologies and Image Guided Therapies (INKA), Institute for Medical Technology, Otto-von-Guericke-University, Magdeburg, 39104 Germany, e-mail: sukreet.pal@st.ovgu.de and nishad.pawaskar@st.ovgu.de.

Comparison of Audio Sensors and Signal Conditioning Strategies for Acquisition and Monitoring of the Signals from the Carotid Artery

R. Salvi, T. Sühn, I. Maldonado, A. Boese, A. Illanes, M. Friebe

***Abstract*— The accumulation of plaque in the arteries arise a severe health condition called Arterial Stenosis. The early diagnosis of the accumulation of plaque can be detected by auscultating and monitoring the carotid artery.**

I. INTRODUCTION

Auscultation is well-established diagnostic tool in cardiology. Diagnostic methods like ultrasound imaging, angiography or magnetic resonance-based imaging depend mainly on the experience of the examining clinician[1]. However, listening to the blood flow in the carotid artery is little investigated but could serve as a screening tool for stenosis[2].While the analysis of these sounds needs experience of a cardiologist, a specific hardware setup for carotid signal acquisition could enable objective assessment. Aim of this work is a comparison of different audio transducers and subsequent signal conditioning strategies, to address the specific requirements for carotid auscultation.

II. MATERIALS AND METHODS

Audio Transducers are available with different packaging like MEMS and normal electret and with different working principles like Electret Condenser, Piezo, Carbon, Dynamic etc. For the application of auscultation of carotid artery MEMS and normal electret both were considered. Four different types of audio sensors were selected according to following specifications: size, frequency response, sensitivity, power requirements and SNR.

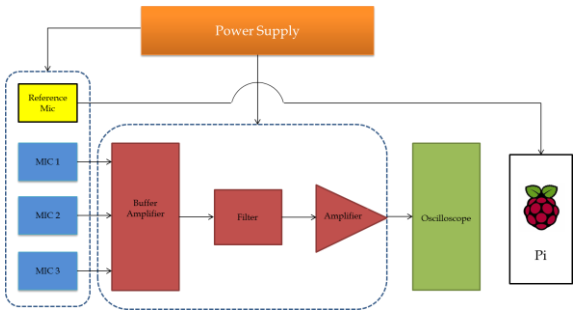

Figure 1: Approach for Signal Acquisition and Conditioning

The sensors M0 (**Knowles SPH0645LM4H-B**, MEMS: Electret Condenser (Digital Output)), M1 (**Knowles SPU0410LR5H-QB**, MEMS: Electret Condenser (Analog Output)), M2 (**Vesper PMM-3738-VM1000-R**, MEMS: Piezo (Analog Output)) and M3 (**Knowles BL21785**, Piezo (Analog Output)) were powered with a regulated power source and attached to a bell shaped structure, resembling the shape of a stethoscope and ensuring a consistent mechanical contact to the skin. Signal conditioning strategies were designed according to the individual requirements of the sensors. Figure 1; illustrates the signal conditioning strategy. Each circuit consists of a buffer, a 4th order Butterworth low-pass filter (cut-off frequency fc=1 kHz) and a preamplifier with a gain set according to the sensor output. Sounds were recorded at the neck of a voluntary subject and in a quiet environment. Different artefacts such as swallowing, intense respiration as well as background talking during the acquisition were introduced. The signal length was 20seconds out of which the first 10 seconds was the ideal condition and next 10 seconds with artefacts. A Periodogram and a Welch were computed and the spectral energies were divided in three different intervals like low frequency (LF = 0-30Hz), medium frequency (MF = 30Hz-100Hz) and high frequency (HF = 100-2300Hz).

III. RESULTS AND DISCUSSION

The recordings from each sensor show noticeable differences in the signal quality. While the filters efficiently eliminated the high frequency distortion signals from the voice and background, the artefacts generated by swallowing and respiration were still present. This could be explained as, since the artefacts breathing and swallowing lie below the cut-off frequency, they were not eliminated. However, background talks lie in the higher frequency range and so the filters were successful in eliminating them. The Microphone M0 is more susceptible to the background talk as compared to the others. MEMS microphones M1 and M2 show good signal strength but lack stability with respect to artefacts. The Microphone M3, show better stability but the signal strength is low as compared to others. However, the MEMS Microphones M1 and M2 have internal amplification circuit additional to the one in the conditioning circuit. Therefore, it can be concluded that the Microphone M3 is good in both; Sensibility and Stability with respect to the artefacts.

REFERENCES

[1] T. Sühn *et al.*, "Computer Assisted Auscultation System for Phonoangiography of the Carotid Artery," vol. 5, no. 1, pp. 1–3, 2019.

[2] I. Maldonado, A. Illanes, A. Boese, and M. Friebe, "Characterization of a carotid distension waveform from audio signal acquired with a stethoscope," *Comput. Cardiol. (2010).*, vol. 44, pp. 1–4, 2017.

Open-source early health technology assessment in regenerative medicine with TESSEE

Cátia Bandeiras, *Member, IEEE,* Joaquim M. Sampaio Cabral, Stan N. Finkelstein, and Frederico Castelo Ferreira

***Abstract*— Cell therapies and regenerative medicine is promising for chronic diseases, being very interesting for healthcare management in an aging population. However, given that these therapies often use cells in their products, they have manufacturing scale limitations that make them very costly to produce. Furthermore, the high reimbursement costs proposed for these therapies make reimbursement by national healthcare systems very difficult. Early health technology assessment (eHTA), can provide insights on manufacturing innovations from an early development stage, in order to better target the costs, pricing, and healthcare benefits necessary towards sustainable adoption. This work aims at presenting eHTA approaches in regenerative medicine, and introduces a focus on TESSEE, an open-source tool for eHTA. TESSEE was developed during a PhD thesis work with the aim to connect bioprocess and health economics, having case studies connected to the development of stem cell therapies. This approach, when combined with engineering design of these products, can contribute to rational development of regenerative medicine based therapies.**

I. INTRODUCTION

Regenerative medicine therapies have very high manufacturing costs and are produced at a much lower scale than small molecule and biological drugs. The scaling-up of stem cell manufacturing is impaired by manufacturing systems with small lot sizes, labor-intensive tasks, long processing times, and costly process components. Early health technology assessment (eHTA) is an emergent field aiming at determining the commercial viability of a new medical technology in the research and development stage. Models for this effect include several uncertainty variables to provide informed estimates for the innovation and development of a new technology.

*Research supported by Fundação para a Ciência e Tecnologia (FCT) through the PhD Fellowship PD/BD/105868/2014.

C. Bandeiras is with the Institute of Bioengineering and Biosciences, Department of Bioengineering, Instituto Superior Técnico, Universidade de Lisboa, Portugal (e-mail: catia.bandeiras@tecnico.ulisboa.pt). She is also an Associate Editor for IEEE Potentials, the IEEE magazine for Students and Young Professionals.

J. M. S. Cabral is with the Institute of Bioengineering and Biosciences, Department of Bioengineering, Instituto Superior Técnico, Universidade de Lisboa, Portugal (e-mail: joaquim.cabral@ist.utl.pt).

S. N. Finkelstein is with the Harvard-MIT Division of Health Sciences & Technology, Cambridge, MA 02139 USA (e-mail: snfinkel@mit.edu).

F. C. Ferreira is with the Institute of Bioengineering and Biosciences, Department of Bioengineering, Instituto Superior Técnico, Universidade de Lisboa, Portugal (e-mail: frederico.ferreira@ist.utl.pt).

II. METHODS

eHTA approaches in regenerative medicine would benefit from a collaborative, open-source approach, that would connect bioprocess modeling for evaluation of engineering and process design innovations to the cost-effectiveness to the final product. Having this in mind, TESSEE was developed. While this tool was developed for specific case studies in stem cell engineering, the framework can be used for other medical challenges and requires only some Python modeling and data science knowledge.

III. RESULTS

As a demonstrative approach of the relevance of eHTA for engineering stem cell therapies, case studies will be presented for the choice of culture media and reactor for expansion, and the manufacturing of medical devices for type 1 diabetes and cystic fibrosis. These analyses show that, at the moment, only a small fraction of patients could benefit of these therapies given national healthcare systems willingness-to-pay thresholds. Current recommendations point towards personalized medicine in the evaluated clinical challenges and support the development of predictive models through machine learning tools.

IV. DISCUSSION & CONCLUSION

eHTA is useful for regenerative medicine and the TESSEE framework could recommend specific stem cell therapies for personalized medicine, while providing recommendations for improved process design. Next steps for the development of TESSEE involve the dissemination of the tool for education and the development of a graphical user interface to improve the user experience. Additionally, the creation of a community of different stakeholders and collaborations is sought after.

ACKNOWLEDGMENT

The authors acknowledge funding from FCT, Institute for Bioengineering and Biosciences (UID/BIO/04565/2019) and also through the project PRECISE (PAC-PRECISE-LISBOA-01-0145-FEDER-016394).

REFERENCES

[1] C. Bandeiras, J.M.S. Cabral, S.N. Finkelstein, and F.C. Ferreira, "TESSEE – Tool for Early Stem Cells Economic Evaluation", in *XV Mediterranean Conference on Medical and Biological Engineering and Computing – MEDICON 2019*, pp. 1912-1932